THE JOURNAL
OF
CHEMICAL PHYSICS

VOLUME 6 SEPTEMBER, 1938 NUMBER 9

Exchange Forces and Electrostatic Forces Between Ions in Solution

RONALD W. GURNEY
Wills Physical Laboratory, University of Bristol, England

(April 5, 1938)

Though the treatment of ionic dissociation by thermodynamic methods has been fruitful, the mechanism can be better understood by the use of statistical mechanics. For this purpose one needs to know the potential energy of the ions as a function of temperature. The work D required to dissociate a molecule or molecular ion consists of two parts, one part D_{el} due to electrostatic forces, and the other D_{non} due to nonelectrostatic forces. As the former varies rapidly with temperature, for each species the value of dD/dT is a guide to the value of D_{el}. It is shown that for acid molecules and molecular ions in aqueous solution the relative values of dD/dT for different types are in the order predicted. Further, the characteristic temperature θ at which the dissociation constant passes through a maximum should depend, not on the value of D, but on the relative magnitudes of D_{non} and D_{el}. It is found that the known values of θ fall into line in accordance with this rule. Between two Hg^+ ions, or two Te^- ions, there will be exchange forces of attraction similar to those which give rise to the molecules Na_2 and Br_2; thus in aqueous solution the ions $(Hg_2)^{++}$ and $(Te_2)^{--}$ are stable, although for them D_{el} is negative.

§1

ALTHOUGH the treatment of gaseous molecules by the methods of quantum mechanics has now become habitual, little has been done to use quantum-mechanical forces to describe the stability and the dissociation of molecules in solution. The author has described[1] the mechanism which determines the heat of ionic dissociation, and suggested that the details of dissociation at different temperatures may be understood by recognizing the magnitude of the exchange forces between pairs of simple ions. Similar ideas have been used, particularly by L. P. Hammett,[2] in accounting for the effect of various substituents on the thermodynamic properties of benzene derivatives, etc., in aqueous solution.

A greater insight into the mechanism of such processes than is possible by a thermodynamic treatment, can be obtained by the use of statistical mechanics. For this purpose we require in the first place a knowledge of the mutual potential energy of the ions. Take then a positive and a negative ion first in a vacuum. Leaving aside the Coulomb forces between them, we know that the nonelectrostatic forces will contribute either (*a*) a repulsion only, or (*b*) an attraction as well as a repulsion; that is to say, this contribution, plotted against the separation r, will have the form either of curve *a* in Fig. 1 or of curve *b*. To obtain the total potential energy, this contribution must be combined with the electrostatic energy. If the latter is given by curve *c*, on adding the ordinates to those of curve *a*, curve *d* is obtained; and similarly from curve *b* curve *e* is obtained.

Between two positive ions or two negative ions there will be an electrostatic repulsion, repre-

[1] Gurney, *Ions in Solution* (1936), Chapter 13.
[2] Hammett, J. Chem. Phys. 4, 613 (1936); J. Am. Chem. Soc. 59, 96 (1937).

sented by curve *f* in Fig. 1. But in some cases there are in addition strong exchange forces of attraction similar to the familiar forces between neutral atoms. In the diatomic molecules Na_2 and K_2 it is well recognized that the exchange forces of attraction are almost as simple as in the

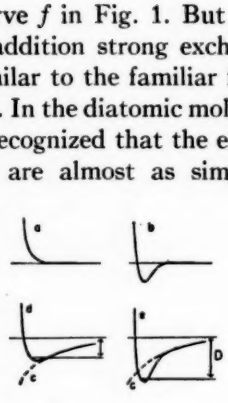

FIG. 1.

hydrogen molecule H_2, the single valence electron in each atom taking part. Consider now a singly charged calcium ion Ca^+; it has the same electronic configuration as the neutral atom of potassium, namely, with one 4*s* electron outside the core; only the charge on the atomic nucleus is one unit higher. If then we bring together two Ca^+ ions, exchange forces of attraction will be present. But, although two K atoms combine to form K_2, two Ca^+ ions will not in a vacuum combine to form $(Ca)_2^{++}$ owing to the electrostatic repulsion between the nuclear charges. If we had some means by which we could cut down the electrostatic repulsion without at the same time cutting down the strength of the exchange forces of attraction, there would be the possibility of obtaining such diatomic ions as $(Ca_2)^{++}$ and $(Hg_2)^{++}$ etc. Now a polar solvent has just the necessary properties. The orientation of the polar solvent molecules causes a large effective reduction in the Coulomb forces. Exchange forces, on the other hand, arise from the rapid circulation of electrons—motion which is so rapid that the heavy solvent molecules can make no response to it. If curve *f* in Fig. 1 represents the potential energy of a weak electrostatic repulsion, then on combining this with curve *b* we obtain curve *g*. In aqueous solution at room temperature the familiar $(Hg_2)^{++}$ ion must possess a potential minimum of this kind sufficiently deep for stability (confirmed by the presence of a Raman spectrum).

Similar exchange forces between halogen atoms give rise to the molecules F_2, Cl_2, Br_2 and I_2. Now the oxygen atom has one electron less than fluorine, and the atoms of sulphur, selenium and tellurium have one electron less than Cl, Br and I, respectively. The singly charged negative ions O^-, S^-, Se^- and Te^- have the same electronic configurations as the halogen atoms, and between any pair of these ions exchange forces of attraction will be present. In any solvent of high dielectric constant the electrostatic repulsion may be so small that diatomic ions with two negative charges are stable. As long ago as 1923 it was, in fact, discovered[3] that in aqueous solution at room temperature tellurium ions exist in the diatomic form $(Te_2)^{--}$.

§2

In the remainder of this paper we are concerned with the potential energy between ions bearing charges of opposite sign, for which curves *d* and *e* in Fig. 1 give the appropriate forms. Let the depth of the minimum of curve *e* be denoted by *D*. In curve *d* the depth of the potential minimum is due entirely to electrostatic forces of attraction; but in curve *e* these electrostatic forces are superimposed on curve *b*, which already has a potential minimum due to the nonelectrostatic forces. We may therefore write

$$D = D_{\text{nonelectrostatic}} + D_{\text{electrostatic}}. \qquad (1)$$

Species of ions for which the potential energy has the form of curve *d* in Fig. 1 may form short range ion pairs. It is only for species for which the potential energy has the form of curve *e* that we can draw a distinction between stable molecules in solution and ion pairs; the depth *D* of the minimum is the dissociation energy of the molecule in solution. The importance of separating this energy into the two parts $D = D_{\text{non}} + D_{\text{el}}$ lies in the fact that exchange forces between a pair of atoms or ions are characteristic of the species concerned and are independent of temperature; while D_{el} depends on the nature and temperature of the solvent. With rise of temperature the curve *c* of Fig. 1 becomes steeper, and the depth of the minimum becomes greater,

[3] Karsanowsky, Zeits. f. anorg. allgem. Chemie **128**, 17 (1923).

the increase in D being equal to the increase in D_{el}. In a solvent of dielectric constant K we shall not expect the increase in D_{el} to be strictly proportional to $1/K$ owing to the familiar electrical saturation of the dielectric in the neighborhood of each ion.

Although the methods of this paper are applicable to the dissociation of all species of molecules and molecular ions, the only types for which recent accurate data are available are acid molecules and ions, where a proton (or deuteron) is transferred from the solute to a solvent molecule; we shall accordingly discuss only these. Some years ago Wynne Jones[4] examined the data on the strength of acids in different solvents, and found that they grouped themselves, as we should expect, into three classes, according as the proton is transferred from (1) a neutral molecule, (2) a negative ion, such as $(H_2PO_4)^-$, or (3) a positive ion such as $(NH_4)^+$.

Since then successful attempts have been made to interpret the effects of polar substituents at room temperature.[5] Hammett[6] has also discussed the change of entropy with temperature, recognizing clearly the separate contributions from the electrostatic and nonelectrostatic forces.

To use the methods of statistical mechanics, we need, in addition to the potential energy, a knowledge of the energy levels of the protons. It is well known that in molecules such as HCl the spacing between the vibrational levels is so large that even at temperatures above room temperature practically all the molecules are in their lowest vibrational level. This is due to the small mass of the proton and will be true of the protons with which we shall be concerned here. Suppose first that in a vacuum we have a molecule of an organic acid ROOH and a water molecule side by side; in the ROOH molecule the proton is in a vibrational level inside the electron cloud of one of the oxygen atoms. The water molecule is capable of accommodating an additional proton, to form $(H_3O)^+$; i.e., in the water molecule is a set of vacant vibrational levels for a proton; we are concerned only with the lowest vibrational level of the set. If the vacant level in the H_2O molecule is higher than the initial occupied level, in order to transfer the proton from one to the other, a certain amount of work will be required. When the proton has been transferred, leaving behind a negative charge on the oxygen atom, an electrostatic field has been created in the surrounding vacuum, having a density of energy equal at every point to $E^2/8\pi$, where E is the intensity of the field; for a molecule in solution similar considerations will apply. The work required to complete the separation of the ions is entirely electrostatic, and D_{el} finally becomes equal to the integral of the energy in the field surrounding the negative ion added to the energy in the field surrounding the $(H_3O)^+$ ion. The latter part is of course the same for all acid molecules. From the usual Born formula,[7] for a molecule which dissociates into a pair of singly charged ions of radius b_+ and b_- we should, in the absence of electrical saturation have

$$D_{el}=\frac{\epsilon^2}{2K}\left(\frac{1}{b_+}+\frac{1}{b_-}\right). \qquad (2)$$

For a pair of small ions in water at room temperature (2) has a value in the neighborhood of 0.1 electron volt. To give the low degrees of dissociation of the familiar weak acids, values of D greater than 0.2 electron volts are required; for most species D_{non} is greater than D_{el}. (If the neutral acid molecule is surrounded by a certain field, because it is polar, the value of D_{el} will more strictly be the difference between the final and initial energies of the field.)

If we consider next processes of the type

$$\begin{aligned}(NH_4)^+ + H_2O &\rightarrow NH_3 + (H_3O)^+ \\ (C_6H_5NH_3)^+ + H_2O &\rightarrow C_6H_5NH_2 + (H_3O)^+\end{aligned} \qquad (3)$$

we see that they are different from the dissociation of a neutral molecule, because initially an electrostatic field exists round the positive ion, and the positive charge is merely transferred elsewhere. If the total energy of the field round the $(H_3O)^+$ ion is, for a particular species, the same as the total energy of the field initially surrounding the positive ion, the value of D_{el}

[4] Proc. Roy. Soc. **A140**, 448 (1933).
[5] Schwarzenbach and Egli, Helv. Chim. Acta **17**, 1183 (1934); Schwarzenbach and Epprecht. ibid **19**, 493 (1935).
[6] Hammett, reference 2, p. 101.
[7] Born, Zeits. f. Physik. **1**, 45 (1920); compare Hammett, reference 2, p. 102.

for this process will be zero. It will be convenient to name this an *isoelectric* transference of a proton. For dissociations similar to (3), even when they are not approximately isoelectric, the value of D_{el} will at any rate be much smaller than in those dissociations where we create a positive and a negative charge.

Intermediate between these two types lie dissociations like that of the glycine ion:

$$NH_3^+CH_2COOH+H_2O\rightarrow NH_3^+CH_2COO^-+H_3O^+. \quad (4)$$

As in (3) we begin with a positive ion, and end with a molecule which as a whole is electrically neutral, but which here bears opposite charges on its two ends; their electrostatic field may possess a considerable energy, though not, of course, as much as a pair of separate ions. The same applies to the other mode of dissociation of glycine:

$$H_2O+NH_2CH_2COO^-\rightarrow OH^-+NH_3^+CH_2COO^-. \quad (5)$$

In this case the electrostatic work of transferring the proton should be diminished by the negative charge already on the glycine ion, which will attract the proton. In (4) above the electrostatic work is diminished by the repulsion of the positive charge on the glycine ion; we expect then a smaller D_{el} than that for a neutral ROOH molecule, as already stated. On the other hand, in the dissociation of a negative ion, for example

$$(H_2PO_4)^-+H_2O\rightarrow(HPO_4)^=+H_3O^+ \quad (6)$$

we expect D_{el} to be greater than for a neutral molecule.

In the next section we shall examine the rate of variation of D with temperature for these four types of dissociation. We shall expect no correlation between this rate and the value of the total D. For a large or small value of D_{el} may be accompanied by a large or small D_{non}; and it is only D_{el} that changes. Over the range of temperature from 0°C to 60°C for which measurements are available, the dielectric constant of water falls from 88.31 to 66.62;[8] the value of $1/K$ rises from 0.01133 to 0.01502, that is, by 33 percent. If then the electrostatic energy were strictly proportional to $1/K$, the value of D_{el} would also increase by 33 percent. Though this will not be so, we must expect that dD/dT will be large when D_{el} is large, and small when D_{el} is small.

[8] Akerlof, J. Am. Chem. Soc. **58**, 1842 (1936).

§3

In expressing the dissociative equilibrium at temperature T, to ensure that the partition functions of the various particles are measured from the same zero of energy, the factor $e^{-D/kT}$ must be inserted. The relation between the activities of the positive and negative ions, a_+ and a_-, and the activity of the neutral molecule a, is then

$$a_+a_-/a=\mathbf{K}=Ce^{-D/kT}, \quad (7)$$

where the statistical factor C depends on the solvent only, and is the same for all solutes. (In the second dissociation of an acid an additional statistical factor $\frac{1}{4}$ enters.) For substances in aqueous solution at room temperature it is well known that for some species the dissociation constant $\mathbf{K}$ increases with rise of temperature, and for others falls. The description given here accounts for the characteristic behavior of each type. For (7) takes the form

$$-\ln \mathbf{K}/C=D_{non}/kT+D_{el}/kT. \quad (8)$$

For a dissociation which is approximately isoelectric the last term will be absent, and (8) is found to take the form

$$-\log \mathbf{K}=A/T+B, \quad (9)$$

where A and B are constants.[9] For neutral molecules, on the other hand, this will not be so. For five species of neutral molecule Harned and his co-workers find that the value of $\mathbf{K}$ passes through a maximum value at a certain temperature θ characteristic of each substance, and the variation of log $\mathbf{K}$ can in each case be represented approximately by a parabola

$$\log \mathbf{K}_{max}-\log \mathbf{K}=p(T-\theta)^2 \quad (10)$$

with the same value of p for all.[10] It will appear that this approximate regularity of behavior is due to the change in the dielectric constant of the water in which all the substances are dissolved.

[9] Pedersen, Dansk. Vidensk. Selsk. 14 (1937); also measurements for the $(NH_4)^+$ ion over the range from 5° to 45°C will be published shortly by Wynne Jones.

[10] Harned and Embree, J. Am. Chem. Soc. **56**, 1050 (1934).

Consider any two substances in aqueous solution at temperature T. Let their dissociation constants be $\mathbf{K}$ and $\mathbf{K}_r$, respectively; and at temperature T' let the values be $\mathbf{K}'$ and $\mathbf{K}_r'$. Then from (7) we shall have the equations

$$\begin{aligned} D'-D&=kT\ln\mathbf{K}-kT'\ln\mathbf{K}'\\ &\quad -kT\ln C+kT'\ln C',\\ D_r'-D_r&=kT\ln\mathbf{K}_r-kT'\ln\mathbf{K}_r'\\ &\quad -kT\ln C+kT'\ln C'. \end{aligned} \tag{11}$$

On subtracting the second from the first, we obtain

$$\begin{aligned} &(D'-D)-(D_r'-D_r)\\ &\quad =kT\ln(\mathbf{K}/\mathbf{K}_r)-kT'\ln(\mathbf{K}'/\mathbf{K}_r'). \end{aligned} \tag{12}$$

If now the dissociation to which $\mathbf{K}_r$ refers is nearly isoelectric, while the other is not, the value of $(D_r'-D_r)$ will be small compared with $(D'-D)$. The variation of $\mathbf{K}_r$ will be given by an expression of the form (9) above. If, taking the observed values of $\mathbf{K}$ for several other species of molecules, we substitute them in (12), we can obtain values of the change in D for each of them relative to a single reference substance (or relative to each other). This has been done for different types in Table I.[11] Similarly the relative values of dD/dT at 25°C have been obtained from the expression

$$(d/dT)(D-D_r)=(d/dT)(kT\ln(\mathbf{K}_r/\mathbf{K}) \tag{13}$$

using the empirical power series given in the original papers. Apart from the figures in the last column, the values have been calculated taking $\log\mathbf{K}_r=A/T+B$, with B equal to 0.614, the value found recently by Pedersen[9] for the anilinium ion. In the last column of the table are given for comparison values calculated taking B equal to 1.772, the value found by Pedersen for the *o*-chlor-anilinium ion.[12]

TABLE I.

	TEMP.	$(D'-D)-(D_r'-D_r)$ ELECTRON VOLTS	$(d/dT)(D-D_r)$ AT 25°C ε-VOLTS PER 1°C	
$(H_2PO_4)^-$	20°–50°C	0.0414 in 30°	13.1×10^{-4}	15.4×10^{-4}
Acetic acid	0°–60°	0.0662 in 60°	10.8	13.1
Glycine $\mathbf{K}_B$	10°–45°	0.0205 in 35°	5.5	7.8
Glycine $\mathbf{K}_A$	10°–40°	0.0126 in 30°	4.2	6.5
Anilinium		(0.00)	(0.0)	2.3

TABLE II.

	TEMP.	D IN ELECTRON VOLTS	dD/dT AT 25°C
$(H_2PO_4)^-$	50°C	0.534	15.3×10^{-4}
	0°	0.486	
Acetic acid	60°	0.433	13.0
	0°	0.353	
Glycine $\mathbf{K}_B$	45°	0.369	7.7
	10°	0.341	
Chloracetic acid	40°	0.289	10.5
	0°	0.247	
Glycine $\mathbf{K}_A$	40°	0.252	6.4
	10°	0.233	
H_3PO_4	50°	0.257	10.2
	0.3°	0.206	
Water *	60°	1.090	15.1
	0°	0.998	
HCl estimate †	25°	−0.31	—

* Harned and Hamer, J. Am. Chem. Soc. **55**, 2194 (1933).
† Ebert, Naturwiss. **13**, 393 (1925); Wynne Jones, J. Chem. Soc. 1064 (1930).

It will be seen that for the different types the values lie in the order predicted above. The most rapid variation with temperature is found for the negative ion $H_2PO_4^-$. Next comes the neutral molecule of acetic acid; and the values for the other similar acids fall here. Then the glycine values lie between acetic acid and the anilinium ion, as they should.

§4

As these results derived from (7) are satisfactory, we may discuss (7) further. When dissociation of a molecule or ion has taken place, the result is that the proton is now vibrating in the interior of a water molecule instead of in the interior of the original molecule or ion. In a solution we need to know the ratio of the number of available levels for the proton in the solvent molecules to the number of levels in the solute; this ratio determines the statistical equilibrium. As we are concerned only with the lowest vibrational level in each case, there is one level for the proton in each water molecule. The activities a_+ and a_- are usually expressed in moles per liter; since one liter of water contains 55.5 mole of water, the value to be assigned to the factor C in (7) according to the above simple scheme is 55.5 for the first dissociation of any acid. For the second dissociation of a dibasic

[11] I have not included values for the $(HSO_4)^-$ ion, derived from the measurements of Hamer (J. Am. Chem. Soc. **56**, 860 (1934)), because in Chicago I learned from Professor T. F. Young that a calorimetric measurement of the heat of dissociation had yielded a value twice as great as that given by Hamer; a still higher value has recently been published by Pitzer (J. Am. Chem. Soc. **59**, 2365 (1937)).

[12] Pedersen, Dansk. Vidensk. Selsk. 15 (1937).

acid, the value will be one-quarter of this, that is 13.9. As it seems worth while at least to explore the simplest assumptions, values of D calculated in this way from experimental values of $\mathbf{K}$ are given in Table II. If 55.5 is held to represent merely an upper limit to the number of available levels in the water molecules, each value of D in the table must be regarded as an upper limit.

It will be noticed that the values of dD/dT are almost identical with the corresponding values in the last column of Table I. The reason for this is that Pedersen's empirical expression for the *o*-chlor-anilinium ion, used above, may be written $\mathbf{K}=59.2e^{-D/kT}$. Or, in other words, use of the value $C=55.5$ is equivalent to expressing results relative to a reference $\mathbf{K}_r$ given by $\log \mathbf{K}_r=A/T+\log 55.5$.

Included in the table are values for the self-dissociation of water: $2H_2O \rightarrow H_3O^+ + OH^-$, which has the equilibrium

$$a_+a_-/a^2=e^{-D/kT}, \qquad (14)$$

where a^2 has been taken equal to $55.5^2=3080$. The very small dissociation of water must be due to the presence of a large D_{non}; there is no reason why D_{el} should be very different, since the dissociation produces a $(H_3O)^+$ ion and a negative ion, as from any neutral molecule. As we are taking the magnitude of dD/dT as a guide to the value of D_{el}, we expect the value of dD/dT for water to be similar to that for acetic acid, or a little larger, since the OH^- ion has a small radius and the energy of its electrostatic field may be somewhat larger than for a $(ROO)^-$ ion. It is satisfactory to see from Table II that this is so.

We have hitherto spoken of the dissociation energy D as if it were necessarily positive. There is, however, no difficulty in imagining a neutral acid molecule in which the energy level of the proton is higher than the vacant level in the solvent molecule. For such a substance in dilute solution nearly all the protons will have been transferred to solvent molecules, the small number remaining behind, to form acid molecules, being in accordance with the Boltzmann law. The electrostatic part of D is necessarily positive; but, when D_{non} has a large negative value, the total dissociation energy D may be negative.

TABLE III.

	$-\log \mathbf{K}$ at 25°	θ	dD/dT at 25°
(1)* H_3PO_4	2.123	−18.0°C	8.0×10^{-4}
(2) Glycine $\mathbf{K}_A$	2.350	+53.9	4.2
(3) Chloracetic acid	2.861	− 5.4	8.6
(4) Formic acid	3.752	+24.7	8.7
(5) Glycine $\mathbf{K}_B$	4.219	93.0	5.5
(6) Acetic acid	4.757	22.6	10.8
(7)† *n*-Butyric acid	4.817	8.0	11.7
(8) $(H_2PO_4)^-$	7.206	43.1	13.1

* Nims, J. Am. Chem. Soc. **56**, 1110 (1934).
† Harned and Sutherland, J. Am. Chem. Soc. **56**, 2040 (1934).

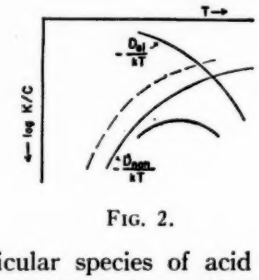

FIG. 2.

For a particular species of acid molecule the value of D may clearly be positive in one solvent and negative in another. For illustration a rough value of D for HCl in water has been included in Table II, based on estimates of $\mathbf{K}$.

§5

The variation of D_{el} with temperature is intimately connected with the characteristic temperature θ at which $\mathbf{K}$ becomes a maximum. As Table III shows, there is no correlation at all between the degree of dissociation of a substance and the value of θ assigned to it. The ideas outlined in this paper may therefore be subjected to a severe test by enquiring whether they account for these seemingly haphazard values.

When with rising temperature the value of $\mathbf{K}$ reaches a maximum, and begins to fall off, this is because the potential minimum of curve *e* in Fig. 1 is becoming rapidly deeper. Eq. (8) may be put into the form

$$-\log \mathbf{K}/C=A/T+f(T), \qquad (15)$$

where $A=D_{\text{non}}/k$, and $f(T)=D_{\text{el}}/kT$. In Fig. 2 the principal intersecting curves are intended to represent $-A/T$ and $-f(T)$, respectively, for a particular species of molecule, e.g., acetic acid. Adding the ordinates of these two curves, one obtains the lower curve with a maximum, which is Harned and Embree's parabola. The diagram shows clearly how the characteristic temperature θ, at which the maximum occurs, depends upon the relative magnitudes of the electrostatic

and nonelectrostatic parts of the dissociation energy. In comparing two different species of molecules, if we have nearly the same electrostatic forces but weaker exchange forces, a curve for D_{non}/kT like the broken line in Fig. 2 will be used for the latter. It is obvious that, on adding the ordinates, the maximum of the lower curve will be shifted upward and to the left; i.e. the substance will be more highly dissociated and the maximum will occur at a lower temperature. The behavior of phosphoric and chloracetic acids, relative to acetic acid, affords an illustration of this. Their values of **K** are respectively about 500 times and 100 times as large as for acetic acid, while θ lies below the freezing point; the values $-18°$ and $-5.4°$ have been assigned to them, respectively. If the high degree of dissociation were due mainly to weak electrostatic forces, θ would be *higher* than for acetic acid, as is clear from Fig. 2. But, as the dissociation creates a positive and a negative ion, we expect a normal D_{el}, and indeed the value of dD/dT shown in Table II indicates a value of D_{el} differing little from the other acids. The low value of D is therefore due to a small D_{non}, and the low value of θ is anticipated. On the other hand, for both dissociations of glycine we believe the electrostatic forces to be small. Their exceptionally high values of θ, namely 53° and 93°C are therefore satisfactory.

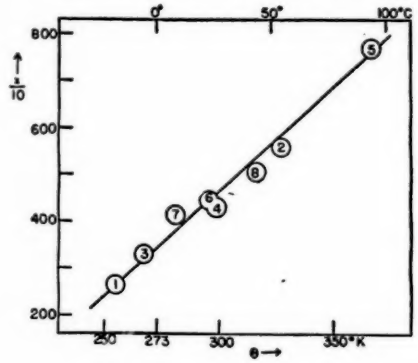

FIG. 3.

In the further dissociation of the $(H_2PO_4)^-$ ion we have strong electrostatic forces, and these by themselves would make the value of θ lower. The observed value of θ is, however, 43.1°, as compared with 22.6° for acetic acid. This is not in disagreement with the theory but affords additional evidence in its favor; for the value of **K** is some 300 times *smaller* than for acetic acid, showing the presence of a much larger D_{non}, which in Fig. 2 shifts the maximum of the curve downwards and to the right. This behavior may be contrasted with that of the bisulphate ion $(HSO_4)^-$; here, in spite of the large D_{el}, the value of **K** is nearly 1000 times *greater* than that of acetic acid; we should expect an exceptionally low value of θ; and, indeed, Harned assigned the value $-27.6°$ to it, a temperature lower than for any other substance investigated.

The value of θ for any substance thus depends upon the relative magnitudes of the two parts of the dissociation energy D_{non} and D_{el}. But it would perhaps be more convincing to express this in terms of experimental quantities, without mentioning D_{non} and D_{el}. Now for different species we have been taking the value of $(d/dT)(kT \ln (\mathbf{K}_r/\mathbf{K}))$ as a relative measure of D_{el}; and for different species the value of $\log \mathbf{K}$ is a relative measure of the total D. Suppose then that for each dissociation we define a quantity x by

$$x=(-\log \mathbf{K})/(dD/dT), \qquad (16)$$

both terms being taken at room temperature, then x is a measure of the ratio of D to D_{el}, and θ should be a smooth function of x (though it shows no correlation with either the numerator or the denominator taken separately). The success of this maneuver, shown in Fig. 3, is satisfactory. In the figure the numbering of the points corresponds to the numbering of the substances in Table III, where they are arranged in the order of $\log \mathbf{K}$. This treatment should have equal success for substances in nonaqueous solution, when sufficient data are available.

The simplified discussion given in these last two paragraphs is merely a step towards a more elaborate statistical treatment.

The Electrostatic Influence of Substituents on the Dissociation Constants of Organic Acids. I.

J. G. KIRKWOOD AND F. H. WESTHEIMER
Department of Chemistry, University of Chicago, Chicago, Illinois

(Received May 11, 1938)

Bjerrum's theory of the influence of substituents on dissociation constants has been extended and amplified. The molecules and ions entering into the ionization equilibria are treated as cavities of low dielectric constant, rather than as structureless regions of the same dielectric constant as the solvent. The theory gives better results than the simple Bjerrum formulation, especially for the short chain dicarboxylic acids, and in the fact that it permits a satisfactory treatment of the influence of dipolar substituents on dissociation constants.

I

THE ratio of the first to the second dissociation constant of a dibasic organic acid is always greater than four, and approaches four as the length of the acid is increased. In 1923 Bjerrum[1] suggested that the ratio of the dissociation constants can be accounted for by the combination of a statistical factor of four and the electrostatic effect of the negative charge of the acid-ion on the dissociation of the second hydrogen, and presented an approximate mathematical discussion. In this paper, following a consideration of the Bjerrum treatment, an extension of the electrostatic theory of dissociation constants will be developed.

A thermodynamic comparison of the dissociation constants K_1 and K_2 of two organic acids HA_1 and HA_2 in the same solvent leads to the following relation

$$RT \log K_1/K_2 = \bar{F}^\circ(HA_1) + \bar{F}^\circ(A_2^-) - \bar{F}^\circ(HA_2) - \bar{F}^\circ(A_1^-), \quad (1)$$

where $\bar{F}^\circ(HA_1)$, $\bar{F}^\circ(A_2^-)$, $\bar{F}^\circ(HA_2)$, and $\bar{F}^\circ(A_1^-)$ are the reference values of the chemical potentials of the respective solute species taken at infinite dilution in the solvent. From a molecular point of view, it is readily seen that $\bar{F}^\circ(HA_1) + \bar{F}^\circ(A_2^-) - \bar{F}^\circ(HA_2) - \bar{F}^\circ(A_1^-)$ is equal to $N\Delta w'$, where N is Avogadro's number and $\Delta w'$ is the average reversible work expended in the transfer of a proton from the carboxylate group of an ion A_2^- to the carboxylate group of an ion A_1^-, situated at an infinite distance from A_2^- in the given solvent. A part of $\Delta w'$ may be regarded as purely electrostatic in origin, that is, work done in moving the proton in the electric field produced by the average charge distributions of the two ions. We may denote this part by Δw. Another contribution arises from an entropy change associated with differences in molecular symmetry, and equal to $k \log [\sigma(HA_1)\sigma(A_2^-)/\sigma(A_1^-)\sigma(HA_2)]$ where $\sigma(HA_1)$, $\sigma(HA_2)$, $\sigma(A_1^-)$ and $\sigma(A_2^-)$ are the symmetry numbers of the respective particles. The symmetry number gives rise, in the ratio of the dissociation constants of a symmetrical dibasic acid, to the well-known statistical factor of four. Finally, and by no means to be overlooked, is the contribution to $\Delta w'$ associated with the intrinsic structure of the carboxyl group and carboxylate ion. However, if the two acids, HA_1 and HA_2, are, let us say, of the form R_1CH_2COOH and R_2CH_2COOH, and the possibility of structural resonance is absent, it is reasonable to suppose that the relatively distant substituent groups R_1 and R_2 will have little influence on the structure of the carboxyl group and carboxylate ion, except perhaps for an electrostatic polarization which may be taken into account in Δw, the electrostatic part of $\Delta w'$. Under these circumstances, the structural contributions to the work expended in detaching the proton from HA_2 will be canceled by a contribution of equal magnitude gained by attaching the proton to A_1^-. The net structural contribution to $\Delta w'$ is then zero, and we may write Eq. (1) in the form

$$RT \log K_1/\sigma K_2 = N\Delta w = 2.303RT\Delta pK$$
$$\Delta w = W(HA_1) + W(A_2^-) - W(HA_2) - W(A_1^-) \quad (2)$$
$$\sigma = \sigma(HA_1)\sigma(A_2^-)/\sigma(A_1^-)\sigma(HA_2),$$

[1] Bjerrum, Zeits. f. physik. Chemie **106**, 219 (1923); see Greenspan, Chem. Rev. **12**, 339 (1933).

where $W(HA_1)$, $W(A_2^-)$, $W(HA_2)$ and $W(A_1^-)$ are the electrostatic free energies of the respective molecules in the given solvent. The Bjerrum theory, in its most general form, is summarized by Eq. (2). Although Bjerrum developed his theory on the basis of a somewhat different argument, his fundamental assumption may be expressed in our terms, namely that the intrinsic structure of the carboxyl group and carboxylate ion is the same in the two acids. Although this assumption can certainly be no more than a close approximation to the facts, that it is essentially correct is supported by the observation that the dissociation constants of two aliphatic acids, R_1CH_2COOH and R_2CH_2COOH generally differ but slightly when R_1 and R_2 are nonpolar radicals.

If we are interested in a comparison of the first and second dissociation constants of a symmetrical dibasic acid, we are concerned with the molecular species H_2A, HA^-, $A^=$ and HA^-. Since the symmetry number ratios, $\sigma(H_2A)/\sigma(HA^-)$ and $\sigma(A^=)/\sigma(HA^-)$ each have the value two, the statistical factor becomes four, and Eq. (2) becomes

$$\begin{aligned} &RT \log K_1/4K_2 = N\Delta w = 2.303RT\Delta pK \\ &\Delta w = W(H_2A) + W(A^=) - 2W(HA^-). \end{aligned} \tag{3}$$

Bjerrum's approximation is obtained if Δw is set equal to the electrical work e^2/DR' required to bring the two charges, $-e$, of the acid ions, HA^- from infinity to their distance of separation, R', in the di-ion $A^=$, in a homogeneous medium having the solvent dielectric constant, D. This leads to results of fair accuracy[2] in the case of elongated straight chain dibasic acids, but with short molecules the values of R' obtained are, in some cases, only a fifth of that expected on the basis of structural considerations.

In the next section we shall describe a more refined calculation of Δw, which, although still somewhat schematic, avoids the treatment of the molecules and ions, in which the charges are imbedded, as structureless regions of dielectric constant D. Instead, we regard the molecules as forming cavities of low dielectric constant, D_i, in the solvent. Of course the introduction of an internal molecular dielectric constant D_i differing from unity is somewhat artificial. Nevertheless, its physical significance is clear, for it provides a crude means of allowing for the polarization of a molecule produced by the average charge distributions of polar or ionic substituent groups. A reasonable estimate of D_i for aliphatic compounds is about 2.00, a value in the neighborhood of the dielectric constant of the liquid paraffin hydrocarbons.

For certain purposes it is convenient to write Eq. (3) in the simple Bjerrum form, with the use of an effective dielectric constant, D_E, defined in terms of Δw, where the distance, R, is the separation of the protons in H_2A

$$\begin{aligned} &kT \log K_1/4K_2 = e^2/D_E R \\ &D_E = e^2/R\Delta w, \end{aligned} \tag{4}$$

rather than that of the negative charges in the di-ion $A^=$. This mode of expression was introduced by Eucken[3] from empirical considerations.

We shall also be concerned with a comparison of the dissociation constants of pairs of monocarboxylic acids similar in structure except for the presence of additional polar groups in one of them. As an example of such a pair, we may mention acetic and chloracetic acids. The statistical factor, σ, is evidently unity in these cases. If we adopt the notation of Eucken, using an effective dielectric constant, D_E, the appropriate form of Eq. (2) is

$$\begin{aligned} &kT \log K_1/K_2 = eM \cos\zeta/D_E R^2 = 2.303kT\Delta pK \\ &D_E = M \cos\zeta/R^2\Delta w, \end{aligned} \tag{5}$$

where M is the dipole moment of the polar group in the acid HA_1, R is the distance from the proton of the point dipole, and ζ its angle of inclination to the line joining it to the proton. We shall also make use of a more complicated form of Eq. (1) in which the charge distribution is not treated merely as a point dipole. Substitution of D, the dielectric constant of the solvent, for D_E leads, as Eucken showed, to calculated values of R as much as six times smaller than might be expected.

Perhaps the most serious approximation in our calculations of Δw which follow is the neglect of possible deviations of the local dielectric constant of the solvent in the neighborhood of a solute molecule from its macroscopic value, D. Such deviations might arise from electrical

[2] Gane and Ingold, J. Chem. Soc. 2153 (1931).

[3] Eucken, Zeits. f. angew. Chemie **45**, 203 (1932).

saturation, electrostriction, and other departures of the local density of the solvent from its bulk value. Ingold[4] has attempted to estimate corrections to the simple Bjerrum formula arising from electrical saturation and electrostriction. However, his calculations are based upon the Clausius-Mosotti equation, which is known to be invalid for polar liquids such as water. Further, even were the general method accurate the effect he calculated would be reduced to a fraction of the indicated magnitude if the solvent were excluded from the volume actually occupied by the molecule. It seems, then, entirely possible that he overestimates the importance of these effects. While the neglect of electrical saturation and electrostriction may lead to some inaccuracy, certainly the present treatment must be undertaken before finer adjustments are considered.

II

In order to calculate the electrostatic free energy of a spherical molecule of radius b, with an arbitrary charge distribution and immersed in a solvent of dielectric constant D, we make use of a formula developed by one of us in another connection.[5] A slightly different zero of energy is used here, since we have to consider changes of state involving the addition and removal of charges in the molecule.

$$W=\tfrac{1}{2}\sum_{k,l=1}^{\nu}\frac{e_k e_l}{D_i r_{kl}} +\tfrac{1}{2}\sum_{n=0}^{\infty}\frac{(D_i-D)(n+1)G_n}{D_i b^{2n+1}[(n+1)D+nD_i]} \quad (6)$$

$$G_n=\sum_{k=1}^{\nu}\sum_{l=1}^{\nu}e_k e_l r_k{}^n r_l{}^n P_n(\cos\vartheta_{kl}),$$

where the set of point charges $e_1\cdots e_i$ characterizes the average distribution of charge in the molecule, r_{kl} is the distance between the charges e_k and e_l, r_k and r_l the distances of e_k and e_l from the center of the sphere, and ϑ_{kl} the angle between r_k and r_l. The functions $P_n(\cos\vartheta_{kl})$ are the ordinary Legendre functions, and D_i is the internal dielectric constant of the molecule. If we consider the set of molecules HA_1, HA_2, A_1^- and A_2^- of equal radii b, in which A_1 contains the charges $e_1\cdots e_s$ in excess of those contained in A_2^-, a simple calculation shows that

$$\Delta w=\frac{e}{D_i}\sum_{k=1}^{s}\frac{e_s}{R_k} +\tfrac{1}{2}\left(\frac{1}{D}-\frac{1}{D_i}\right)\sum_{n=0}^{\infty}\frac{(n+1)\Delta G_n}{[(n+1)+nD_i/D]b^{2n+1}} \quad (7)$$

$$\Delta G_n=2er^n\sum_{k=1}^{s}e_k r_k{}^n P_n(\cos\vartheta_k),$$

where e is the protonic charge, R_k is the distance between e_k and the proton in HA_1, r and r_k are the lengths of the vectors joining the center of the sphere with the proton and the charge e_k, respectively, and ϑ_k the angle between r and r_k. We note that a similar formulation is possible when the excess of charge of A_1^- over A_2^- is continuously distributed with density ρ. If the ions are those involved in the first and second dissociation of a symmetrical dibasic acid, the charge distribution of the acid-ion HA^-, which corresponds to A_1^-, contains a proton in excess of that of $A^=$, which corresponds to A_2^-. If we denote by x the ratio $(r/b)^2$, where r is the distance of each proton in H_2A from the center of the spherical cavity of radius b, Eq. (7) becomes

$$\Delta w=\frac{e^2}{b}\left\{\frac{1}{D_i}\frac{1}{(2x(1-\cos\vartheta))^{\frac{1}{2}}} +\left(\frac{1}{D}-\frac{1}{D_i}\right)\sum_{n=0}^{\infty}\frac{(n+1)x^n P_n(\cos\vartheta)}{n+1+nD_i/D}\right., \quad (8)$$

where ϑ is the angle between the lines joining the two protons of H_2A to the center of the molecule. Unless we refer our calculation to the distance between the protons rather than the distance between negative charges in the ions, we neglect the effect of the carboxyl dipole. Although the sum in Eq. (8) may be expressed as a definite integral, an adequate approximation is obtained by expanding in powers of D_i/D, and neglecting all terms in powers of D_i/D higher than the first. Then, making use of the properties of the Legendre functions, the series involved may be summed. When the resulting expression is sub-

[4] Ingold, J. Chem. Soc. 2179 (1931).
[5] Kirkwood, J. Chem. Phys. **2**, 351 (1934).

stituted in Eq. (3), we obtain

$$\log_{10} K_1/4K_2=\frac{e^2}{2.303RkT}\left[\frac{f_1}{D}+\frac{f_2}{D_i}\right]$$

$$f_1=\frac{2(2x(1-\cos\vartheta))^{\frac{1}{2}}}{(1-2x\cos\vartheta+x^2)^{\frac{1}{2}}}-\frac{(2x(1-\cos\vartheta))^{\frac{1}{2}}}{x}$$

$$\times\log_e\frac{(1-2x\cos\vartheta+x^2)^{\frac{1}{2}}+x-\cos\vartheta}{1-\cos\vartheta}$$

$$f_2=1-\frac{(2x(1-\cos\vartheta))^{\frac{1}{2}}}{(1-2x\cos\vartheta+x^2)^{\frac{1}{2}}}$$

$$R=b(2x(1-\cos\vartheta))^{\frac{1}{2}}, \qquad (9)$$

where R is the distance between the protons in H_2A. If we make use of the notation of Eq. (4), in which an effective dielectric constant appears, we have

$$1/D_E=f_1/D+f_2/D_i. \qquad (10)$$

In Fig. 1 the values of D_E are shown for all values of $\sqrt{x}$ from zero to one, and for three values of $\cos\vartheta$, namely, -1, $-1/2$ and 0, corresponding to the cases in which the protons are on a diameter, placed at an angle, computed from the center, of 120°, and at right angles. D was taken as 78 for water at 25°; D_i was assigned the value 2.00. The effective dielectric constant rises, with increase of $\sqrt{x}$, from D_i when the charges are in the center of the sphere and $\sqrt{x}=0$ to values above the dielectric constant of water when the charges are on the edge of the sphere and $\sqrt{x}=1$. The fact that the effective

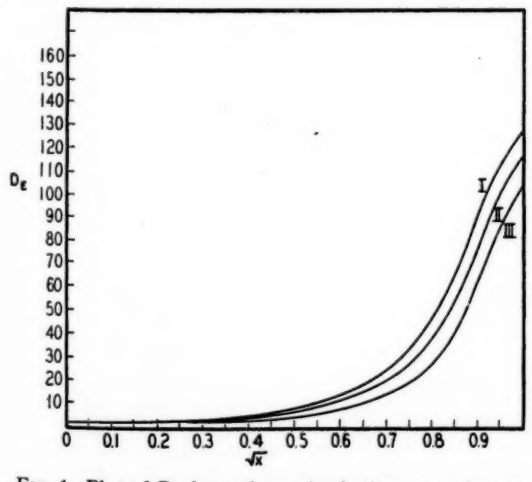

FIG. 1. Plot of D_E for a charged substituent against $\sqrt{x}$. In curve I $\cos\vartheta=-1$, in curve II $\cos\vartheta=-1/2$ and in curve III $\cos\vartheta=0$. D_i is 2.00 throughout.

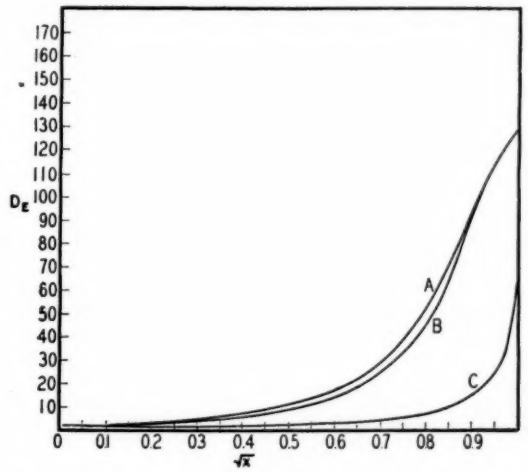

FIG. 2. Curve A, plot of D_E against $\sqrt{x}$ for a charged substituent with $D_i=2.50$. Curve B, same except $D_i=2.00$. Curve C, plot of D_E against $\sqrt{x}$ for a dipolar substituent. In all cases $\cos\vartheta=-1$.

dielectric constant is greater, at the edge of the sphere, than the dielectric constant of the medium may at first glance be surprising. This need cause no concern, for D_E is only a dielectric constant by convention, being so defined that our equations take on the simple Bjerrum form. The result is in no way dependent upon the approximation made when Eq. (8) was expanded in powers of D_i/D. In part IV of this paper, the sum in Eq. (8) is expressed as a definite integral, and the exact value of D_E for charges at the edge of a sphere and on a diameter obtained.

In the computation of D_E, no arbitrary parameters enter except the internal molecular dielectric constant, D_i. However, it is assigned a reasonable value, common to all aliphatic molecules, and is not readjusted to meet the demands of individual cases. Further, the value of D_E depends primarily upon the existence of a low internal dielectric constant, and only secondarily upon the exact value assigned to it. In Fig. 2, curve A was computed for charges on a diameter, with $D_i=2.5$, while curve B was computed for charges on a diameter, with $D_i=2.0$. The difference, while real, is small.

Besides the effect of substituents bearing a total net charge, we wish to determine the electrostatic free energy difference, Δw, when HA_1 contains a polar group in excess of HA_2. We may regard the dipole as two equal and opposite

charges, so placed and of such a magnitude that the product of charge by the distance of separation is equal to the dipole moment. Eq. (18) gives the value of Δw in this case. We can also regard the charge distribution as a point dipole. If we restrict our attention to those cases in which the dipole and proton both lie equidistant from the center on a diameter, then

$$\frac{1}{D_E}=\frac{1}{D_i}\left[1-\frac{4x^{\frac{1}{2}}}{(1+x)^2}\right]+\frac{1}{D}\left[\frac{8x^{\frac{1}{2}}}{(1+x)^2}+\frac{4x^{\frac{1}{2}}}{1+x}-\frac{4}{x^{\frac{1}{2}}}\log(1+x)\right], \quad (11)$$

where all the symbols have their usual significance. In Fig. 2, curve C is a plot of D_E, obtained from Eq. (11), against $\sqrt{x}$.

III

From the known dissociation constants of organic acids and Eqs. (4) and (5) an experimental value of D_E can be obtained for the cases in which HA_1 differs from HA_2 either by a charged or by a dipolar substituent. With charged substituents, D_E varies from 15 to about the dielectric constant of water, with dipolar substituents from about 3 to about 10; in both cases D_E is greater for greater values of r/b. For values of r/b between 0.5 and 0.9 which correspond to actual molecules, Figs. 1 and 2 show that D_E, obtained by our theoretical treatment, varies in a similar manner. We note that the effective dielectric constant is much smaller for a dipolar than for a charged substituent at the same value of r/b.[6] In this section we wish to present the computations for the application of our equations to a few simple cases.

The exact location of the proton in the carboxyl group is still open to question. Available evidence[7] seems to favor a double potential energy minimum for the proton adjacent to each of the oxygen atoms, at approximately the position of the proton in the normal O−H bond. To avoid undue complications in the calculations, we shall adopt the extended chain model, and conventionally place the proton on the extension of the bond between the carboxyl carbon atom and its nearest carbon neighbor. Some convention, of which this is the most convenient is necessary solely for the purpose of estimating ϑ, the angle between the lines joining the protons to the center.

The selection of a structural distance between the protons of a dicarboxylic acid for comparison with the value computed from the dissociation constant ratio is further complicated by present ignorance relative to internal rotations in the molecule. We obtain a probable upper limit for the structural distance by using the extended chain model with the proton conventionally located at a distance of 1.45A from the respective carboxyl carbon atoms on the extensions of the terminal carbon to carbon bonds. The distance of 1.45A is actually the greatest distance of the projection of the proton on the extension of the terminal carbon-carbon bond, when attached to either oxygen at the covalent distance 0.94A and with an angle of 90° between the C−O and O−H bonds. For the purpose of comparison we have also calculated the root mean square separation of the protons on the basis of free rotation. In this computation, we have employed the following formula for the mean square distance $\bar{R}_n^2$ between the terminal atoms in a chain containing n bonds[8]

$$\bar{R}_n^2=\sum_{k=1}^{n} l_k^2+2\sum_{k=1}^{n}\sum_{s=1}^{k-1} l_k l_s \prod_{m=s}^{k-1}\eta_{m,\,m-1},$$

where $\eta_{m,\,m-1}$ is the cosine of the supplement of the angle between the m and $m-1$ bonds, and l_k is the length of the k'th bond. We are aware of the fact that the free rotation value does not provide an absolute lower bound for the average structural distance. However, it is not unreasonable to suppose that the average structural separation of the protons lies between the extended chain and the free rotation value. In Table I we have presented the data for a few acids which are at least approximately spherical. It is seen that the distance computed from the

[6] Smallwood [J. Am. Chem. Soc. **54**, 3048 (1932)] has shown by means of a Born cycle that D_E will be unity if certain cancellations in the free energies of solvation, from the hypothetical gaseous state, of the acids and ions occur.

[7] See Price and Evans, Proc. Roy. Soc. **A162**, 110 (1937).

[8] A special case of the formula developed by Eyring, Phys. Rev. **39**, 746 (1932). It is worth while pointing out that for the above formula to be valid, free rotation is not actually necessary. The only requirement is that the mean values of cos φ and sin φ vanish for adjacent bonds, φ being the angle specifying the projection of the $i+1$'th bond on a plane perpendicular to the i'th bond. This may occur even if the rotation is highly inhibited.

TABLE I. *Separation of protons in dicarboxylic acids.* Distance in A.*

ACID	MAXIMUM	FREE ROTATION	THIS PAPER	BJERRUM
Oxalic acid	4.44	3.50	3.85	0.91
Dimethyl malonic acid	4.87	4.12	4.15	1.34
Tetramethyl succinic acid	6.66	4.66	4.80	0.96

* The values in column 4 are given to the nearest 0.05A. Since the computed values of R in Table I refer to a single configuration of the molecule, they are not strictly suitable for comparison with mean distances calculated on the basis of free or inhibited internal rotation. Nevertheless, we have stated the maximum and free rotation distances in order to exhibit a possible range of variation of the interprotonic distance in the acids. With internal rotation, we should properly compute an average value of ΔpK over all internal configurations for comparison with the experimental value. Such a calculation is very tedious and does not seem worth while on the basis of free rotation, since in actual molecules the rotation is doubtless inhibited. We are unable to make the calculation for inhibited rotation, until future information about the hindering torques becomes available.

dissociation constant ratio by means of our equation do actually fall between the suggested limits, while the values computed with the simple Bjerrum formula lie considerably below the free rotation value and are almost certainly too small on any basis. We remark that the Bjerrum formula is by no means as unsatisfactory for the longer chain acids. We have selected for discussion a group of short chain acids the shapes of which roughly approximate spheres, since it is in these cases that the Bjerrum theory needs refinement. In a later paper, we shall develop a formula, on the basis of an ellipsoidal model, which passes asymptotically into the simple Bjerrum formula as the chain length increases. A knowledge of the torques hindering internal rotation would permit a more exact application of our formulas involving a calculation of the average value of ΔpK over all internal configurations of the acids and ions.

For these computations it was necessary to estimate the radii of the spheres. In the absence of specific information, we have fallen back on Traube's rule.[9] The partial molar volume of dimethyl malonic acid in water, then, is about 99.1 cc, and the diameter of the molecule, considered as a sphere, is 6.77A. Further, since we have decided, conventionally, to place the protons on the extensions of the terminal carbon to carbon bonds, we may assign the angle $\cos\vartheta=-0.333$ to the lines joining the protons to the center. From Eq. (4) we obtain

$$\sqrt{x}D_E=\frac{e^2}{2.303bkT\Delta pK(2(1-\cos\vartheta))^{\frac{1}{2}}},$$
$$r/b=\sqrt{x}.$$

[9] Traube, Saml. chem. chem-tech.. Vortr. **4**, 255 (1899).

Substituting the value of 2.29 for ΔpK for dimethyl malonic acid found by Gane and Ingold[2] in this expression, we find $\sqrt{x}D_E$ equal to 19.1. Values of $\sqrt{x}D_E$ computed with the aid of Eq. (10) are given in Table II for varying $\sqrt{x}$ and $\cos\vartheta$. Using this table, the value of $\sqrt{x}$ can be obtained in any particular case by linear interpolation. The computations for the other acids were carried out in a similar fashion, again using the data of Gane and Ingold. The angle between the protons for oxalic and tetramethyl succinic acids was chosen as 180°.

As an example of the effect of a simple dipolar substituent we present the computations for the ratio of the dissociation constant of acetic to chloracetic acids. Since the molecule does not approach a true sphere, we arbitrarily placed the center at the midpoint of the line joining the proton with the midpoint of the carbon-chlorine bond. We employed the value 1.56×10^{-18} e.s.u. for the dipole moment of the C−Cl bond;[10] the values of the dissociation constants of acetic and chloracetic acids were taken from Landholt-Börnstein.[11] The data for chloracetic acid are given in Table III. Other calculations have shown that, in chloracetic acid, the acidity is relatively little effected by multipole moments of higher order than the second.

Finally we may mention that, in common with the previous electrostatic theories of dissociation, the temperature coefficients experimentally determined[12] do not agree with those calculated, on the basis of a constant value of R. Although a real variation of the average value of R with

TABLE II. *Values of* $\sqrt{x}D_E(x)$.

$\sqrt{x}$	$\cos\vartheta=-1$	$\cos\vartheta=-\frac{1}{3}$	$\cos\vartheta=0$
0.00	0.00	0.00	0.00
0.10	0.25	0.24	0.23
.20	0.64	0.60	0.55
.30	1.31	1.16	1.02
.40	2.45	2.11	1.76
.50	4.59	3.82	3.02
.60	8.79	7.15	5.42
.70	17.6	14.2	10.6
.80	37.5	30.9	23.3
.90	79.2	68.9	56.4
.95	106.6	96.3	83.2
1.00	127.0	116.3	103.5

[10] Smyth, Am. Chem. Soc. Symposium on Molecular Structure, p. 209 (1937).

[11] Landholt-Börnstein, *Physikalische-Chemische Tabellen*, Eg IIIc.

[12] Jones and Soper, J. Chem. Soc. 133 (1936).

TABLE III. *Distance between proton and dipole in chloracetic acid in A.*

MAXIMUM	FREE ROTATION	MINIMUM	THIS PAPER	BJERRUM
3.39	2.99	1.84	2.90	0.55

temperature is not unlikely, it may be that a more refined theory is necessary before accurate estimates of temperature coefficients can be made. In any case, the temperature coefficients are not large.

IV

In this section we shall present some of the mathematical details omitted earlier in the paper. Eq. (7) may be written in the following form.

$$\Delta w = e\sum_{k=1}^{s} e_k H_k$$

$$H_k = \frac{1}{D_i R_k} + \frac{1}{b}\left(\frac{1}{D} - \frac{1}{D_i}\right) S(x_k, \cos\vartheta_k) \quad (12)$$

$$S(x, \alpha) = \sum_{n=0}^{\infty} \frac{(n+1)x^n P_n(\alpha)}{1+n(1+\omega)},$$

where x_k is equal to rr_k/b^2 and ω is the ratio, D_i/D. From the properties of the Legendre functions, we may write

$$S_0(t, \alpha) = \sum_{n=0}^{\infty} t^n P_n(\alpha) = \frac{1}{(1-2\alpha t+t^2)^{\frac{1}{2}}}. \quad (13)$$

It is readily verified that $S(x, \alpha)$ may be expressed in the form

$$S(x, \alpha) = \frac{\partial}{\partial x}\left[x^{\omega/(1+\omega)} \int_0^{x^{1/(1+\omega)}} S_0(t^{1+\omega}, \alpha) dt\right]. \quad (14)$$

Simplification of Eq. (14) leads to

$$S(x, \alpha) = \frac{1}{1+\omega}\left\{S_0(x, \alpha) + \frac{\omega}{1+\omega} S_1(x, \alpha)\right\}$$

$$S_1(x, \alpha) = x^{-1/(1+\omega)} \int_0^x t^{-\omega/(1+\omega)} \times [1-2\alpha t+t^2]^{-\frac{1}{2}} dt. \quad (15)$$

Expansion in powers of ω with the neglect of terms in ω^2 gives

$$S(x, \alpha) = So(x, \alpha) + \omega[S_1^0(x, \alpha) - So(x, \alpha)]$$

$$S_1^0(x, \alpha) = \frac{1}{x} \log\left[\frac{(1-2x+x^2)^{\frac{1}{2}} + x - \alpha}{1-\alpha}\right]. \quad (16)$$

Evaluation of $S_1(x, \alpha)$ by graphical quadrature shows that the expansion (16) is adequate in all cases of interest although D_E calculated from (10) is 2 percent high at $x=1$. Substitution in Eq. (12) gives

$$H_k = \frac{1}{Db}\left\{2[1-2x_k\cos\vartheta_k + x_k^2]^{-\frac{1}{2}} - \frac{1}{x_k}\log\left[\frac{(1-2x_k\cos\vartheta_k+x_k^2)^{\frac{1}{2}} + x_k - \cos\vartheta_k}{1-\cos\vartheta_k}\right]\right\} + \frac{1}{D_i}\left\{\frac{1}{R_k} - \frac{1}{b}[1-2x_k\cos\vartheta_k + x_k^2]^{-\frac{1}{2}}\right\}. \quad (17)$$

Eq. (9) for the symmetrical dibasic acid follows at once from Eqs. (12) and (17), only one term occurring in the sum of Eq. (12). For a dipolar distribution consisting of two point charges $+e$, and $-e$, Eq. (12) takes the form

$$\Delta w = e^2[H_+ - H_-], \quad (18)$$

where H_+ and H_- are to be computed from Eq. (17) for the respective charges. We note that H_k may be regarded as a function $H(\mathbf{r}_k, \mathbf{r})$ where $\mathbf{r}_k$ and $\mathbf{r}$ are the vectors extending from the center of HA_2 to the charge k and the carboxyl proton, respectively. Thus for a point dipole, we may write

$$\Delta w = e\mathbf{M}\cdot\nabla_1 H(\mathbf{r}_1, \mathbf{r}), \quad (19)$$

where $\mathbf{M}$ is the vector moment and ∇_1 the gradient operator associated with the position $\mathbf{r}_1$ of the dipole. The general expression is rather complicated and will not be given. However, for a molecule in which the proton and dipole are located on a diameter, Eqs. (17) and (19) yield Eq. (11) of Section II.

The Electrostatic Influence of Substituents on the Dissociation Constants of Organic Acids. II.

F. H. WESTHEIMER AND J. G. KIRKWOOD
University of Chicago, Chicago, Illinois

(Received June 4, 1938)

The theory of the influence of substituents on dissociation constants presented in an earlier article of the same title is extended to acids ellipsoidal in shape. Bjerrum's formula is obtained in the limiting case of unit eccentricity of the elliptical section of a prolate ellipsoid of revolution. The influence of dipolar as well as ionic substituents can satisfactorily be treated.

I

IT has been proposed by Bjerrum[1] that the influence of a polar substituent on the dissociation constant of an organic acid is primarily electrostatic in origin. On the basis of this hypothesis, the ratio of the dissociation constants of two similarly constituted acids may be calculated from electrostatic work necessary to transfer a proton from the first acid to the ion of the second. Because of the fruitfulness of Bjerrum's idea, we considered it desirable to introduce certain refinements into the calculation of the work of transfer. In a previous article, we showed[2] that the electrostatic work is dependent not only upon the charges present and the distance between them, but also upon the shape of the molecule and upon the positions of the charges. We have already presented the equations for a spherical model, and have applied them to several aliphatic acids which approximate a sphere in shape. In the present paper, similar considerations lead to the equations for an ellipisod of revolution, a model well fitted to treat the longer aliphatic dibasic acids.

We are concerned with four ellipsoids, representing the molecular species HA_1, A_1^-, HA_2 and A_2^-. For the sake of simplicity, we have assumed that the protons of the carboxyl group and the dipoles in the molecules lie on the line connecting the foci of the ellipsoid, and, in the actual computations, have further assumed that the charges are actually at the foci, although this latter limitation is not inherent in the equations developed. In the present discussion, it is convenient to use confocal elliptical coordinates. If r_1 and r_2 are the distances of a point from the two foci, and R the distance between the foci, then $\lambda=(r_1+r_2)/R$, $\mu=(r_1-r_2)/R$, and φ is the angle by which the point has been rotated past a fixed plane through the major axis. Since we have chosen an ellipsoid of revolution with all charges on the major axis, the model is axially symmetrical and the angle φ does not enter the formulation.

Following the same reasoning advanced for the spherical model, we approximate the total free energy increment in the reaction $HA_1+A_2^- \rightleftarrows HA_2+A_1^-$ by the sum of the electrostatic contribution, Δw, and the symmetry contribution RT log σ, where σ is the statistical factor, equal to four for symmetrical dibasic acids.

$$kT \log K_1/\sigma K_2 = 2.303\, kT\Delta pK = \Delta w$$
$$\Delta W = W(HA_1)+W(A_2^-) - W(HA_2) - W(A_1^-), \quad (1)$$

where $W(HA_1)$, $W(A_2^-)$, $W(HA_2)$ and $W(A_1^-)$ are the electrostatic free energies of the respective molecular species. In order to determine the electrostatic work, Δw, it is first necessary to solve Laplace's equation in confocal elliptical coordinates. Then, from the electrostatic potential of the charges, the electrostatic work

TABLE I. *Effective dielectric constant for varying* λ_0.

λ_0	D_E (CHARGE)	D_E (DIPOLE)
2.3	7.8	2.7
2.0	11.2	3.3
1.8	15.5	4.0
1.6	25.3	5.7
1.4	51.	11.2
1.3	74.	20.4
1.2	94.	49.
1.1	94.	90.
1.0	78.	78.

[1] Bjerrum, Zeits. f. physik. Chemie **106**, 219 (1923).
[2] Kirkwood and Westheimer, J. Chem. Phys. **6**, 506 (1938).

can be computed. The actual mathematical treatment is presented in Part III of this paper. In that section it will be shown that, if HA_1 differs from HA_2 by a protonic charge, then

$$\Delta pK=\frac{e^2}{2.303kTR}\times\left\{\frac{1}{D_i}+\left(\frac{1}{D}-\frac{1}{D_i}\right)\sum_{n=0}^{\infty}\frac{U_n}{1+(D_i/D)C_n}\right\} \quad (2)$$

$$U_n=(2n+1)\frac{Q_n(\lambda_0)}{P_n(\lambda_0)}(-1)^n$$

$$C_n=\frac{\lambda_0-P_{n-1}(\lambda_0)/P_n(\lambda_0)}{\lambda_0-Q_{n-1}(\lambda_0)/Q_n(\lambda_0)}.$$

Further, if HA_1 differs from HA_2 by a point dipole of moment M inclined at an angle ζ to the major axis of the ellipsoid, then

$$\Delta pK=\frac{eM\cos\zeta}{2.303kTR^2}\times\left\{\frac{1}{D_i}+\left(\frac{1}{D}-\frac{1}{D_i}\right)\sum_{n=0}^{\infty}\frac{Y_n}{1+(D_i/D)C_n}\right\} \quad (3)$$

$$Y_n=n(n+1)(2n+1)\frac{Q_n(\lambda_0)}{P_n(\lambda_0)}(-1)^n.$$

In these formulas, P_n represents a Legendre function of the first kind, D is the dielectric constant of the solvent, D_i the internal molecular dielectric constant[2] and $\lambda=\lambda_0$ is the equation of the ellipsoidal cavity in the solvent created by the molecule.

Q_n represents a Legendre function of the second kind; Q_0 and Q_1 are given by the equations

$$Q_0(\lambda)=\tfrac{1}{2}\log_e\frac{\lambda+1}{\lambda-1}$$

$$Q_1(\lambda)=\frac{\lambda}{2}\log_e\frac{\lambda+1}{\lambda-1}-1$$

and the rest can be obtained from the first two by means of the recursion formula,

$$(n+1)Q_{n+1}(\lambda)=(2n+1)Q_n(\lambda)-nQ_{n-1}(\lambda).$$

As in the previous article, an effective dielectric constant, D_E, is defined in terms of the Bjerrum equation.[1, 3] For the case in which HA_1 has a charge in excess of HA_2,

$$\Delta pK=e^2/2.303D_ERkT \quad (4)$$

and in the case in which HA_1 contains a dipole in excess of HA_2

$$\Delta pK=eM\cos\zeta/2.303D_ER^2kT. \quad (5)$$

In Table I the values of D_E accurate to 1 percent for molecules in water at 25° computed from Eqs. (2), (3), (4) and (5) for both dipolar and charged substituents are recorded for typical values of λ_0. D_i, as previously, has been set equal to 2.00.

In Fig. 1, D_E has been plotted against λ_0. At large values of λ_0 the charges are brought close together in the medium of low dielectric constant, and D_E approaches the internal molecular dielectric constant D_i. On the other hand, as λ_0 decreases toward 1, the ellipsoid thins out into a rod, and at λ_0 equal to 1 disappears altogether, leaving the charges immersed only in the solvent. As in the spherical case, the values of the effective dielectric constant depends primarily upon the existence of a low internal dielectric constant, only secondarily upon its exact value.

With the ellipsoid as with the sphere, values of D_E greater than the dielectric constant of the solvent are obtained. With the ellipsoid, how-

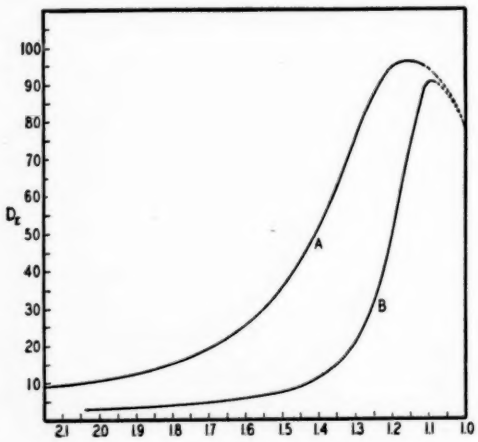

FIG. 1. Curve A is the plot of D_E for a charged substituent against λ_0, curve B is the plot for a dipolar substituent. The slope of the curves at $\lambda_0=1$ has not been determined.

[3] Eucken, Zeits. f. angew. Chemie **45**, 203 (1932).

ever, since the effective dielectric constant must approach D as the ellipsoid vanishes, the values of D_E go through a maximum.

Here again our theoretical treatment is in agreement with the experimental fact that, for the same value of λ_0 the effective dielectric constant is much greater in the case in which the substituent is charged than in the case in which the substituent contains a dipole.

II

The equations presented in Part I will now be applied to some actual molecules which approximate an ellipsoid of revolution. We have compared the first and second dissociation constants of three dicarboxylic acids, succinic, glutaric and suberic, and have compared the dissociation constants of chloracetic acid and of β-chlorporpionic acid with the dissociation constants of the corresponding unsubstituted acids. Chloracetic acid, intermediate in shape between a sphere and an ellipsoid, has been treated by both methods. In order to fix the boundries of the molecules, we have again estimated the partial molar volume in aqueous solution from Traube's rule,[4] and have made use of the following equation relating λ_0, R, and the molecular volume, V, of an ellipsoid of revolution:

$$\lambda_0^3-\lambda_0=(6/\pi)(V/R^3). \qquad (6)$$

This equation must be solved simultaneously with Eqs. (4) and (5) and with Fig. 1 to obtain the value of R in particular cases. We note that

$$\frac{D_E\ (\text{charge})}{(\lambda_0^3-\lambda_0)^{\frac{1}{3}}}=\frac{e^2}{2.303kT\Delta pK}\left(\frac{\pi}{6V}\right)^{\frac{1}{3}}$$

and

$$\frac{D_E\ (\text{dipole})}{(\lambda_0^3-\lambda_0)^{\frac{2}{3}}}=\frac{eM\cos\zeta}{2.303kT\Delta pK}\left(\frac{\pi}{6V}\right)^{\frac{2}{3}}.$$

We have prepared a table of D_E (charge)/$(\lambda_0^3-\lambda_0)^{\frac{1}{3}}$ and D_E (dipole)/$(\lambda_0^3-\lambda_0)^{\frac{2}{3}}$ for various values of λ_0 and can, then, estimate the value of λ_0 for any particular case by linear interpolation. From this value of λ_0 and Eq. (6), R is easily obtained. These values are presented in Table II. The values of R, computed for the acids selected, with the aid of Table II, are presented in Table III.

[4] Traube, Saml. chem. chem-tech., Vortr. **4**, 255 (1899).

TABLE II.

λ_0	D_E (CHARGE)/$(\lambda_0^3-\lambda_0)^{\frac{1}{3}}$	D_E (DIPOLE)/$(\lambda_0^3-\lambda_0)^{\frac{2}{3}}$
2.3	3.6	0.60
2.0	6.1	0.99
1.8	9.7	1.58
1.6	18.7	3.1
1.4	46.	9.2
1.3	77.	22.0
1.2	117.	74.
1.1	154.	239.
1.0	∞	∞

TABLE III. *R in* A.

ACID	ΔpK	MAXIMUM	FREE ROTATION	THIS PAPER*	BJERRUM
Succinic acid	0.77	6.66	4.66	5.85	3.99
Glutaric acid	0.47	7.39	5.15	7.00	6.53
Suberic acid	0.28	11.46	6.38	9.30	10.9
Chloracetic acid	1.90	3.39	2.99	2.90	0.55
β-Chlorpropionic acid	0.85	4.61	3.69	4.20	1.06

* The values of R in this column are given to the nearest 0.05A. For the chloracids, ζ was computed as the angle between the carbon-chlorine bond and the line joining the midpoint of this bond with the point of location of the proton on the extension of the terminal carbon-carbon bond into the carboxyl group. The values of cos ζ are 0.59 and 0.94 for chloracetic and β-chlorpropionic, respectively. The carbon-chlorine bond moment was taken as 1.56 Debye units.

Since the computed values of R in Table III refer to a single configuration of the molecule, they are not strictly suitable for comparison with the mean distances calculated on the basis of free or inhibited rotations. Here, as in the previous paper,[2] we have stated the maximum and the free rotation distances in order to exhibit a possible range of variation of the interprotonic distance. The values of ΔpK were taken from Landholt-Börnstein.[5]

It is at once seen that both the Bjerrum formula and the present treatment give reasonable values for the long aliphatic dibasic acids. The advantage of the present treatment over the simple Bjerrum approximation is most clearly exemplified in the cases of the chloro-acids.

The approximations and possible sources of error involved in this formulation have been discussed in the previous paper.[2] They include neglect of electrical saturation and electrostriction, the use of an internal molecular dielectric constant, the use of Traube's rule, and

[5] Landholt-Börnstein, *Physikalische-Chemische Tabellen*, Erg. IIIc.

the difficulty in obtaining a structural value of R with which to compare our value, due to present ignorance concerning rotation in polyatomic molecules in aqueous solution. We are further limited by the fact that we have placed the charges or dipoles at the foci of the ellipsoid.

III

In the third part of this paper, we wish to derive the equations presented in Part I. Laplace's equation, in confocal elliptical coordinates for an axially symmetric potential ψ, is

$$(\lambda^2-1)\frac{\partial^2\psi}{\partial\lambda^2}+2\lambda\frac{\partial\psi}{\partial\lambda}+(1-\mu^2)\frac{\partial\psi}{\partial\mu^2}-2\mu\frac{\partial\psi}{\partial\mu}=0. \quad (7)$$

This equation must be satisfied both inside and outside the ellipsoid, λ_0, forming the boundary between the molecule of dielectric constant D_i and the solvent of dielectric constant D. The potential ψ_i in the interior of the molecule, satisfying Eq. (7) may be written as follows

$$\psi_i=\frac{1}{D_i}\sum_{k=1}^{\nu}\frac{e_k}{|r-r_k|}+\sum_{n=0}^{\infty}B_nP_n(\mu)P_n(\lambda), \quad (8)$$

where the B_n are constants, ψ_i having no singularities except at the positions of the point charges $e_1\cdots e_2$, characterizing the average charge distribution of the molecule. Since the potential must vanish at an infinite distance from the molecule, the solution, ψ_e, of Eq. (7) outside the boundary ellipsoid may be expressed in the form

$$\psi_e=\sum_{n=0}^{\infty}A_nP_n(\mu)Q_n(\lambda), \quad (9)$$

where the P_n and Q_n are the Legendre functions of the first and second kinds, respectively. The boundary conditions namely, continuity of the potential and of the normal component of the dielectric displacement everywhere on the boundary ellipsoid, λ_0, require the following relations to be satisfied.

$$\psi_i(\lambda_0,\mu)=\psi_e(\lambda_0,\mu) \qquad -1\leq\mu\leq+1$$
$$D_i\left(\frac{\partial\psi_i}{\partial\lambda}\right)_{\lambda=\lambda_0}=D\left(\frac{\partial\psi_e}{\partial\lambda}\right)_{\lambda=\lambda_0}. \quad (10)$$

Before applying the boundary condition we introduce into Eq. (8) the Neumann expansion for each of the terms $1/|r-r_k|$

$$\sum_{k=1}^{\nu}\frac{e_k}{|r-r_k|}=\frac{2}{R}\sum_{n=0}^{\infty}(2n+1)\beta_nP_n(\mu)Q_n(\lambda) \quad (11)$$
$$\beta_n=\sum_{k=1}^{\nu}e_kP_n(\mu_k)$$

valid when each charge e_k is situated at a point μ_k on the ellipse, $\lambda=1$, which is the line joining the foci. R is the distance between the foci. Substitution of (8) and (9) into Eq. (10) and use of the property of orthogonality of the $P_n(\mu)$ in the interval, $-1\leq\mu\leq+1$, yields the following set of linear equations for the determination of the A_n and B_n

$$(2/R)(2n+1)(\beta_n/D_i)Q_n(\lambda_0)+B_nP_n(\lambda_0)=A_nQ_n(\lambda_0)$$
$$D_iB_nP_n'(\lambda_0)+(2/R)(2n+1)\beta_nQ_n'(\lambda_0)=DA_nQ_n'(\lambda_0). \quad (12)$$

Solution gives the following expression for the B_n

$$B_n=\frac{2(2n+1)\beta_n}{R}\left(\frac{1}{D}-\frac{1}{D_i}\right)\times\frac{Q_n(\lambda_0)Q_n'(\lambda_0)}{P_n(\lambda_0)Q_n'(\lambda_0)-(D_i/D)P_n'(\lambda_0)Q_n(\lambda_0)}, \quad (13)$$

where $P_n'(\lambda_0)$ and $Q_n'(\lambda_0)$ are the first derivatives of the Legendre functions. The derivatives may be eliminated with the aid of the recursion formula,

$$(\lambda^2-1)P_n'(\lambda)=n[\lambda P_n(\lambda)-P_{n-1}(\lambda)]$$
$$B_n=\frac{2(2n+1)\beta_n}{R}\left(\frac{1}{D}-\frac{1}{D_i}\right)\frac{Q_n(\lambda_0)}{P_n(\lambda_0)}\times\left[1+\left(\frac{D_i}{D}\right)\frac{\lambda_0-P_{n-1}(\lambda_0)/P_n(\lambda_0)}{\lambda_0-Q_{n-1}(\lambda_0)/Q_n(\lambda_0)}\right]^{-1}. \quad (14)$$

The electrostatic work of charging the molecule is obtained by substitution of Eqs. (8) and (14) into the general formula

$$W=\tfrac{1}{2}\sum_{k=1}^{\nu}e_k\psi_i(1,\mu_k), \quad (15)$$

all charges being located on the line $\lambda=1$. We are interested in calculating ΔW for a set of molecules HA_1, HA_2, A_1^- and A_2^-.

$$\Delta W = W(HA_1)+W(A_2^-) - W(HA_2)-W(A_1^-). \quad (16)$$

Use of Eqs. (8), (14) and (15) under the assumption that all species have the same size and shape yields

$$\Delta W=\frac{e}{D_i}\sum_{k=1}^{s}\frac{e_k}{r_k} + \frac{1}{R}\left(\frac{1}{D}-\frac{1}{D_i}\right)\sum_{n=0}^{\infty}(2n+1)\alpha_n\frac{Q_n(\lambda_0)}{P_n(\lambda_0)} \times\left[1+\left(\frac{D_i}{D}\right)\frac{\lambda_0-P_{n-1}(\lambda_0)/P_n(\lambda_0)}{\lambda_0-Q_{n-1}(\lambda_0)/Q_n(\lambda_0)}\right]^{-1} \quad (17)$$

$$\alpha_n=2e\sum_{k=1}^{s}e_kP_n(\mu_k),$$

where the sums extend over the set of charges $e_1\cdots e_2$ which the acid HA_2 contains in excess of those of HA_1 and r_k is the distance of charge e_k in HA_2 from the proton, e, located at the focus (1, 1) of the ellipsoid. In the symmetrical dibasic acid, the set of charges $e_1\cdots e_2$ consists of a single proton, e, located at the other focus, $(1,-1)$ and Eq. (17) becomes, since $P_n(-1)=(-1)^n$,

$$\Delta W=\frac{e^2}{R}\left\{\frac{1}{D_i}+\left(\frac{1}{D}-\frac{1}{D_i}\right)\sum_{n=0}^{\infty}2(2n+1)(-1)^n \times\frac{Q_n(\lambda_0)}{P_n(\lambda_0)}\left[1+\left(\frac{D_i}{D}\right)\frac{\lambda_0-P_{n-1}(\lambda_0)/P_n(\lambda_0)}{\lambda_0-Q_{n-1}(\lambda_0)/Q_n(\lambda_0)}\right]^{-1}\right. \quad (18)$$

Eqs. (1) and (18) lead to Eq. (2). When HA_2 contains a dipole moment located at the focus $(1,-1)$, in addition to the charges constituting HA_1, we find

$$\alpha_n=2eM\cos\zeta \lim_{x\to 0}\left\{\frac{1}{x}\left[P_n\left(\frac{2x}{R}-1\right)-P_n(-1)\right]\right\} \quad (19)$$

$$=-2(-1)_n n(n+1)\frac{eM\cos\zeta}{R},$$

where $M\cos\zeta$ is the component of the dipole moment along the axis of the ellipsoid. By symmetry it is readily seen that its component perpendicular to the axis contributes nothing. Eqs. (1), (17) and (19) lead to Eq. (3).

Photochemical Studies. XXVII. The Effect of Radiation on Mixtures of Nitrogen Dioxide and Nitrous Oxide and its Relationship to the Photochemical Decomposition of Nitrous Oxide

F. C. Henriques, Jr., A. B. F. Duncan and W. Albert Noyes, Jr.
Metcalf Chemical Laboratory, Brown University, Providence, R. I.

(Received June 14, 1938)

Oxygen atoms were produced in NO_2-N_2O mixtures by the photochemical decomposition of NO_2 alone. No reaction of these atoms with N_2O could be detected. Results of calculations give a minimum activation energy of 14,000 cal. for the reaction $O+N_2O=2\,NO$ and a probable maximum activation energy of 24,000 cal. The activation energy of the reaction $O+NO_2=NO+O_2$ is estimated to be 4000 cal. It is concluded that *two primary processes* are necessary to explain the direct photochemical decomposition of N_2O, $N_2O+h\nu=N_2+O$ and $N_2O+h\nu=NO+N$. The latter reaction must be followed by $N+N_2O=NO+N_2$ to explain previously determined quantum yields. The energy of activation of this reaction is probably less than 10,000 cal.

IN a previous article[1] the number of molecules formed upon irradiation of nitrous oxide per absorbed quantum, and which were uncondensed by liquid air, was determined. It was found that the over-all reaction could be represented empirically by the equation

$$4N_2O=2.8N_2+2.5NO+0.7O_2, \qquad (1)$$

which agrees roughly with results previously obtained by Macdonald.[2] It had also been established definitely that nitric oxide is one of the products by Wulf and Melvin[3] who showed that the bands of this substance appear in absorption when nitrous oxide is irradiated. Since nitrogen dioxide appears after condensation with liquid-air oxygen, also, must be formed as shown by Macdonald.[2]

The value of the quantum yield for nitrous oxide decomposition will depend upon the mechanism assumed for the primary process and for the secondary reactions. Molecular oxygen can only be formed if at least part of the primary process is

$$N_2O+h\nu=N_2+O. \qquad (2)$$

Since nitric oxide is formed, if (2) is the sole primary process a secondary reaction

$$O+N_2O=2NO \qquad (3)$$

must occur. An accompanying reaction

$$O+O(+M)=O_2(+M) \qquad (4)$$

must occur either on the walls or as the result of termolecular collisions to explain the known production of O_2.

It was suggested[1] that an alternative explanation could be based on two primary processes, namely (2) and (5)

$$N_2O+h\nu=NO+N. \qquad (5)$$

The fate of the nitrogen atoms might be either

$$N+N_2O=NO+N_2 \qquad (6)$$

or

$$N+N(+M)=N_2(+M) \qquad (7)$$

or both. It should be re-emphasized that (5) cannot be the sole primary process unless a reaction between nitrogen atoms and NO is used to explain the appearance of O_2. The latter is improbable in view of the small amount of reaction which was allowed to occur and the fact that the extent of the reaction did not affect in any marked manner the value of the yield.

The present experiments were undertaken with a view to obtaining evidence for or against reaction (3), thus permitting a decision to be made as to whether primary process (2) alone or both primary processes occur. It is true that Musgrave and Hinshelwood[4] have postulated reaction (3) to explain the appearance of NO

[1] W. A. Noyes, Jr., J. Chem. Phys. **5**, 807 (1937).
[2] J. Y. Macdonald, J. Chem. Soc. 1 (1928).
[3] O. R. Wulf and E. H. Melvin, Phys. Rev. **39**, 180 (19); L. Henry, A.-M., Compt. rendus **200**, 656 (1935).
[4] Musgrave and C. N. Hinshelwood, Proc. Roy. Soc. (London) **A135**, 23 (1932).

during the thermal decomposition of nitrous oxide, but their experiments were carried out at about 1000°K so that this reaction might have an energy of activation too high to permit it to be of importance at room temperature.

A convenient source of oxygen atoms is found in the primary dissociation of nitrogen dioxide by ultraviolet light, since this substance absorbs in a region where nitrous oxide is transparent. Henri[5] reports that nitrogen dioxide possesses two regions of predissociation, one near 3700A and the other below 2450A leading to the production of ^3P and ^1D oxygen atoms, respectively. The photochemical decomposition of nitrogen dioxide has been investigated by Norrish[6] and by Dickinson and Baxter.[7] Approximately two molecules of nitrogen dioxide decompose per quantum absorbed, a fact which may be explained by the reactions

$$NO_2+h\nu=NO+O, \tag{8}$$

$$O+NO_2=NO+O_2. \tag{9}$$

Experimental Method

Nitrogen dioxide was obtained from pure, dry lead nitrate and purified by fractional distillation with liquid air through anhydrous magnesium perchlorate. The middle fraction was vaporized into a series of small tubes with capillary ends, which were sealed off. The nitrous oxide was a commercial product and was purified by bubbling slowly through saturated potassium hydroxide. It was fractionally distilled several times through anhydrous magnesium perchlorate with liquid air and the final middle fraction was collected in a bulb provided with a stopcock.

In order to observe possible separate effects due to ^3P and ^1D oxygen atoms two light sources and reaction vessels were used. The normal ^3P atoms were produced from nitrogen dioxide by using a Pyrex tube 100 cm long with plane Pyrex windows sealed on and as a light source a General Electric type H3 mercury lamp. The Pyrex windows did not transmit radiation below 3000A. A fused silica vessel 20 cm long with sealed on plane windows was used for the ^1D atoms. This was illuminated with a cadmium spark operated at 2 kva, 25,000 volts. Radiation between 2150 and 2350A was isolated by filters. Two cm of 0.05 m acetic acid containing 1 percent acetone absorbed from 2350 to 2900A and below 2150A. Five centimeters of chlorine gas at atmospheric pressure absorbed from 2800 to 4300A, above which the nitrogen dioxide is not dissociated.[6, 7] The acetic acid-acetone solution was renewed every three hours. The reaction cells were attached as shown in Fig. 1.

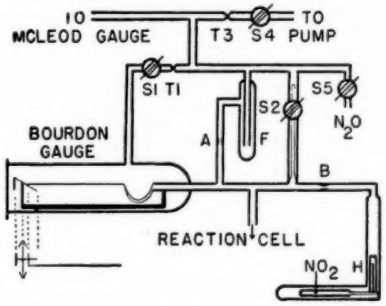

Fig. 1.

Pressures were measured with a glass Bourdon gauge which operated a lever carrying a small mirror. Images of a graduated scale placed at a distance of fifteen feet were read with a telescope. Readings were reproducible to 0.3 cm on the scale. Temperature variation over a period of time decreased this to perhaps 0.5 cm. Three gauges, designated *A*, *B* and *C*, were used during the course of the work. Calibrations showed that a 1 cm scale reading was equivalent to 0.00460, 0.00719 and 0.00201 cm of mercury, respectively, for the three gauges.

In Fig. 1, *S* indicates stopcocks lubricated with low pressure grease, *T* indicates mercury cut-offs and *A* and *B* constrictions for sealing off. Projecting through *S*2 is a capillary tube sealed at the upper end whose use will be apparent.

To explain the procedure used to obtain the results it is necessary to refer to reactions (3), (8) and (9) as well as the sum of (8) and (9)

$$2NO_2=2NO+O_2 \tag{4'}$$

and the sum of (3) and (8)

$$NO_2+N_2O=3NO. \tag{5'}$$

After illumination there will be a pressure increase $\Delta P_4+\Delta P_5$ due to reactions (4') and (5').

[5] V. Henri, Nature **125**, 202 (1930).
[6] R. G. W. Norrish, J. Chem. Soc. 761 (1927); 1158, 1604, 1611 (1929).
[7] R. G. Dickinson and W. P. Baxter, J. Am. Chem. Soc. **50**, 744 (1928).

It is known that the termolecular reaction $2NO+O_2=2NO_2$ goes to completion at liquid-air temperatures. This was verified in our experiments. Hence the increase in pressure after illumination is $\Delta P_4+\Delta P_5$ and the residual pressure after freezing down a number of times is ΔP_5.

Bourdon gauge readings are called *R*1, *R*2, etc. Some of these were made merely to check constancy of conditions and do not appear in later calculations. No readings were taken until the temperature difference between the gauge and reaction vessel was approximately 0.2–0.3° which seemed to be the value most easy to maintain.

The entire system was pumped and baked out until the pressure was less than 10^{-5} mm and the reading *R*1 made. *S*4 and *T*3 were closed and N_2O introduced through *S*5 to a pressure of 10–20 cm and the pressure read on *T*3 after which *S*5 was closed. The N_2O was then frozen out by placing liquid air on *F* and the system pumped through *S*4. *T*3 and *S*4 were closed, the N_2O evaporated at −80°C and the pressure was read on *T*3. The reading *R*2 was made, *S*1 was closed and the apparatus sealed off at *A* and the reading *R*3 made.

NO_2 was introduced by breaking the capillary end of a tube with the magnetic hammer, *H*, and *R*4 made. Side tubes attached to the reaction vessel and gauge jacket were simultaneously cooled with liquid air (to avoid breaking the gauge) and *R*5 taken. The liquid air was removed and one hour allowed for diffusion, after which *S*1 was closed and *R*6 made. The N_2O-NO_2 mixture was next illuminated for a period of four to nine hours, after which *R*7 was made.

After illumination the gases were continually distilled between two wide side tubes attached to the reaction vessel. At about two hour intervals the liquid air was removed and the gases evaporated. This was continued until readings *R*8 (with liquid air) and *R*9 (without liquid air) became constant. *S*2 was then turned, breaking the capillary, and *S*1 and *T*1 opened to equalize the pressure. *R*10 was made and in every case agreed with *R*1, *R*2 and *R*5 within experimental error. In experiments with ^1D atoms, the system was sealed off at *B* before *R*6 was made.

For experiments at higher temperatures, the reaction vessel was covered first with wire gauze, then asbestos and wrapped with resistance wire. The vessel was heated between readings *R*6 and *R*7.

Results

The necessary pressures, $P(NO_2)$, ΔP_f (final pressure increase while frozen down), ΔP_4, ΔP_5 are obtained from gauge readings as follows: (a) $P(NO_2)=R4-R3$; (b) $\Delta P_4+\Delta P_5=R7-R6$; (c) $\Delta P_5=R9-R6$; (d) $\Delta P_f=R8-R5$. During distillation of the gases by liquid air after illumination, the pressure decreased steadily for two hours and then remained constant for three to five hours. This reading is called ΔP^0. Thereafter the pressure decreased again and finally reached ΔP_f. Since the volume of the fused silica cell was much less than that of the Pyrex cell, the

Table I. *Summary of experimental results. (Pressures are in centimeters of Hg).*

Exp.	$P(N_2O)$	$P(NO_2)$	$\Delta P_4+\Delta P_5$	ΔP^0	ΔP_f	ΔP_5	Temp. (during illum.)	Time of illum. hr.	Gauge
1*A*	0	0.5	0.198	0	0	0.002	26°C	4	*A*
1*B*	0	0.5	0.078	0	−0.002	0	26	2	*A*
2(1)	10.0	0.384	0.175	0.021	0.021	0.030	25	6	*A*
3*A*	11.2	0.293	0.146	0.044	0	0.002	26	9	*A*
3*B*	11.2	0.293	0.137	0.039	0	0	26	8	*A*
4	12.4	0.186	0.089	0.021	−0.002	0	180±15	5	*A*
5	18.5	0.216	0.090	0.040	−0.0036	−0.0036	265±16	6.5	*B*
6*A*	12.6	0.371	0.226	—	0	0.004	25	8	*B*
6*B*(2)	12.6	0.371	0.176	—	0.036	0.032	215±15	8	*B*
7*A*(2)	15.7	0	0.043	—	0.012	0.043	205±15	5.5	*C*
7*B*	15.7	0	0	—	0	0	215±15	4.5	*C*
8*A*(3)	13.0	0.3±0.05	0.107	—	0	0.036	25	8	*C*
8*B*	13.0	0.3±0.05	0.056		−0.002	0.002	24	9	*C*
8*C*	13.0	0.3±0.05	>0.140		−0.002	−0.002	225±15	9	*C*
9*A*	16.8	0.191	0.076		−0.002	0.002	25	8.5	*C*
9*B*	16.8	0.191	0.068		−0.001	0.003	240±15	6.5	*C*

time to bring $\Delta P_4+\Delta P_5$ to ΔP_f was only three to five hours in the experiments with ^1D atoms. The relative rapidity of the reverse reaction $2NO+O_2=2NO_2$ prevented the observation of a ΔP^0 here. In the experiments with ^3P atoms, ΔP^0 may possibly indicate a solid complex, resulting from a system containing N_2O, NO_2, NO and O_2 which has an appreciable vapor pressure at liquid-air temperatures.

The results are recorded in Table I. Experiments $1A$–5 were made with ^3P atoms and $6A$–$9B$ with ^1D atoms.

(1) In this run no distillations were made. The ΔP_f obtained was probably ΔP^0.

(2) Although the reaction cell was flamed before the N_2O was introduced, the pressure increase was probably due to gas coming off the walls. The facts that in $7A$ there is no difference between $\Delta P_4+\Delta P_5$ and ΔP_5 and that the photochemical decomposition of N_2O leads to NO and O_2 verify this belief.

(3) ΔP_5 may be due to that fact that some mercury was present. This was avoided in subsequent runs by protecting the reaction system with a dry-ice-ether mixture during evacuation.

At the nitrogen dioxide pressures used, less then four percent of this substance was present as N_2O_4 at room temperature and less than one percent at the higher temperatures.

Discussion

Following the primary process (8), there are two competing reactions for oxygen atoms

$$O+NO_2=NO+O_2 \text{ (rate}=k_9(O)(NO_2)), \quad (9)$$

$$O+N_2O=2NO \text{ (or } N_2+O_2) \text{ (rate}=k_3(O)(N_2O)). \quad (3)$$

Within experimental error all of the oxygen atoms reacted with NO_2. Although this does not exclude the possibility of reaction (3), k_9 must be very much greater than k_3. It is possible, from the experimental data, to fix a lower limit to the activation energy of (3). From the previous results[1] on the photochemical decomposition of nitrous oxide (assuming reactions (2), (3) and (4)) it is possible to calculate an approximate upper limit to the activation energy of (3).

Assumption of a steady state gives

$$d(NO_2)/d(N_2O) = (2k_9(NO_2)+k_3(N_2O))/k_3(N_2O) = (K(NO_2)/(N_2O)+1). \quad (10)$$

This is of the form $dy/dx-Ky/x=1$.

Integration gives

$$(NO_2)(N_2O)^{-K}-(N_2O)^{1-K}/(1-K)=\text{const.} \quad (11)$$

In run 5, which will give the highest value of the lower limit, $P(N_2O)$ (initial) is 18.5 cm and $P(NO_2)$ (initial) is 0.216 cm. ΔP_4 is assumed to be 0.0036 cm. The final $P(N_2O)$ is $18.5-\Delta P_4=18.496$ cm, the final $P(NO_2)=0.216-2\Delta P_5-\Delta P_4=0.040$. ($\Delta P_4+\Delta P_5=0.090$ cm, $T=265$°C.)

Therefore

$$(0.216)(18.5)^{-K}-(0.040)(18.496)^{-K} = \frac{(18.5)^{1-K}-(18.496)^{1-K}}{(1-K)}, \quad (12)$$

which reduces to

$$0.216-0.040\times(1.000195)^K = (18.5-18.4964\times(1.000195)^K)/(1-K). \quad (13)$$

Remembering that $(1+A)^K \leqq 1+KA$ if A is small, one finds

$$K \leqq 2.2\times10^4 \quad \text{and} \quad k_9/k_3 \leqq 1.1\times10^4. \quad (14)[8]$$

Now $k=fk^0 \exp(-E/RT)$ for a bimolecular reaction where f is a steric factor and $k^0=\sigma^2(8\pi RT(1/M_1+1/M_2))^{\frac{1}{2}}$ (σ is the mean of the molecular diameters and the M's are molecular weights). Certainly the mean molecular diameters and masses are almost the same and therefore $k_3^0 \leqq k_9^0$. The steric factors should be about 0.01 and there is no reason for believing that they are different for the two reactions.

Spealman and Rodebush[9] estimate that $k_9=10^{-5}\,k_9^0$ at 40°C. From their results we calculate the energy of activation of (9) to be 4300 cal. and hence that of (3) to be 14,000 cal.

[8] Schumacher (J. Am. Chem. Soc. **52**, 2377 (1930)) illuminated mixtures of nitrogen dioxide and hydrogen and assumed from his results that there were two competing reactions (a) $O+H_2=OH+H$; (b) $O+NO_2=NO+O_2$. In order to account for the fact that all of the oxygen atoms seemed to react with the nitrogen dioxide, he states that (a) must be at least 10^4 times as fast as (b). It is interesting to compare this result with our value of k_9/k_3.

[9] M. L. Spealman, and W. H. Rodebush, J. Am. Chem. Soc. **57**, 1474 (1935).

We may now calculate the maximum energy of activation of (3) from the previous results[1] using reactions (2), (3), (4) and (15)

$$O+\text{walls}=\tfrac{1}{2}O_2 \text{ (rate}=k_{15}(O)/2(N_2O). \quad (15)$$

Assuming a steady state and integrating we obtain

$$(O_2)=k_4(O)^2(N_2O)t+k_{15}(O)t/2(N_2O), \quad (16)$$

$$(NO)=2k_3(O)(N_2O)t. \quad (17)$$

Assuming the usual formula for k_3, we obtain from (16) and (17)

$$4(O_2)(N_2O)/(NO)^2 = (k_4 \exp(2E_3/RT))/t(f_3)^2(k_3^0)^2 + (k_{15} \exp(E_3/RT))/f_3k_3^0(NO)(N_2O). \quad (18)$$

It is possible to evaluate k_{15}/k_3^0 by Smoluchowsky's equation $Z=3\pi X^2/4L^2$ where Z is the number of collisions suffered by the oxygen atoms with the nitrous oxide molecules before they reach the wall, X is the mean displacement of the atoms in reaching the wall and L is the mean free path of the oxygen atoms.

With a nitrous oxide pressure of 10 cm at 25°C[1] and assuming diameters of 1.6A and 4.6A for oxygen atoms and nitrous oxide molecules respectively, 10^{-4} cm is found for L. X is approximately 1.25 cm. Hence $Z=4\times10^8$. Therefore

$$k_{15}/k_3^0=(N_2O)^2/4\times10^8. \quad (19)$$

Reaction (4) must certainly be a very efficient process requiring little or no activation energy. It will be shown below that (4) is of no importance even if the steric factor were as large as unity; hence $f_4 \exp(-E_6/RT)$ will be assumed to be 0.1. Therefore

$$k_4^0/k_3^{02}=1.25\times10^{-12}. \quad (20)$$

Introducing (19) and (20) into (18) it is found that

$$4(O_2)(N_2O)/(NO)^2=(\exp(2E_3/RT))/8\times10^9t+(\exp(E_3/RT))/4\times10^6. \quad (21)$$

The ratio of oxygen to nitric oxide is 0.28[1] and with a time of 3600 sec. and a final pressure of NO of 3.8×10^{-4} cm, one obtains

$$1=(\exp(2E_3/RT))/8.4\times10^{17}+(\exp(E_3/RT))/4.5\times10^6. \quad (22)$$

The first term on the right (arising from triple collisions) obviously can be neglected. Thus $E_3=9200$ cal.

A comparison of the energy of 14,000 cal. for (3) calculated from the data in this article with the 9200 cal. obtained from the previous data[1] indicates that practically all of the oxygen atoms produced by photochemical decomposition of nitrous oxide will form oxygen molecules by collisions with the walls.

Since nitric oxide is known to be formed,[1-3] primary process (2) must be accompanied by (5), which will be followed by (6) and (23)

$$N+\text{walls}=\tfrac{1}{2}N_2, \quad (23)$$

since the homogeneous termolecular combination of nitrogen atoms may be neglected for the same reasons as (4).

Since the number of molecules of N_2 and NO together formed per quantum absorbed is 1.9,[1] (6) must occur if (3) is excluded. For the speed of (6) to be comparable with that of (23) it can be shown by the above methods that E_6 must be less than 10,000 cal.

From the results of Musgrave and Hinshelwood,[4] the activation energy of (3) must be less than 24,000 cal. if this reaction is to compete successfully with (15). The 10,000 cal. difference between this figure and the minimum found in the present article might well explain why reaction (3) takes place to a small extent at 1000°K.

On the Interaction of Atoms in Alloys

WILLIAM SHOCKLEY
Bell Telephone Laboratories, Inc., New York, N. Y.
(Received May 4, 1938)

A generalization of Bethe's theory of superlattices so as to take into account the interactions between atoms which are not nearest neighbors in the lattice is considered. This process will not furnish any great improvement in agreement between theory and experiment because it predicts, in disagreement with experiment, that many properties of binary alloys are symmetrical between the two constituents. It is further shown to be in disagreement with certain fundamental features of the interactions of atoms in alloys.

BETHE[1] has given a treatment of the order-disorder transformation in binary alloys of 50 atomic percent composition based upon ideas of the interaction between atoms which are nearest neighbors in the lattice. If the two species of atoms are A and B, then the interaction energy between a pair of nearest neighbors is V_{AA}, V_{BB}, or V_{AB} according to the nature of the pair. It is assumed that these three energy parameters are strictly constants and do not vary with the state of order; and it is further assumed that the configurational free energy, i.e., that due to the arrangement of the A and B atoms upon the lattice sites, can be separated from all other free energies and treated separately.

Several writers[2,3] have generalized Bethe's treatment to arbitrary compositions while restricting themselves to the case in which the lattice type (but not necessarily the spacing) remains the same by assuming that the interaction parameters are independent of composition. The results of these investigations show that the theories are along the right lines but the quantitative agreement with experiment is generally poor. In particular, the theory predicts that the phase diagrams for the order-disorder transformation should be symmetrical about fifty atomic percent, a prediction in disagreement with experiment. A natural extension of the theory consists of introducing three more energy parameters describing interactions between *next* nearest neighbors;[4] indeed even more remote interactions may be considered. We shall use the phrase "nth neighbor assumption" to describe the case in which interactions are included between all atoms which neighbors of the nth or less degree. One intuitively feels that the contribution of any one atom to the energy of the alloy will be dependent upon the arrangement of the atoms in its immediate vicinity, i.e., those within the neighboring unit cells. For this reason we might expect that an nth neighbor assumption with a reasonably small value of n would mimic quite well the actual situation. It is the purpose of this note to point out that such expectations are not well founded and to mention some other lines of attack.

In the first place, we shall prove that the assumption of interactions between neighbors of any order does not interfere with the symmetry of the phase diagram about fifty atomic percent. Let us denote by V_{1AA}, V_{1BB}, and V_{1AB}, the interactions between nearest neighbors in the lattice and by Z_1 the number of nearest neighbors of each atom (these are the quantities used in Bethe's theory) and by V_{2AA}, V_{2BB}, V_{2AB}, and Z_2 corresponding quantities for next nearest neighbors, etc. In this proof, which is formally identical with that given by the writer for nearest neighbor interactions,[3] it is assumed that the lattice is of a simple type, such as simple cubic, face-centered cubic, or body-centered cubic so that all lattice sites are equivalent as regards their distribution of neighbors (for other lattices, such as the fluorspar structure, interactions between nearest neighbors may give asymmetry). Let us denote by Q_{nAA}, Q_{nBB}, Q_{nAB} the numbers of pairs of atoms which are nth degree neighbors and are formed of AA, BB and AB, respectively. Then

[1] H. A. Bethe, Proc. Roy. Soc. **150A**, 552 (1935).
[2] C. E. Easthope, Proc. Camb. Phil. Soc. **33**, 502 (1937) and **34**, 68 (1938).
[3] W. Shockley, J. Chem. Phys. **6**, 130 (1938).
[4] This case has been treated by T. S. Chang, Proc. Roy. Soc. London **161A**, 546 (1937).

the contribution of these nth degree interactions to the energy E of alloy is:

$$E_n = V_{nAA}Q_{nAA} + V_{nBB}Q_{nBB} + V_{nAB}Q_{nAB}.$$

If the total number of atoms in the alloy is N and if fractions F_A and F_B of them are A and B, then

$$2Z_nF_AN = 2Q_{nAA} + Q_{nAB},$$
$$2A_nF_BN = 2Q_{nBB} + Q_{nAB}.$$

If we compare the energy of the alloy with that of two crystals of the pure metals, we find that the energy due to the nth degree interactions is

$$E_n' = -V_nQ_{nAB},$$
where $$V_n = \tfrac{1}{2}(V_{nAA} + V_{nBB}) - V_{nAB}.$$

This energy term is obviously symmetrical in A and B and so are the terms due to the interactions of all other orders.

Another reason for being skeptical of any of the nth neighbor assumptions is that they represent emasculated central force treatments of the alloy. Let us assume (1) that the atoms interact in pairs, the potential energies being $V_{AA}(r)$, $V_{BB}(r)$ and $V_{AB}(r)$, where r is the distance between atoms and (2) that the lattice of sites is a rigid unalterable framework. Then the distance r_1 between nearest neighbors is a fixed quantity and the same is true of r_2, the distance between next nearest neighbors, etc. These assumptions correspond to the ∞ th neighbor assumption with $V_{nAA} = V_{AA}(r_n)$. The fact that this correspondence arises directly from (2) constitutes a severe criticism of the nth neighbor assumption: for (2) is a quite unreasonable assumption denying the variations of lattice constant with composition which are recognized empirically by Vegard's law and which would otherwise follow from a difference in equilibrium radii of the three V's.

This reasoning suggests that even the nearest neighbor assumption should be modified by allowing the interatomic distances to vary, entailing corresponding changes in the V's; that is, we should use central force potential energies between the nearest neighbors. Hume-Rothery[5] has discussed the formation of a superlattice in Fe_3Al on this basis: this alloy is characterized by having no pairs of Al atoms as nearest neighbors and a minimum number as next nearest neighbors. Although this situation can be readily explained by assuming next-nearest-neighbor interactions, it may equally well be explained, as Hume-Rothery has pointed out, by considering the strains produced by the interactions of nearest neighbors of different atomic diameters; these strains being least when most evenly distributed, that is, when the Al atoms are as far apart as possible. A. H. Wilson[6] has carried out an analytical investigation of the nearest neighbor central force theory for a case corresponding to superstructure formation in CuAu. He predicts a latent heat and a change of lattice constant with order.

The next-nearest-neighbor assumption without allowance for change in atomic spacing has been used by Chang,[4] who finds that as compared with the nearest-neighbor assumption it gives improved agreement with experiment by leading to higher specific heats near the critical temperature of order; and by Bitter,[7] who shows that it can lead to intermetallic compounds. However, the predictions of the nearest neighbor assumption are greatly altered if change in atomic spacing is permitted as has been shown both by the calculations of Wilson[6] and by considerations of the entropy of lattice vibrations;[8] furthermore suitable assumptions about the interatomic forces lead to the expectation of intermetallic compounds. From this we conclude that the introduction of next-nearest-neighbor interactions is not required until the nearest-neighbor central-force picture has been further investigated.

Although improvement may be justifiably expected to follow the introduction of potential energies between nearest-neighbors, it is known that the central force picture is inadequate for metals. This conclusion is drawn from the failure of the Cauchy relations for the elastic constants, and the reason for this failure is well understood from the work of Fuchs[9] using the modern theory of metals. The work of Mott[10] on β-brass has shown that for the superlattice formation in this

[5] W. Hume-Rothery and H. M. Powell, Zeits. f. Krist. **91**, 23 (1935). (See also reference 8, p. 40.)

[6] A. H. Wilson, Proc. Camb. Phil. Soc. **34**, 81 (1938).
[7] F. Bitter, J. Chem. Phys. **6**, 339 (1938).
[8] For a discussion see F. C. Nix and W. Shockley, Rev. Mod. Phys. **10**, 1 (1938).
[9] K. Fuchs, Proc. Roy. Soc. **157**, 622 (1936).
[10] N. F. Mott, Proc. Phys. Soc. **49**, 258 (1937).

alloy the central force picture is untenable. He finds that the atoms do not interact directly in pairs and that the major part of the energy of the superlattice arises from electrostatic interactions between the Cu and Zn atoms, which are unequally charged. This difference in charge depends upon the manner of occupation of the neighboring sites of each of the two atoms; it is greatest when they are occupied as in a superlattice and least when each atom is surrounded by neighbors of its own species, the atom tending in the latter case to be neutral as in the pure metal. Thus the interaction between any two atoms depends very considerably upon the other atoms which surround them and this is a complete refutation of the central force picture. Mott has suggested an interpretation of the high specific heat of β-brass on this basis.

SEPTEMBER, 1938 JOURNAL OF CHEMICAL PHYSICS VOLUME 6

The Vibrational Spectrum and Thermodynamic Properties of Nickel Carbonyl

BRYCE L. CRAWFORD, JR.,* *Mallinckrodt Chemical Laboratory, Harvard University, Cambridge, Massachusetts,*
AND
PAUL C. CROSS,† *Department of Chemistry, Stanford University, California*

(Received June 24, 1938)

The infra-red absorption spectrum of nickel carbonyl has been measured in the gas phase from 4 to 23μ, and in the liquid phase from 1 to 8μ. Normal coordinate treatments of both the square and tetrahedral models of the AB_4C_4 molecule have been applied to the infra-red and Raman data; the results give further evidence of the tetrahedral structure of nickel carbonyl. An analysis of the vibrational spectrum has been made, based on the tetrahedral model, and has been applied to the statistical calculation of the entropy, heat capacity, and free energy function.

INTRODUCTION

THE theory of directed valence predicts a tetrahedral structure for a nickel carbonyl molecule consisting of four carbonyl groups singly bonded to a neutral nickel atom.[1] Electron diffraction studies[2] appear to confirm this structure. However, the observed nickel-carbon distance indicates strong resonance with a structure involving nickel-carbon double bonds, which may or may not tend to alter the tetrahedral configuration. A square configuration has frequently been proposed, in analogy with the known square configuration of quadricovalent compounds of bivalent nickel.[2] A qualitative analysis of the Raman spectrum of nickel carbonyl was interpreted as favoring the square structure;[3] however, it has been shown that the selection rules were violated in this analysis.[4]

We have therefore undertaken a quantitative analysis of the vibrational spectrum, including infra-red data, considering both the square and tetrahedral models. It was our hope to obtain a new and independent determination of the structure; indications favoring the tetrahedral configuration were found, but the square con-

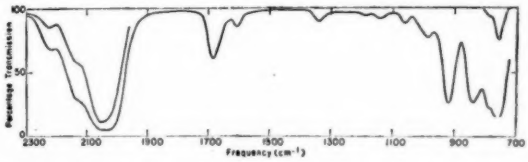

FIG. 1. Absorption spectrum of nickel carbonyl vapor, rocksalt region (20 cm path length, 300 mm pressure).

---

* National Research Fellow in Chemistry.
† Present address: Brown University, Providence, R. I.
[1] L. Pauling, J. Am. Chem. Soc. **53**, 1367 (1931).
[2] L. O. Brockway and P. C. Cross, J. Chem. Phys. **3**, 828 (1935).
[3] A. B. F. Duncan and J. W. Murray, J. Chem. Phys. **2**, 636 (1934).
[4] E. B. Wilson, Jr., J. Chem. Phys. **3**, 59 (1935).

TABLE I. *Observed and calculated infra-red active frequencies.*

OBSERVED (cm^{-1})	INTENSITY	CALCULATED (cm^{-1})	ASSIGNMENT	OBSERVED (cm^{-1})	INTENSITY	CALCULATED (cm^{-1})	ASSIGNMENT
		90	ω_5 (δ)	920	50	920	$\omega_1+\omega_7$ (ν)
		160	$\omega_3+\omega_5$ (δ)			960	$\omega_7+\omega_9$ (δ)
		180	$2\omega_5$ (δ)	990	4	990	$\omega_1+\omega_3+\omega_7$
		300	ω_6 (ν)			1000	$\omega_4+\omega_7$ (δ)
		370	$\omega_3+\omega_6$ (ν)	1060	1	1060	$\omega_1+2\omega_3+\omega_7$
		390	$\omega_5+\omega_6$ (ν)			1080	$2\omega_7$ (δ)
475	20	470	$\omega_1+\omega_5$ (ν)	1140	0	1130	$\omega_1+3\omega_3+\omega_7$
		490	$\omega_3+\omega_9$ (δ)			1150	$\omega_3+2\omega_7$
		510	$\omega_5+\omega_9$ (δ)	1340	1	1340	$2\omega_4+\omega_9$
545	60	540	ω_7 (δ)	1590	(liquid)	1590	$\omega_8-\omega_4$
		550	$\omega_4+\omega_5$ (ν)	1610	0	1620	$3\omega_7$
595	0	600	$2\omega_6$ (ν)			1630	$\omega_8-\omega_9$
		610	$\omega_3+\omega_7$ (δ)	1660	(liquid)	1670	$\omega_8-\omega_1$
		630	$\omega_5+\omega_7$ (δ)	1682	20		
680	10	680	$\omega_1+\omega_6$ (ν)	1740	(liquid)	1750	$\omega_8-\omega_6$
		720	$\omega_6+\omega_9$ (ν)			1960	$\omega_8-\omega_5$
760	70	760	$\omega_4+\omega_6$ (ν)			1980	$\omega_8-\omega_3$
790	10	800	$\omega_1+\omega_9$ (ν)	2050	100	2050	ω_8 (ν)
840	50	840	$\omega_6+\omega_7$ (ν)			2120	$\omega_3+\omega_8$ (ν)
		840	$2\omega_9$ (δ)	2150	20	2140	$\omega_5+\omega_8$ (ν)
		880	$\omega_4+\omega_9$ (δ)	2230	4	2230	$2\omega_5+\omega_8$

TABLE II. *Assignment of observed Raman active frequencies.*

OBSERVED (cm^{-1})	INTENSITY	CALCULATED (cm^{-1})	ASSIGNMENT
82	100 p	70	ω_3
		90	ω_5
382	20 P	380	ω_1
463	8 D	460	ω_4
601	4	600	$2\omega_6$
718	0	720	$\omega_6+\omega_9$
833	2	840	$\omega_1+\omega_4$
872	2	880	$\omega_4+\omega_9$
913	2	920	$2\omega_4$
1609	0	1620	$\omega_2-\omega_9$
2043	30 p	2040	ω_2
2132	5	2130	$\omega_2+\omega_5$
2223	1	2220	$\omega_2+2\omega_5$

Data from reference 3; D=depolarized, P=polarized, p=partly polarized.

figuration cannot be conclusively eliminated on the basis of this analysis.

Using the tetrahedral model, a satisfactory assignment of fundamental frequencies was made, and thermodynamic properties calculated.

EXPERIMENTAL

The infra-red absorption in the rocksalt region was studied using the spectrometer at the University of Wisconsin.[5] The absorption of the liquid was studied from 1 to 8μ; that of the vapor from 4 to 14μ. The absorption of the vapor in the region from 12 to 23μ was also studied, using the spectrometer at Harvard University.[6] The absorption curves are given in Figs. 1 to 3. The frequencies of the maxima of the bands are given in Table I; the Raman data of Duncan and Murray[3] are summarized in Table II.

After our measurements had been completed, a report of a similar study by Bailey and Gordon appeared.[7] The agreement between their observations and ours is very satisfactory, although there are some differences. Several of the weak bands which we found are not given by Bailey and Gordon, and their relative intensities for certain bands do not agree with ours. They resolved the band at 680 cm^{-1} into three components; in our measurements we find some

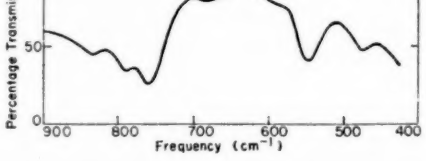

FIG. 2. Absorption spectrum of nickel carbonyl vapor, KBr region (20 cm path length, 200 mm pressure).

[5] P. C. Cross and F. Daniels, J. Chem. Phys. **1**, 48 (1933). These measurements were made by P. C. Cross, who wishes to express his gratitude to Professor Daniels and to the Wisconsin Alumni Research Corporation for the grant which made possible this study.

[6] H. Gershinowitz and E. B. Wilson, Jr., J. Chem. Phys. **6**, 197 (1938). These measurements were made by B. L. Crawford, Jr., who wishes to thank Professor Wilson and Dr. Gershinowitz for the use of this instrument and for their continued interest in this work.

[7] Bailey and Gordon, J. Chem. Phys. **6**, 225 (1938).

indication of such structure, but of such an uncertain nature that we can attach no significance to it. Certainly the possible side-components are not comparable in intensity to the peak at 680 cm^{-1}.

Normal Coordinate Treatment

Both the square and tetrahedral configurations of the molecule AB_4C_4 were treated, using the methods of group theory[8] in finding the normal coordinates and selection rules. The reduced representations for the internal vibrations were found to be, for the square model ($\mathbf{D}_{4h}$),

$$\Gamma = 2A_{1g}+A_{2g}+2B_{1g}+2B_{2g} +E_g+2A_{2u}+2B_{2u}+4E_u.$$

and for the tetrahedral model ($\mathbf{T}_d$),

$$\Gamma = 2A_1+2E+4T_2+T_1.$$

The normal coordinates for the two models are sketched approximately in Figs. 4 and 5; the selection rules for the fundamentals are also indicated.

Frequency expressions, based upon valence-force type potential energy expressions, were calculated for both models. For the tetrahedral model, the following five-constant potential function was used:

$$2V = K_1\Sigma(\Delta R_i)^2+K_2\Sigma(\Delta r_i)^2 +H_1R^2\Sigma(\Delta\alpha_{ij})^2+H_2r^2\Sigma(\Delta\beta_i)^2 +hR^2\Sigma(\Delta\alpha_{ij})(\Delta\alpha_{kl}).$$

Here R_i is the distance from the nickel to the ith carbon atom, r_i the carbon-oxygen distance in the ith CO group, α_{ij} the angle between the ith and jth nickel-carbon bonds ($\alpha_{ij}^0 = 109°28'$) and β_i the angle between the ith nickel-carbon and carbon-oxygen bonds ($\beta_i^0 = 180°$). K_1 and K_2 are the force constants for stretching of the nickel-carbon and carbon-oxygen bonds, respectively; H_1 and H_2 are force constants for distortion of the valence angles; h is the constant for interactions between opposite valence angles of the nickel atom, the last summation being taken over the three pairs of opposite angles α_{ij}.

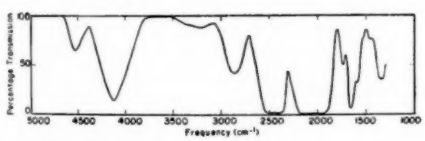

FIG. 3. Absorption of liquid nickel carbonyl (2 mm path length).

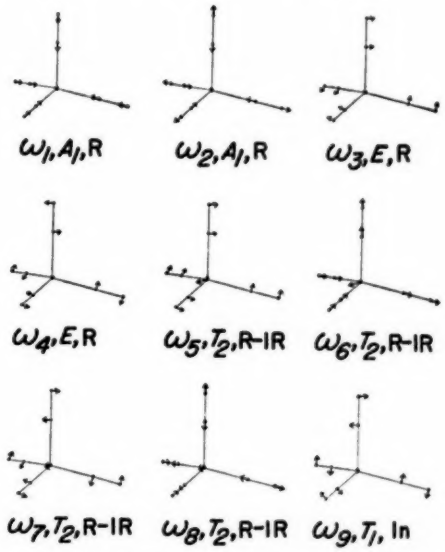

FIG. 4. Approximate modes of vibration of the tetrahedral AB_4C_4 type molecule, T_d.

FIG. 5. Approximate modes of vibration of the square AB_4C_4 type molecule, D_{4h}

[8] E. Wigner, *Göttinger Nachrichten* (1930), p. 133; E. B. Wilson, Jr., Phys. Rev. **45**, 706 (1934); J. E. Rosenthal and G. M. Murphy, Rev. Mod. Phys. **8**, 317 (1936). We are grateful to Professor Wilson for making available to us some preliminary work on the AB_4C_4 molecule, and for his suggestions and criticisms.

This potential function leads to the frequency expressions given below, in which $\lambda_i = 4\pi^2 c^2 \omega_i^2$. Fundamentals marked *R* are Raman active, those marked *IR* are infra-red active, and those marked *In*, inactive in both Raman and infra-red.

$2A_1$; ω_1, ω_2; $R(\rho \leq \frac{3}{4})$:

$$\lambda^2 - \lambda[(K_2/m) + (K_1+K_2)/M] + K_1K_2/mM = 0$$

$2E$; ω_3, ω_4; R:

$$\lambda^2 - \lambda[(H_2/m) + (3H_1' + f^2H_2)/M] + 3H_1'H_2/mM = 0$$

$4T_2$; ω_5, ω_6, ω_7, ω_8; $R-IR$:

$$\begin{vmatrix}
-3MS\lambda & & & \\
+(K_1+4H_1'') & 2(K_1-2H_1'') & -(K_1+4H_1'') & QH_2 \\
+NQH_2 & -QH_2 & -QUH_2 & \\
 & -3M\lambda & & \\
(K_1-2H_1'') & +2(K_1+H_1'') & -(K_1-2H_1'') & -(2K_2+H_2) \\
+(K_2-NH_2) & +(2K_2+H_2) & -U(K_2-H_2) & \\
 & & -3M\lambda & \\
W(K_1+4H_1'') & 2W(K_1-2H_1'') & -W(K_1+4H_1'') & 2(K_2-PH_2) \\
-(K_2+2NPH_2) & -2(K_2-PH_2) & +U(K_2+2PH_2) & \\
 & & & -3m\lambda \\
-(K_2-NH_2) & -(2K_2+H_2) & U(K_2-H_2) & +2K_2+H_2
\end{vmatrix} = 0$$

T_1: ω_9; *In*:

$$\lambda = H_2(M+mf^2)/mM$$

where

$$H_1' = H_1 + (h/2) \qquad P = 1 - Wg$$
$$H_1'' = H_1 - (h/2) \qquad Q = 2gSUW$$
$$f = (R+r)/R \qquad U = (M+m)/m$$
$$S = M_0/(M_0+4M+4m) \qquad W = 4m/M_0$$
$$N = 1 + (4MSr/M_0R)$$

and M_0, M and m refer to the masses of the *A*, *B*, and *C* atoms, respectively.

Frequency expressions were also calculated for the square model, using a similar potential function (seven constants). Since this model was rejected, it does not seem worth while to give these expressions in detail. Fig. 6, which shows the relation between the frequencies of the tetrahedral and square models, plotted qualitatively on an energy scale, will serve to show approximately the relative magnitudes of the frequencies. It is to be emphasized that this figure is a qualitative one; the actual separations of the levels in the square model will depend on the relative magnitudes of the bending force constants for distortion in the plane of the molecule and perpendicular to this plane.

Vibrational Analysis

Consideration of the square model

While we have not found conclusive evidence from this analysis against the square configuration, there are certain features of the spectrum which are difficult to reconcile with this model. The strong Raman line at 82 cm^{-1} appears to be, as Duncan and Murray[3] describe it, "very broad, unsymmetrical, and of unusually great intensity which suggests that it is complex." This would require, on the basis of the square model, two *g* type frequencies lying near 80 cm^{-1}. This is supported by the appearance of two series of bands; one occurring in the infra-red at 920,

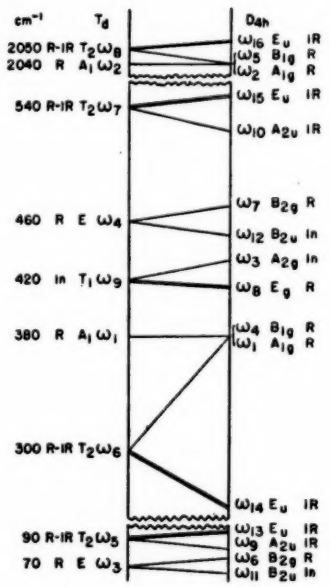

FIG. 6. Relation between the fundamental frequencies of the tetrahedral and square models for nickel carbonyl. The frequencies are located on an energy scale; the magnitudes are noted, in cm^{-1}, for the tetrahedral model; the locations for the square model are *qualitative* only.

990, and 1060 cm^{-1}, and most satisfactorily assigned to combinations involving a g type frequency of 70 cm^{-1}; and the other occurring in both the infra-red and the Raman spectra, at 2040, 2130, and 2220 cm^{-1} (Raman frequencies), and similarly suggesting a g type frequency of 90 cm^{-1}.

There can be, however, but one g type frequency of this magnitude. The discussion of the Raman data given below in connection with the tetrahedral model applies also to the square configuration; thus the polarized lines at 382 and 2043 cm^{-1} must be assigned to ω_1 and ω_2, and the low lying frequency of about 80 cm^{-1} to ω_6. Several choices may be made as to the other assignments of the g type frequencies; we have been unable, however, to find a set of assignments which would give reasonable force constants and yield another g type frequency near 80 cm^{-1}. (See Fig. 6.)

These indications, together with the electron-diffraction evidence, and the satisfactory assignment obtained with the tetrahedral model, have led us to abandon further consideration of the square configuration.

Consideration of the tetrahedral model

The totally symmetric radial frequencies ω_1 and ω_2 should appear in the Raman effect as strong, polarized lines; they must therefore be assigned to 382 and 2043 cm^{-1}. We may regard the broad 82 cm^{-1} line as composed of two components at 70 and 90 cm^{-1}, the frequencies indicated by the series mentioned above. The frequency expressions then favor the assignment $\omega_3=70$, $\omega_5=90$ cm^{-1}. We may then assign ω_4 to the next strongest Raman line, at 463 cm^{-1}; or we may regard this line as a combination of $\omega_1+\omega_3$ and assign ω_4 to 601 cm^{-1}. From either assignment we may calculate K_1, K_2, H_1', and H_2, and hence should be able to calculate the other five frequencies, adjusting the interaction constant h to fit the infra-red spectrum. If we take $\omega_4=601$, then we must adjust h to make $\omega_7=760$, since the frequency expressions are such that ω_7 must lie above ω_4 (see Fig. 6), and no infra-red band between 600 and 760 cm^{-1} is sufficiently intense to encourage the assignment of a fundamental within that region. This would lead to a value of about 220 cm^{-1} for ω_6 and about 580 cm^{-1} for ω_9; these values give no possible fundamental or binary combination for the intense band at 545 cm^{-1}, and hence must be rejected. If we take $\omega_4=463$ cm^{-1}, on the other hand, we are led to the following force constants:

$$K_1 = 2.52\ (10^5)\ \text{dynes/cm.}$$
$$K_2 = 15.89$$
$$H_1 = 0.089$$
$$H_2 = 0.377$$
$$h = -0.010.$$

Table III gives the values of the fundamental frequencies thus calculated, and also the assigned values, which are used in the calculation of com-

TABLE III. *Fundamental frequencies.*

	CALCULATED (cm^{-1})	ASSIGNED (cm^{-1})
ω_1	(382)	380
ω_2	(2043)	2040
ω_3	(70)	70
ω_4	(463)	460
ω_5	110	90
ω_6	310	300
ω_7	(545)	540
ω_8	2050	2050
ω_9	430	420

Frequencies in parentheses were used to determine force constants.

bination frequencies and are to be regarded as the "true" fundamental frequencies of the molecule. The agreement is satisfactory when the approximate nature of the potential function is considered.

TABLE IV. *Thermodynamic values.*

TEMP. (°K)	S^*	$-(F^0-E_0^0)/T$	C_v
298.1	97.0	73.4	32.8
316.1	99.1	74.8	33.5
350.0	102.7	77.4	34.5
400.0	107.7	80.8	35.8
450.0	112.2	84.1	36.8
500.0	116.4	87.1	37.7

The calculated values for all infra-red active fundamentals, first overtones, and binary combinations which lie below 2250 cm^{-1} are given in Table I, compared with the observed spectrum. (The table also contains calculated values and assignments for certain higher combinations and difference tones, which are needed to completely fit the observations.) If we divide the nine fundamental frequencies approximately into those of "valence" type (ω_1, ω_2, ω_6, ω_8) and those of "deformation" type (ω_3, ω_4, ω_5, ω_7, ω_9) we find an interesting intensity pattern exhibited in Table I. The combinations which involve at least one valence type component (marked ν in Table I) are more strongly infra-red active than the pure deformation type combinations (marked δ), which indeed are so weak as not to appear. The single real exception to this generalization is the fact that no band is found at 720 cm^{-1}, the calculated value of $\omega_6+\omega_9$. The possible significance of this intensity pattern is an interesting subject; however, in view of our present inadequate knowledge concerning vibrational intensities, we prefer not to attempt any interpretation.

It will be noted that the difference tones arising from the two low lying fundamentals, with calculated frequencies at 1960 and 1980 cm^{-1}, are not found. This is rather surprising in view of the appearance of other difference tones. It should be pointed out, however, that this is not to be regarded as disagreeing with the particular assignment of frequencies given here; any assignment must include a Raman active frequency near 80 cm^{-1}, which should give a difference frequency at about 1970 cm^{-1}.

The assignments and calculated frequencies, which account for the Raman spectrum, are given in Table II, together with the observed frequencies.[3]

The value found for the C−O bond stretching force constant, 15.89×10^5 dyne/cm, lies between the value[9] associated with the C−O double bond, 12.3×10^5, and that associated with the C−O triple bond, 18.6×10^5; it is very close to the value found in carbon dioxide, 15.24×10^5. This is in agreement with the resonance hybrid character of the bond suggested by Brockway and Cross[2] on the basis of the interatomic distances.

Both the C−O and the Ni−C bond force constants, when used in Badger's relation[10] between force constants and interatomic distance, give fairly good agreement: Ni−C distance, calculated 1.85A, observed 1.82A; C−O distance, calculated 1.17A, observed 1.15A.

THERMODYNAMICS

By standard methods of statistical mechanics, the virtual entropy, free energy function, and heat capacity of nickel carbonyl (perfect gas at 1 atmos. pressure) have been calculated for the temperatures 298.1, 316.1 (boiling point) 350, 400, 450, and 500°K. The moments of inertia were calculated from the interatomic distances[2] Ni−C=1.82A, C−O=1.15A; the product $(ABC)=5.03\ (10^{-112})\ g^3\ cm^6$. The thermodynamic values are given in Table IV.

In view of the fact that several of the fundamentals, including the low lying frequencies, were not directly observed, but assigned on the basis of combination assignments and frequency calculations, these thermodynamic values cannot be taken as highly accurate. After considering the effects of various frequency changes, however, we believe that the error is not greater than 2 percent in the entropy and free energy function, and somewhat less in the heat capacity.

[9] H. W. Thompson and J. W. Linnett, J. Chem. Soc. 1384 (1937).
[10] R. M. Badger, J. Chem. Phys. **3**, 710 (1935).

Vibration Spectra and Molecular Structure

IV. The Infra-Red Absorption Spectra of the Double and Single Molecules of Formic Acid

LYMAN G. BONNER* AND ROBERT HOFSTADTER
Palmer Physical Laboratory, Princeton University, Princeton, New Jersey

(Received May 21, 1938)

In the present study the absorption spectrum of formic acid vapor between 1 and 15.5μ has been investigated under a variety of temperature conditions. The spectrum at room temperature gives essentially the absorption of the double molecules alone, while that at 140°C gives the absorption of the single molecules. The results are interpreted in terms of the hydrogen bonding existing in the double molecule. In addition an attempt to prepare and investigate pure formic acid-*d* is reported.

AS is well known, the vapor of formic acid exists, at the vapor pressure of the liquid, largely as double molecules at room temperature, but is readily dissociated. A temperature of 150°C, at this same pressure, suffices to almost completely dissociate the material to single molecules. According to electron diffraction measurements of Pauling and Brockway[1] the double molecules are associated through the OH to give a structure HC(=O)OH···O(H)CH in which the O—O distance is 2.67A. The purpose of the present work has been, in part, to study the structure and constants of the formic acid molecule both in the single and double states, and in part to investigate the nature of the hydrogen bond. Formic acid is one of the simplest and most symmetrical molecules in which this type of bonding exists and seemed, therefore, to be a logical starting point.

Depending on the nature and state of aggregation of the substance under investigation, O—H containing molecules seem to fall into three classes: those exhibiting a sharp infra-red absorption near 3700 cm^{-1}, those with a more diffuse band near 3400 cm^{-1}, and those which seem to exhibit no absorption characteristic of the O—H bond. The first type is exemplified by the vapors and dilute solutions of alcohols, acids, etc. To the second belong liquid alcohols and higher acids and in the third class fall chelate compounds of the type discussed by Wulf *et al.*[2] and the lighter fatty acids. These three classes and their probable differences have been discussed recently by Buswell, Deitz and Rodebush,[3] by Errera and Mollet[4] and by Badger and Bauer.[5] Undoubtedly the normal undisturbed oscillation frequency of the O—H bond is 3700 cm^{-1} and the existence of the other two classes is a result of varying types or degrees of hydrogen bonding. Absence of the characteristic O—H absorption (3400 cm^{-1} in liquid samples) has been used as a criterion for the existence of a chelate ring or other structure involving the OH, but the OH frequency in these extreme cases is a matter of some concern since it certainly cannot disappear altogether. Buswell, Deitz and Rodebush and Badger and Bauer have suggested that the frequency shift is just sufficient to superimpose the OH on the CH frequency, near 3000 cm^{-1}. It is the belief of the present authors that this contention is supported by our observations on the spectrum of formic acid vapor.

MATERIALS AND APPARATUS

To obtain pure anhydrous formic acid, Kahlbaum's product was treated by the method of vacuum distillation and sublimation prescribed by Coolidge[6] until the vapor pressure reached the

* Now at Duke University, Durham, N. C. This work was performed while the author was the holder of a National Research Council Fellowship in Chemistry.

[1] Pauling and Brockway, Proc. Nat. Acad. Sci. **20**, 336 (1934).

[2] Hilbert, Wulf, Hendricks and Liddel, J. Am. Chem. Soc. **58**, 548 (1936).

[3] Buswell, Deitz and Rodebush, J. Chem. Phys. **5**, 84 (1937); J. Chem. Phys. **5**, 501 (1937).

[4] Errera and Mollet, Nature **138**, 882 (1936).

[5] Badger and Bauer, J. Chem. Phys. **5**, 839 (1937).

[6] Coolidge, J. Am. Chem. Soc. **50**, 2166 (1928).

value given by this author. Coolidge mentions the possibility of dissociation to CO and H_2O and since this question was important in the present work, a sample of this vapor in a one liter flask was maintained at 150°C for 36 hours. At the end of this time there was no perceptible pressure increase to indicate a dissociation of this nature.

TABLE I. *Positions of dimer and monomer absorption bands.*

DIMER		MONOMER	
$\lambda(\mu)$	$\nu(cm^{-1})$	$\lambda(\mu)$	$\nu(cm^{-1})$
3.25	3080	2.80	3570
3.95	2530	3.40	2940
4.20	2380	4.30	2325
5.25	1905		
5.75	1740	5.75	1740
7.40	1350		
8.30	1205		
9.15	1093	9.15	1093
10.9	917		
15.0	667	15.2	658

For our absorption cell, a 15 cm length of glass tubing was sealed at the ends with rocksalt plates and 5 cm lengths of tubing, also closed with rocksalt, were placed at each end to provide a dead air space. The problem of providing glass to rocksalt seals, vacuum tight at 150°C was considerable since none of the usual waxes or resins can withstand this temperature. This difficulty was finally surmounted by placing small asbestos washers between the glass and the salt plate, clamping the whole assembly tightly in a brass frame, and painting the joints with glyptal. Although the glyptal softened at the highest temperatures used in these experiments, the asbestos usually kept it from sucking in. Two identical cells were made and mounted side by side and the furnace wrapped around both. One cell was evacuated to serve as a dummy and the other provided with a side tube projecting beyond the furnace to hold liquid formic acid at room temperature, thereby determining the pressure of vapor in the cell. In one set of runs this side tube was immersed in ice to reduce the pressure in the cell. Vapor pressures of formic acid are, according to Coolidge, 44 mm at 25°C and 11.2 mm at 0°. The temperature of the cells was determined by means of a thermocouple inside the furnace.

The spectrometer used was the rocksalt prism instrument described by Barnes, Brattain and Seitz.[7] Percent transmission measurements were made throughout the region 1–15.5μ at $\cdot 0.1\mu$ intervals. The accuracy of the band positions listed in Table I is therefore limited to about this value.

RESULTS

Figures 1 and 2 show series of runs with the vapor at various temperatures between 25° and 140°C, and with the side tube in air, and in an ice bath, respectively. In the first case the side tube was warmed by the furnace, increasing the vapor pressure to the figures shown on the curves. In Table I are listed the wave-lengths and frequencies of all bands considered significant in the monomer and dimer spectra. As may be seen, there is a marked transition from the complex

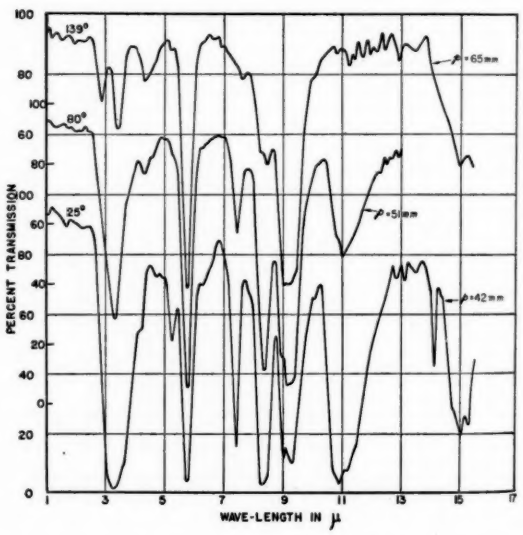

FIG. 1. Absorption bands in formic acid vapor; side tube in air.

dimer spectrum at room temperature to the comparatively simple monomer spectrum at higher temperatures. From the point of view of O−H bond considerations the region 2.5–3.5μ is of particular interest. In the low temperature, completely associated spectrum there appears one very broad absorption with center at approximately 3.3μ. As the temperature is increased this band decreases in intensity, changes in

[7] Barnes, Brattain and Seitz, Phys. Rev. **48**, 582 (1935).

shape, and ultimately, at the highest temperature, corresponding to nearly complete dissociation, resolves into two sharp and comparatively weak bands at 2.8 and 3.35μ, respectively. The C−H band, at 3.35μ in the monomer, is almost

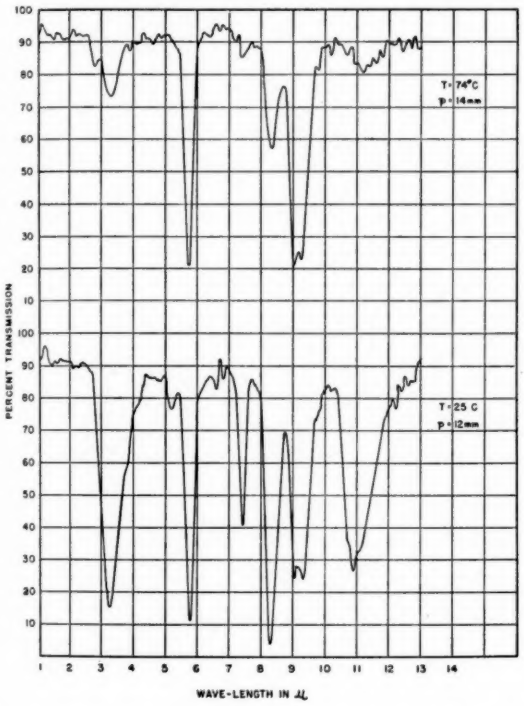

FIG. 2. Absorption bands in formic acid vapor; side tube in ice bath.

certainly very little affected by the association. It is, therefore, a reasonable assumption that the greatly enhanced intensity in this region in the dimer spectrum is due to a shifting of the O−H absorption down from 2.8μ. It is to be noted that the monomer O−H, at 3570 cm^{-1}, falls, as might be expected, in the region customarily assigned to O−H in vapors and dilute solutions.

Using the method of rigid groups and the equations presented in a previous paper[8] it is possible to calculate C−O and C=O force constants for the monomer. We obtain for these 5.4 and 11.8×10^5 dynes/cm, respectively. A considerable amount of evidence already presented[8] indicates that the normal value of the C−O force constant is not far from 4.5. We interpret the above value as indicating the existence of single-double bond resonance in the monomer, in accord with the prediction of Pauling and Sherman.[9] This interpretation is further borne out by an apparent shortening of the C−O bond in formic acid, recently found by Bauer and Badger.[10] The amount of resonance energy must, however, be less than that predicted by Pauling and Sherman.

DEUTERO-FORMIC ACID

Since the intensity arguments presented above are perhaps not sufficient proof of the coincidence of C−H and O−H−O frequencies in this type of molecule, an attempt was made to prepare the monodeutero derivative HCOOD. In this molecule, of course, the C−H frequency should remain unchanged and the O−D−O band should differ by a factor of approximately root two from its position in the normal molecule. The reduction to normal intensity of the C−H band and the appearance at approximately 4.25μ of an absorption band would confirm the above-mentioned coincidence.

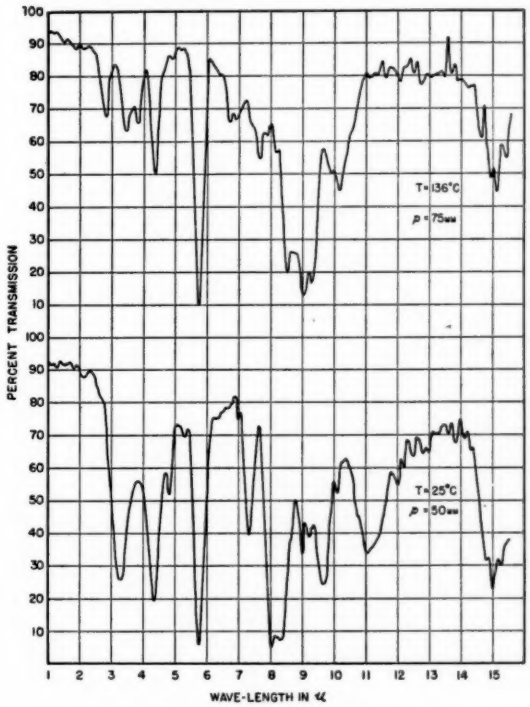

FIG. 3. Absorption bands in heavy formic acid vapor. The high temperature run shows that this material is actually an isotopic mixture of all four possible acids.

[8] Bonner, J. Chem. Phys. **5**, 293 (1937).

[9] Pauling and Sherman, J. Chem. Phys. **1**, 606 (1933).

[10] Bauer and Badger, J. Chem. Phys. **5**, 852 (1937).

An attempt was made to prepare HCOOD by passing D_2S (prepared from D_2O and Al_2S_3*) through a column of powdered lead formate at 100°C. The product was purified by distillation and the spectrum obtained over a temperature range as before. These spectra are reproduced in Fig. 3. It is to be noted that the highest temperature curve shows the presence of about equal amounts of C−H, C−D, O−H and O−D in the monomer. From this we conclude that adsorption and exchange has taken place on the surface of the hot lead formate powder and that the dimer curves represent the absorption of a statistical mixture of the four possible formic acids. That the exchange took place in the preparation and not in the cell was demonstrated, we believe, by a room temperature run in which the formic acid was placed in a cell sealed with glyceryl phthallate resin. The curve was identical with that obtained using a cell sealed with asbestos and glyptal.

As a result of further experiments by one of us (R. H.) it has been found possible to prepare the pure HCOOD by a different method and to observe its spectrum. These results will be published very shortly.

* We are indebted to Dr. John Turkevitch, of the Princeton Chemistry Department for supplying us with the pure Al_2S_3.

SEPTEMBER, 1938 JOURNAL OF CHEMICAL PHYSICS VOLUME 6

Vibration Spectra and Molecular Structure

V. Infra-Red Studies on Light and Heavy Acetic Acids[1]

R. C. HERMAN AND R. HOFSTADTER
Palmer Physical Laboratory, Princeton, New Jersey

(Received June 1, 1938)

The infra-red absorption spectra of CH_3COOH and CH_3COOD between 1 and 15.5μ have been obtained with a rocksalt prism spectrometer. The association of CH_3COOD has been studied and a value of the heat of dissociation obtained. Positions of the hydrogen and deuterium bonded O−H−O and O−D−O frequencies are given. Making certain assumptions, a value for the shorter O−H and O−D distances in the dimer rings is found to be 1.07A.

INTRODUCTION

AT room temperature the vapor of acetic acid consists chiefly of double molecules whose structure may be assumed to be similar to that of formic acid. The structure frequently assumed is the following:

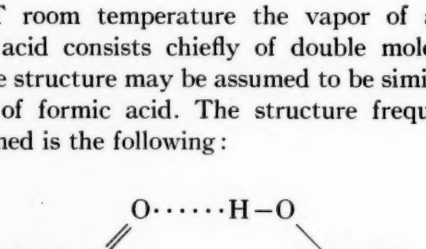

in which the two single molecules are linked by two hydrogen bonds. Several years ago Gillette and Daniels[2] studied the effect of association on the infra-red absorption spectrum of acetic acid vapor. By raising the temperature they were able to obtain the spectrum of the single molecules since from recent vapor density measurements[3] it is known that dissociation into single molecules is almost complete at about 150°C. Shifts and changes of intensity of certain bands were reported. However, no changes are mentioned in the high frequency region where vibrations involving hydrogen atoms are known

[1] Preliminary accounts of this work were given at the Washington meeting of the American Physical Society, April 1938, and in a Letter to the Editor, J. Chem. Phys. **6**, 110 (1938).

[2] Gillette and Daniels, J. Am. Chem. Soc. **58**, 1139 (1935).

[3] F. H. MacDougall, J. Am. Chem. Soc. **58**, 2585 (1936).

to occur.[4] Since the dissociation involves the breaking of two hydrogen bonds, one would expect some changes here if there is an infra-red active band associated with the hydrogen bond. In order to obtain more information concerning this point it was thought desirable to study d-substituted acetic acid (CH_3COOD). Such a substitution would alter the frequency of a band associated with the hydrogen bond, shifting it to about 4.3μ if this hydrogen vibration originally lay in the region of C−H valence vibrations.[5] The suggestion that the hydrogen bond vibration appears fused with the C−H valence vibration was made by Buswell, Deitz and Rodebush.[5] The close proximity of these two bands has also been mentioned by Badger and Bauer.[6] Whereas the "free" O−H valence vibration (fundamental at 2.75μ) has been observed, only weakly if at all, in the spectrum of the double molecule, Badger and Bauer report the second harmonic band to be characteristic of the single molecule of acetic acid. Errera and Mollet[7] have found corresponding results in the liquids of some fatty acids.

Experimental

Heavy acetic acid was prepared in vacuum by reacting Kahlbaum acetyl chloride with 99.6 percent pure heavy water. This method was previously employed by Engler.[8] The DCl as well as a small excess of acetyl chloride were chiefly removed by pumping. The CH_3COOD was further purified by three distillations. In each case all but a middle fraction was rejected. The vapor pressure of the final sample at low pressures (4 to 15 mm), agreed with that of Kahlbaum glacial CH_3COOH. In order to determine the ratio of deuterium to hydrogen in the acid position, the heavy acetic acid was reacted with magnesium and the evolved D_2-H_2 mixture was analyzed in a mass spectrograph.[9] This analysis yielded a D/H ratio of 95± about 0.1 percent.

The cells employed were constructed from Pyrex cylinders, 22 cm long, having ground glass flanges at either end to which cleaved rocksalt plates were sealed by means of a thin coating of glyptal No. 1201. This technique differs from that of Ebers and Nielsen[10] only in the use of cleaved instead of polished rocksalt windows. The glyptal was usually air dried over night and then baked out for several hours. A second coat of glyptal was then applied and treated in a similar manner. Both the cell for the substance and a similarly constructed vacuum cell were placed in a furnace provided with rocksalt windows. A side tube on the sample cell was led outside the furnace through a hole in one of the end plates. Before distilling the liquid to be studied into the side tube, the sample cell was baked out at about 140°C and simultaneously pumped for several hours. Throughout these experiments, the vapor was in equilibrium with liquid and its pressure was consequently the

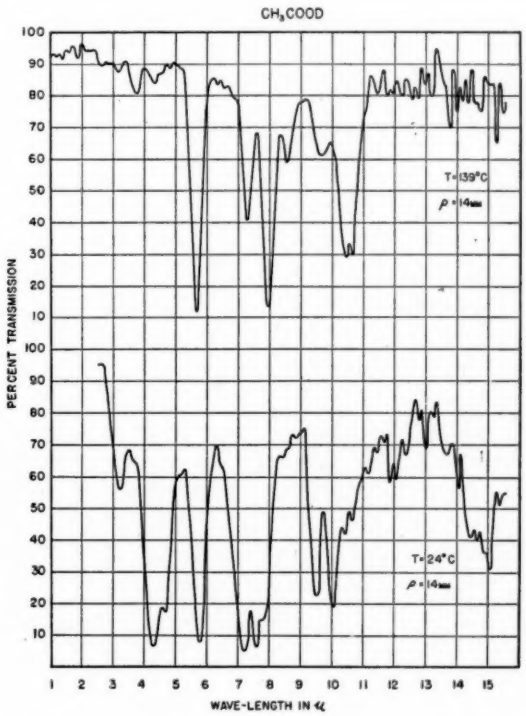

Fig. 1. Absorption spectrum of heavy acetic acid. Length of cell 22 cm.

[4] They report that the band at 2985 cm^{-1}, which they assign to the CH bond, is not affected by increase of temperature.
[5] Buswell, Deitz and Rodebush, J. Chem. Phys. **5**, 84, 501 (1937).
[6] Badger and Bauer, J. Chem. Phys. **5**, 839 (1937).
[7] Errera and Mollet, J. de phys. et rad. **6**, 2811 (1935).
[8] W. Engler, Zeits. f. physik. Chemie **B32**, 471 (1936).
[9] We wish to thank Drs. Hipple and Delfosse for kindly making these analyses.
[10] Ebers and Nielsen, J. Chem. Phys. **5**, 822 (1937).

vapor pressure of the liquid. A temperature bath surrounding the side tube permitted the pressure to be varied. Pressures were measured by means of a mercury manometer. A thermocouple was inserted in the furnace to measure the temperature which did not vary by more than about five degrees over the length of the cells. The furnace could be raised and lowered on ways so that it was possible to place either of the cells in the path of the radiation from the source. The technique described prevented the condensation of liquid on the windows. The rocksalt prism spectrometer employed has been previously described.[11] In obtaining the infra-red curves the transmission of the sample cell was compared to that of the vacuum cell at every tenth of a μ, several readings being taken per point whenever the transmitted energy was low. Certain band centers were located by taking readings about every fiftieth of a μ. All the spectra shown, except the exchange spectrum, have been obtained more than once, in particular at different pressures. Room temperature runs in cells sealed with Picein instead of glyptal gave the same spectra. Likewise, room temperature runs of samples that had previously been run at high temperatures showed no changes.

Results and Discussion

1. By the method described we have obtained the spectrum of heavy acetic acid at 24°C and at 139°C. These results are shown in Fig. 1. From dissociation data the calculated degrees of dissociation for these two cases are 9 percent and 97 percent, so that these curves very nearly represent the dimer and monomer spectra. It is to be noted that the band appearing at 4.35μ (2299 cm^{-1}) is very sensitive to changes in temperature. This fact alone makes it highly probable that this band is to be attributed to the deuterium bonded O−D−O vibration, since such a high frequency fundamental can be assigned to no other bond. If this frequency is increased by approximately a factor $\sqrt{2}$ which is demanded by a hydrogen replacement one would expect this band to be shifted to about 3.1μ in light acetic acid, and to be temperature sensitive as well. On comparing this expected behavior with the results reported by Gillette and Daniels,[2] it was felt desirable to restudy light acetic acid. The results of this investigation are shown in Fig. 2. The degrees of dissociation are 9 percent and 98 percent for the low and high temperature runs, respectively. The positions of the observed bands are in good agreement with those found by Gillette and Daniels with the exception of the band at 3.20μ (3125 cm^{-1}) which they report at 3.35μ (2985 cm^{-1}). As the curves show we again find a marked temperature dependence in conformity with the expectation that this frequency is to be associated with the hydrogen bonded O−H−O vibration.[12]

As the temperature is raised the ratio of single to double molecules increases and while the O−H−O or O−D−O bonded frequency diminishes in intensity, the "free" O−H or O−D appears. These frequencies appear at 2.75μ (3640 cm^{-1}) and 3.77μ (2653 cm^{-1}) respectively. The more or less normal values of

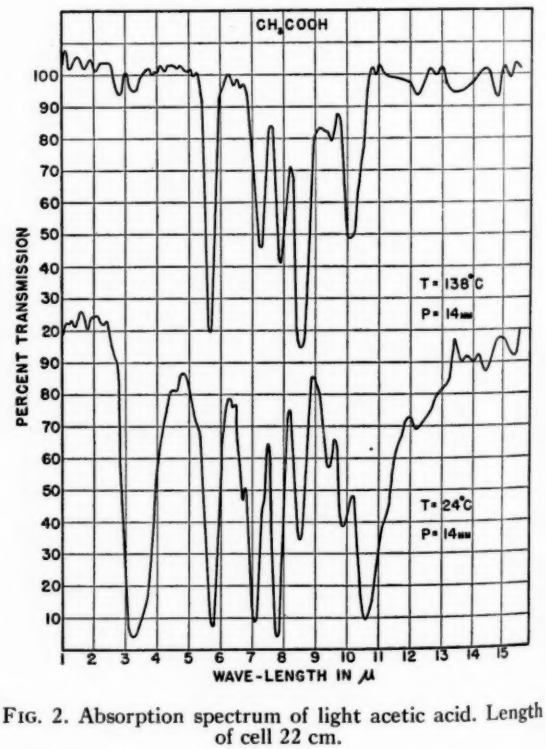

Fig. 2. Absorption spectrum of light acetic acid. Length of cell 22 cm.

[11] Barnes, Brattain and Seitz, Phys. Rev. **48**, 582 (1935).

[12] Buswell and Rodebush, J. Chem. Phys. **5**, 296 (1938), from their studies on the carboxylic acids, believe that the hydrogen bond absorption lies near 3.2μ.

these frequencies suggest that the H or D atoms are linked to only one oxygen atom in the single molecule.

In both light and heavy acetic acids the monomer and dimer spectra are quite different. Apart from the changes already mentioned, which are concerned with hydrogen vibrations, we find numerous changes in intensity, the disappearance of certain bands, the appearance of others, as well as shifts.

In Table I we have tabulated our frequency

TABLE I.*

CH_3COOH			CH_3COOD		
MONOMER	DIMER	PROBABLE ASSIGNMENT	MONOMER	DIMER	PROBABLE ASSIGNMENT
3640±70		O−H	3840±140		
	3125±19	O−H−O			
3030±45	?	C−H	3175±70	3125±50	C−H
			2653±15		O−D
			2299±15†	2299±11	O−D−O
				2127±25	
1770±7	1739±9	C=O	1770±6	1736±6	C=O
	1493±20				
1381±5	1418±4	δC−H	1377±3	1387±4	δC−H
				1315±9	
1266±8	1282±8	*C−O*	1266±8	1258±8‡	*C−O*
1176±6	1176±6	*δO−H*	1176±6§		
1053±10	1058±5		1042±10	1058±5	
	1010±5			1000±5	
985±10		*C−C*	953±5	953±9‡	*C−C*
	938±7				
	820±10			840±8	
				667±30	

* The italicized *C−O*, *δO−H* and *C−C* assignments have been suggested by preliminary work on CD_3COOD.
† Probably due to a small amount of dimer.
‡ Probably due to a small amount of monomer.
§ Possibly due to five percent impurity of CH_3COOH.

measurements of the more prominent bands found in CH_3COOH and CH_3COOD with rather generous estimates of probable errors. The complexity of all these spectra make impossible a complete assignment of bands at the present time. However, certain bands may be identified with confidence. These identifications have been noted in the table.

In light acetic acid three bands shift appreciably. The C=O frequency which appears at 1739 cm^{-1} in the dimer shifts to 1770 cm^{-1} in the monomer, a change of 31 cm^{-1}. A slightly larger shift occurs for the band at 1418 cm^{-1} in the dimer. The fact that so large a shift is observed in the latter case is surprising if this is really a C−H bending vibration. The band at 1282 cm^{-1} shifts by 16 cm^{-1}, appearing at 1266 cm^{-1} in the monomer. Gillette and Daniels

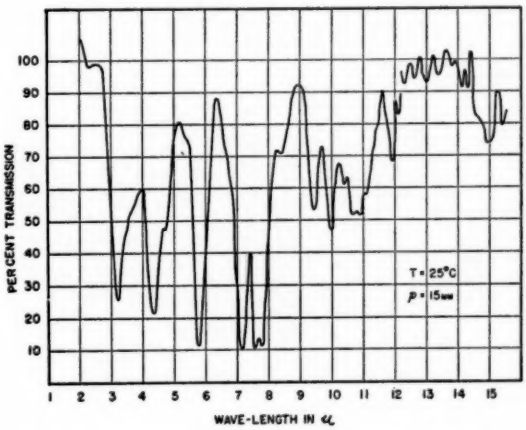

FIG. 3. Exchange spectrum. Length of cell 15 cm.

report two bands in the dimer spectrum at 1740 and 1435 cm^{-1} which shift by 46 and 37 cm^{-1}, appearing in the monomer at 1786 and 1398 cm^{-1}, respectively. They also find a band in the dimer at 1296 cm^{-1} which is reported at 1288 cm^{-1} in the monomer. Thus we find qualitative agreement in the directions and approximate magnitudes of the shifts although the band centers are in slight disagreement. In the region beyond 9.1μ in the monomer spectrum we find the appearance of a new band at 985 cm^{-1}.

It is of interest to note the great intensity of the O−D−O band in CH_3COOD, which suggests the highly polar character of the hydrogen bond.[13] A smaller band occurs at 2127 cm^{-1} on the long wave-length side of the O−D−O band. A similar result has been found in the spectrum of formic acid.[14] The O−H−O band at 3125 cm^{-1} is likewise of great intensity and shows an asymmetry on its long wave-length side. The asymmetry can possibly be correlated with the 2127 cm^{-1} band. The C=O frequency in heavy acetic acid is observed at the same position as in light acetic acid and shifts in the same direction by the same amount, within the experimental error. The 1377 cm^{-1} band shifts by the small amount of 10 cm^{-1}. The new band in the monomer spectrum at 953 cm^{-1} probably corresponds to the 985 cm^{-1} frequency of the CH_3COOH monomer. Among the differences between the dimer spectra of the light and heavy acids one

[13] M. L. Huggins, J. Org. Chem. 1, 407 (1936).
[14] R. Hofstadter, Paper No. VI of this series.

further change appears especially noteworthy. The band at 938 cm^{-1} in CH_3COOH appears to shift to 667 cm^{-1} in CH_3COOD and therefore seems to be due to a vibration directly involving a hydrogen atom.

In one run upon CH_3COOD some asbestos paper was present in the form of washers between the windows and cell. After heating the vapor in this cell to 124°C the temperature was reduced to room temperature and a run taken. The curve obtained is shown in Fig. 3. This is clearly the result of an exchange because the superposition of the spectra of light and heavy acetic acids shows all the bands observed in this spectrum. It is not clear whether the exchange occurred catalytically between the methyl and acid group or is a result of impurity within the asbestos.

2. The heat of dissociation of molecules held together by hydrogen bonds can be obtained from the dependence of the equilibrium constant on temperature as determined by means of vapor density measurements. According to Fenton and Garner[15] the heat of dissociation of acetic acid is 13,790 cal. per mole, whereas Nernst and von Wartenburg[16] find 15,000 cal. per mole. MacDougall[3] made what is probably the most careful determination and obtained 16,400 cal. per mole. Since there are two O−H−O bridges in the dimer ring this last value corresponds to a dissociation energy of 8200 cal. per mole for each hydrogen bond. Recently Badger and Bauer[17] investigated the dependence on temperature of the intensity of the second harmonic of the O−H band in acetic acid. They remark that because of the difficulty of making photometric determinations of intensity, their individual determinations do not claim the accuracy of MacDougall's measurements. However, in the region where their accuracy was greatest, the best straight line through their points does not deviate greatly from MacDougall's which is represented by

$$\log_{10} K_p = 11.789 - 3590/T.$$

We have made an attempt to find the heat of dissociation using one of the fundamental bonds of CH_3COOD. Since the hydrogen bonded O−H−O frequency falls in the region of C−H valence vibrations [5, 6, 1, 18] it was not possible to investigate light acetic acid by means of its fundamental bridge frequency. The substitution of a D for an H atom in the acid position shifts this frequency, now the deuterium bonded O−D−O frequency, to a region unoccupied by other bands, making it possible to study the dependence of association on temperature in CH_3COOD.

Setting the spectrometer at the center of the 2299 cm^{-1} band, intensity measurements were made for various total pressures at given temperatures between room temperature and 145°C. In order to obtain a greater percentage of dimer in the vapor than we have worked with, it would have been necessary to cool the vapor below room temperature. This would have been very inconvenient with our experimental arrangement. However, if one were to cool the vapor to 5°C the degree of dissociation would only change from 9 percent to 6 percent. Since it was not possible to obtain 100 percent dimer, we could not directly determine the dependence of transmission on the number of grams of dimer in the cell. This dependence can be obtained by means of the "free" O−D band at 3.77μ, since at or slightly higher than 145°C the vapor is almost completely dissociated. However, the resolving power of the instrument employed was not great enough to study this band; the neighboring 4.35μ band affected the results. Instead, we assumed MacDougall's values for the degree of dissociation α at 38.5°C and calculated the partial pressure of dimer P_D from the relation

$$P_D = \frac{1-\alpha}{1+\alpha} p,$$

in which p is the total pressure. Since our total pressures were low, rarely greater than 22 mm, we may apply the gas law

$$P_D V = N_D R T,$$

to find the number of moles of dimer in the volume of the cell, V, at a given temperature T.

[15] Fenton and Garner, J. Chem. Soc. 694 (1930).
[16] Nernst and von Wartenburg, Zeits. f. Elektrochem. u. angew. physik. chemie **22**, 37 (1916).
[17] Badger and Bauer, J. Chem. Phys. **5**, 605 (1937).
[18] Bonner and Hofstadter, J. Chem. Phys. **6**, 531 (1938).

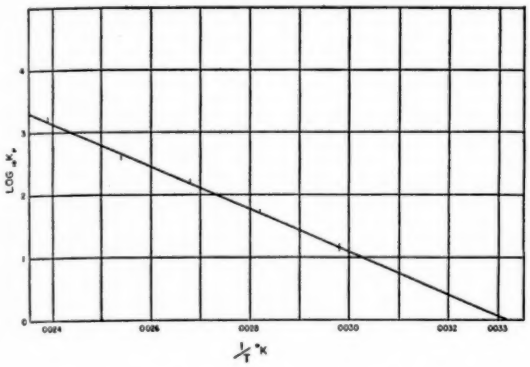

FIG. 4. Equilibrium constant for CH_3COOD.

This leads to a knowledge of the dependence of the transmission on $\rho_D = N_D/V$ since we experimentally determined its dependence on p at a given temperature. Employing this calibration curve it was possible to find α from the relation

$$\alpha = (p - \rho_D RT)/(p + \rho_D RT).$$

At each temperature the dissociation constant K_p can be evaluated from the equation

$$K_p = 4\alpha^2 p/(1-\alpha^2).$$

K_p is defined as p_M^2/p_D in which p_M and p_D are the partial pressures of monomer and dimer, respectively. Fig. 4 gives the plot of $\log_{10} K_p$ *vs.* $1/T$. The heights of the vertical lines give the spread in $\log_{10} K_p$, and contain on the average about five points. From the slope of the curve one finds the heat of dissociation to be 15,900 cal. per mole or 7,950 cal. per mole per bond. This is to be compared with MacDougall's value 8200 calories. Our experimental error estimated at roughly ± 700 cal. is too large to distinguish between the heats of dissociation of light and heavy acetic acids.

The use of a deuterium substitution for investigating dissociation processes spectroscopically may be of some value in examining other aliphatic or aromatic compounds.

3. The electron diffraction experiments of Pauling and Brockway[19] have shown that in formic acid the O−O distance is 2.67A. Since this work did not locate the hydrogen atoms in the ring some calculations have been made in an attempt to do so. For instance, a quantum-mechanical calculation by Gillette and Sherman[20] indicated that the dimer ring of formic acid is stable if the hydrogen atoms lie on the O−O line of centers and at the normal O−H distances. The system was shown to be less stable if the hydrogen atoms lie midway between the oxygens. With the H atoms at the normal O−H distances, values of the bridge length and heat of dissociation were calculated and found to be in poor agreement with experiment. Barnes, Bonner and Condon[21] assumed that the hydrogen lies somewhere along the perpendicular bisector of the line joining the oxygen atoms considered stationary and calculated frequencies for various configurations. They obtained an upper limit of 2390 cm^{-1} for the frequency in the case in which the hydrogen atom is situated midway between the oxygen atoms. This does not agree with the experimentally observed bridge frequency of about 3100 cm^{-1}, which was not known at that time.

We have made a similar calculation with the acetic acid dimer ring considered to have a structure identical with that of formic acid. We have assumed that the O−H−O and O−D−O groups in the dimer rings of light and heavy acetic acids can be treated approximately as asymmetric linear triatomic molecules. We have further assumed that the force constants involved vary inversely with the cube of the equilibrium distance according to Badger's formula[22]

$$k = \frac{1.86 \times 10^5 \text{ dynes}}{(r_e - d_{ij})^3} \frac{}{\text{cm}},$$

in which d_{ij} is a constant depending on the atoms involved. Calculations were made for various O−H and O−D distances. If the shorter O−H or O−D distance is taken as 1.07 ± 0.01A the experimental O−H−O and O−D−O frequencies, 3125 and 2299 cm^{-1}, respectively, are checked to within better than 1 percent. This distance is to be compared with the normal O−H distance of 0.97A. In view of the assumptions

[19] Pauling and Brockway, Proc. Nat. Acad. Sci. **20**, 336 (1934).

[20] Gillette and Sherman, J. Am. Chem. Soc. **58**, 1135 (1936).

[21] Barnes, Bonner and Condon, J. Chem. Phys. **4**, 772 (1936).

[22] R. M. Badger, J. Chem. Phys. **2**, 138 (1934).

made we do not feel that too much confidence can be placed in this value for the distance. However, if we use the distances 1.07 and 1.60A, the stretching force constants appear to be 4.68 and 0.91×10^5 dynes/cm.

Acknowledgments

We wish to express our appreciation to Mr. R. R. Brattain for considerable assistance and helpful advice. Professors Dougherty and Wallis of the Chemistry Department have very kindly discussed some chemical problems with us. We are thankful to Mr. René Puech for assistance in taking some readings. Professor W. Bleakney has taken an interest in this work which we sincerely appreciate. Finally, we are very grateful to Professor R. Ladenburg for his sustained interest and encouragement.

SEPTEMBER, 1938 JOURNAL OF CHEMICAL PHYSICS VOLUME 6

Vibration Spectra and Molecular Structure

VI. Infra-Red Absorption Spectrum of Heavy Formic Acid[1]

ROBERT HOFSTADTER
Palmer Physical Laboratory, Princeton, New Jersey
(Received June 1, 1938)

The infra-red absorption spectra between 1 and 15.5μ of the monomer and dimer of HCOOD have been found with a rocksalt prism spectrometer. The position of the vibration characteristic of the "deuterium bond" in HCOOD has been determined and permits an approximate calculation of the shorter OD distance in the dimer ring. As in CH_3COOD the distance is found to be 1.07A.

Introduction

SOME time ago Dr. L. G. Bonner and the author[2] were interested in investigating light formic acid vapor (HCOOH) in the infra-red with the hope of finding particulars concerning the hydrogen bond and molecular structure of the acid. Electron diffraction studies of formic acid[3] indicate that the structure of the double molecule is that shown below.

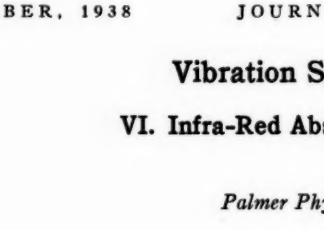

Since the vapor of the acid consists of an equilibrium mixture of double and single molecules[4] it was hoped that by raising the temperature and thus promoting the dissociation, the absorption band or bands associated with the hydrogen bond might be recognized and followed as the transition between the double and single molecules progressed. In agreement with these ideas, profound changes were observed in the spectrum on passing from room temperature to higher temperatures. However, these results alone were not sufficient to fix unambiguously either the position or relative intensity of the hydrogen bond band in formic acid, for a very great decrease in intensity of absorption was observed at about 3.25μ where unfortunately the CH commonly appears. One could not say whether this change was due to a changing CH intensity or, indeed, to the hydrogen bond, although the latter possi-

[1] These results were reported in part in the Washington Meeting of the American Physical Society, April 1938.
[2] Phys. Rev. **51**, 1017 (1937) and Paper No. IV in this series.
[3] Pauling and Brockway, Proc. Nat. Acad. Sci. **20**, 336 (1934).
[4] A. S. Coolidge, J. Am. Chem. Soc. **50**, 2166 (1928).

bility seemed more plausible.[5, 6] It was therefore decided to investigate the deuterium substituted acid (HCOOD). In this case the "deuterium bond" would have a frequency smaller than that of the hydrogen bond by a factor of approximately $\sqrt{2}$. If the band at 3.25μ were really to be connected with the hydrogen bond, then a new one ought now to appear at roughly 4.3μ.

To obtain HCOOD the reaction $D_2S+PbFo_2 = PbS+2DFo$ was used. Unfortunately only a statistical mixture of the light and heavy acids was produced. Apparently internal exchange occurred on the surface of the $PbFo_2$ column, so that the four forms HCOOH, HCOOD, DCOOH, DCOOD were finally present in equal amounts. CD and OD, of course, behaved exactly as CH and OH; consequently, no more could be learned than from a study of HCOOH. Moreover there was a great complexity and richness of bands in the spectrum.

Recently it has been possible to prepare moderately pure HCOOD, and it is with this compound that the present paper is concerned.

Experimental

Preparation

The first attempt to eliminate the mixed forms was to reduce the temperature of the $PbFo_2$ column from 100°C previously used to room temperature. This gave no appreciable improvement so that an entirely different method of preparation was used. At the suggestion of Professor Taylor and Dr. Turkevich, a simple exchange was tried between HCOOH and 99.5 percent D_2O, with subsequent drying of the acid-water mixture with anhydrous $CuSO_4$.[7] The HCOOD samples obtained by this process were still not entirely pure, probably because of exchange with light water introduced in the drying process. However, the mixtures obtained by this method contained only the two monomeric forms HCOOD and HCOOH as shown by the absence of any CD absorption in the monomer spectrum. The ratios of the amounts of heavy to light forms, denoted by D/H, of several samples were respectively 3.5, 8, 12.4. The first and last of these ratios were determined by analysis in a mass spectrograph of the H_2-D_2 mixtures obtained by reacting Mg strips with the acid samples.[8] The middle ratio was found by comparing the depths of the OD and OH bands found in a high pressure run of the monomer spectrum. Good agreement between these two methods was obtained for the ratios D/H = 1.0, 3.5. This investigation confirmed the earlier conclusions regarding the amounts of the four forms present in the mixed acid.[2]

The HCOOH was supplied by Kahlbaum and was distilled until the vapor pressure agreed with the determinations of Coolidge.

Analysis

All spectra were obtained with the spectrometer described by Barnes, Brattain and Seitz.[9] The cells, furnace, etc. were all similar to those used in an investigation of acetic acid.[10] After the high temperature runs were taken, the region $1-5\mu$

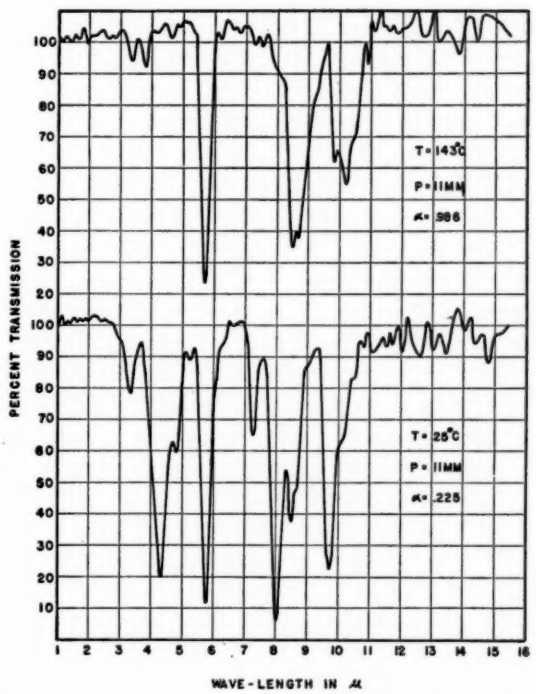

FIG. 1. Absorption spectrum of HCOOD. D/H = 8.0. Length of cell = 22 cm.

[5] Buswell, Deitz and Rodebush, J. Chem. Phys. **5**, 84, 501 (1937).
[6] Badger and Bauer, J. Chem. Phys. **5**, 839 (1937).
[7] That this exchange goes was proved by Münzberg and Oberst, Zeits. f. physik. Chemie **B31**, 18 (1935).
[8] I wish to thank Drs. Hipple and Delfosse for kindly doing these analyses.
[9] Barnes, Brattain and Seitz, Phys. Rev. **48**, 582 (1935).
[10] Herman and Hofstadter, Paper No. V in this series.

was re-run at room temperature to see whether any exchange had taken place in the cell. No significant changes were observed other than those which were due to differences in running conditions. Even after several days there were no important changes. This indicates that spontaneous exchange within or between HCOOD molecules is slow, if it exists at all. This is in agreement with the work of Münzberg and Oberst mentioned above.

Results and Discussion

Figures 1 and 2 show the spectra obtained for two samples with the D/H ratios 8 and 12.4. Even though the samples were run at different pressures one may see from the curves that further purification would probably lead to no serious changes.[11] Indeed, the sample for which the D/H ratio was 3.5 presented a very similar set of spectra. The degree of dissociation, α, was determined from the dissociation data of Coolidge.

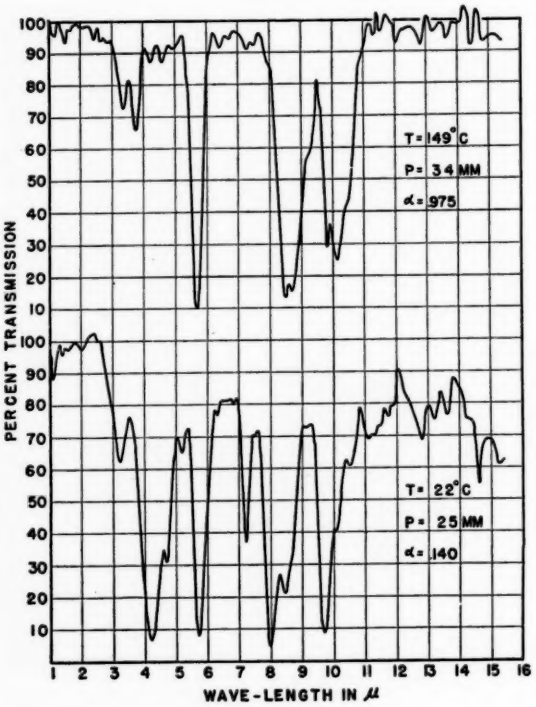

Fig. 2. Absorption spectrum of HCOOD. D/H = 12.4. Length of cell = 22 cm.

[11] The ratios of dimers containing one H and one D to those containing two D's are only half the above values, namely 4 and 6.2.

Since the degree of dissociation at room temperature and the pressures shown is in the neighborhood of 18 percent we may consider the lower curves to represent the dimer. The upper curves are certainly spectra of the monomer for α is very close to 1. Table I lists the frequencies found by averaging the band centers for the corresponding curves in the two figures.

Table I. HCOOD.

Monomer			Dimer		
cm^{-1}		Probable Assignment	cm^{-1}		Probable Assignment
3003	±60	C−H	3030	±46	C−H
2667	35	O−D			
2347	35*		2347	33	O−D−O
2105	30*		2105	22	
			1916	16	
1764	16	C=O	1736	15	C=O
			1381	11	
			1253	10	
1163	6	C−O?	1181	7‡	C−O?
1081	15†				
1030	5		1030	5	
980	5		985	10‡	
953	8		950	8‡	
			901	7†	

* Very small and probably due to small amount of dimer.
† Probably due to 7.5 percent impurity of HCOOH.
‡ Probably due to small amount of monomer.

The dimer spectrum of HCOOD shows a strong, broad band at about 4.26μ (2347 cm^{-1}) which is overlapped somewhat by a weaker band on the long wave-length side at 4.75μ (2105 cm^{-1}). The band at 4.26μ must then be that which characterizes the deuterium bond in heavy formic acid. Further proof that this assignment is correct is obtained from the dissociation results, for this band is absent in the monomer and belongs solely to the dimer, where the deuterium bonds occur. No other reasonable choice for such a high frequency can be made. One sees how small the CH bands of the monomer and dimer are. The strong absorption at 3.25μ found in light formic acid may now be explained as being chiefly due to the hydrogen bond, in agreement with the earlier ideas.[2] Correlated with the disappearance of the bonded band, we see the emergence of a small band at 3.75μ (2667 cm^{-1}). This is to be attributed to a "free" OD valence vibration. Results similar to those just mentioned have been found in light and heavy acetic acids[10]

TABLE II.

HCOOH		HCOOD	
Obs.	Calc.	Obs.	Calc.
1740 cm^{-1}	1744 cm^{-1}	1764 cm^{-1}	1741 cm^{-1}
1093	1093	1162	1083
650?	579	667	572

and in the liquid of ethyl alcohol where a similar association has been assumed to take place.[12]

From the position of the O−D−O band in the dimer, the approximate distance between the D and the nearest oxygen in the dimer ring may be calculated. It is assumed here that the O−D−O vibration frequency in the molecule may be computed from a linear asymmetric triatomic model where the O−O distance is 2.67A, with force constants evaluated by application of Badger's rule.[13] A similar calculation can be made using the O−H−O frequency at 3077 cm^{-1}. The best fit for the shorter O−H, O−D distance is 1.07A. Using this distance the two calculated frequencies check the observed ones to better than 2.6 percent. This same calculation for the acetic acid dimers furnishes the identical value, 1.07A.[10]

The monomer spectrum of HCOOD presents an interesting detail in the appearance of an intense band at 8.6μ (1163 cm^{-1}). In comparison with one of the fundamentals of HCOOH (1093 cm^{-1}), this band is shifted towards higher frequency. The similar shape and approximate position of this band suggest that it is to be attributed to the same bond (C−O), since the band at 1093 cm^{-1} in HCOOH has definitely been assigned to this vibration. If this assignment for the 8.6μ band be correct, the shift towards greater frequency cannot be explained as a mere mass effect, for one would expect a decrease in frequency on substitution of a heavier mass in the hydroxyl group (see Table II).

One may calculate the frequencies of a simplified triatomic model of the HCOOD molecule by the method of rigid groups. This method was previously employed in finding the force constants for a similar triatomic model of HCOOH.[2] The force constants yielded in this way, 11.8, 5.4, 0.4×10^5 dynes/cm, were used to compute the new frequencies shown in Table II, where for convenience the data on HCOOH are also collected.

In connection with this anomalous behavior it is to be noticed that the calculated frequency for the C−O bond lies about midway in the frequency interval between the bands at 8.6μ (1163 cm^{-1}) and 10.2μ (980 cm^{-1}). No adequate explanation for this behavior has been worked out, although there is a possibility that these two bands furnish another example of an accidental degeneracy.

No interpretation of the dimer spectrum has been made beyond 6.0μ.

ACKNOWLEDGMENT

I wish to thank Professors Taylor and Menzies and Dr. Turkevich of the Chemistry Department for suggestions concerning the chemical preparation. I also wish to thank Professor Eyring of the Chemistry Department for a very profitable conversation. I am obliged to Mr. R. C. Newton, who kindly performed a chemical determination. Professors Ladenburg, Bleakney and Smyth have given me encouragement and helpful criticism for which I am grateful. Finally, I am indebted to Mr. R. R. Brattain for his kind assistance and advice.

[12] Errera and Mollet, Comptes rendus **204**, 259 (1937).
[13] R. M. Badger, J. Chem. Phys. **2**, 128 (1934).

Raman Spectrum and Fluorescence of Dioxane

HUGH W. HUNTER
Department of Physics, Indiana University, Bloomington, Indiana
(Received June 13, 1938)

A. The Raman spectrum of dioxane is shown to include eleven lines, some of which have been reported by one or both of two previous investigators. B. Dioxane, when irradiated by the ultraviolet light from a mercury arc, gives scattered light whose spectrum shows a broad continuous band in the visible region. Intensity of the scattered band diminishes rapidly with increasing temperature of the dioxane. Shortened time exposures bring out two maxima at about 5800A and 4500A. A similar phenomenon has been observed in work on cyclohexane.

A. RAMAN SPECTRUM OF DIOXANE

DURING an investigation on the conductance of solutions of certain organic salts, it became desirable to know something as to the Raman frequencies of the solvent dioxane, 1–4 diethylene oxide. Dioxane has been studied previously by two independent experimenters, Villars[1] and Wolkenstein and Syrkin,[2] but their results were not completely in agreement, even though both used the same region of the mercury spectrum for their work. The former reported ten frequencies, the latter eleven, with agreement on only six values. Since the frequency shifts measured in the first work were duplicated almost identically in the second, the disagreement obviously arose from doubtful assignment of shifted lines to proper "parent" mercury frequencies.

The values reported here rest upon measurements, made in the near ultraviolet, of frequency shifts from the pair of mercury lines 3125.6A and 3131.6A. These two lines, being almost equal in intensity, gave modified lines that were paired in characteristic fashion, and it was possible to relate each shifted line with its unmodified "parent" without ambiguity.

Dioxane was prepared by Dasher.[3] The commercial product was frozen (freezing point 11.7–11.8°C) to remove the major part of the water, melted and refluxed with sodium hydroxide to remove methylene acetal, and then repeatedly refluxed, first with quick-lime and then with sodium, until the resultant solvent did not tarnish bright sodium. The final product had a specific conductivity of $1\text{–}2\times10^{-16}$ ohm^{-1}, and a density of 1.02766 (25°C).

The spectrograph employed was a Hilger E-3 quartz spectrograph, having a dispersion in the region of the spectrum used (3000–4000A) of about twenty angstroms per millimeter. Exposure time varied from one to eight hours. The light source was a quartz mercury arc with a luminous column ten centimeters long. Both glass and quartz containing tubes were used, and their shape and arrangement were according to that described by Wood.[4] The temperature of the dioxane was controlled by a smooth sheet of water that flowed over the tube and was carried away by an aluminum reflector below.

Results are indicated in Table I. Eleven frequency shifts were measured, the modified

TABLE I. *Raman frequency shifts for dioxane in wave numbers per centimeter. Numbers in parentheses indicate relative intensities.*

I	II	III	IV
VILLARS	WOLKENSTEIN, SYRKIN	THIS DETERMINATION	AVERAGE
291 (0)		288 (0)	290
434 (00)?	427 (3)		
	487 (3)	493 (1)	490
519 (00)?			
837 (4)	836 (10)	837 (5)	*837*
	940 (2)		
	1017 (5)	1018 (4)	1018
1117 (1)	1115 (5)	1113 (3)	*1115*
1214 (1)	1213 (3)	1211 (2)	*1213*
	1306 (5)	1303 (4)	1304
1442 (2)	1450 (6)	1450 (5)	*1450*
2720 (00)		2724 (2)	2722
2864 (3)	2862 (10)	2858 (10)	*2861*
2967 (3)	2971 (10)	2976 (10)	*2972*

[1] Villars, J. Am. Chem. Soc. **52**, 4612 (1930).
[2] Wolkenstein, Syrkin, J. Chem. Phys. **3**, 594 (1935).
[3] Paul J. Dasher, thesis, Indiana University (1937).
[4] R. W. Wood, Phil. Mag. **6**, 729 (1928); Phys. Rev. **36**, 1421 (1930).

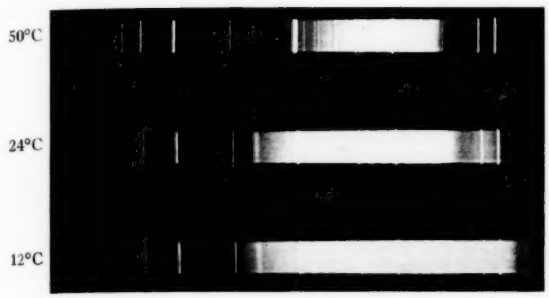

FIG. 1.

lines in every case appearing in pairs having the configuration of the originating mercury lines, 3125.6 and 3131.6A. Measurements were accurate to ±6 wave numbers per centimeter. The six values previously reported both by Villars[1] and by Wolkenstein and Syrkin[2] were confirmed closely; of the remaining five, two agreed with Villars' original report, and three agreed with the values given by Wolkenstein and Syrkin.

In Table I, the first two columns list final values taken from the two earlier reports. The results of the present determination appear in the third column, and shifts verified definitely by two independent determinations are given in column four. The six frequency shifts confirmed in all three cases are italicized.

B. FLUORESCENCE

In the course of the determination of the Raman spectrum of dioxane, it was observed that the spectrum of the scattered light exhibited a strong continuous band in the visible region when a quartz mercury arc and a quartz containing tube were used. Reduced time exposures brought out distinct bands, with maxima at about 5800A and 4500A. The band of shorter wave-length was the broader of the two, extending well below 4000A.

When a glass containing tube of the same dimensions was substituted for the quartz tube, the continuous background disappeared. A thin glass filter produced the same result, an indication that the fluorescence was due to the irradiation of the dioxane by ultraviolet light below 2900A.

The intensity of the fluorescence was found to diminish rapidly with increasing temperature of the dioxane. At 12°C (freezing point 11.8°C) there resulted a strong continuous spectrum extending from 3400A entirely through the visible range. With higher temperatures of the dioxane, and with all other conditions unchanged, the two maxima were evident, and the extent of the spectrum was reduced at both ends. At temperatures as high as 50°C the long wave-length component disappeared, and the remaining band was limited to a region between about 4000A and 5000A. These results are shown in Fig. 1 which represents three exposures made consecutively on the same plate. The only factor changed during the series was the temperature of the dioxane, as indicated. Exposure was for three hours.

Continued irradiation of the dioxane with ultraviolet light did not affect the transparency of the liquid. Dioxane exposed for a period of three days showed the same fluorescence as that exhibited by a fresh sample.

A phenomenon similar to that just described was found by Karl Haberl[5] during an investigation on the intensity of the Raman lines of cyclohexane, C_6H_{12}. He reported that the intensity of the fluorescence from cyclohexane was negligible for temperatures above 20°C, increasing rapidly with diminishing temperatures to 8°C, the liquid freezing at 5°C. He also found two maxima, at 4000A and 2900A.

[5] Karl Haberl, Ann. d. Physik **21**, 301 (1934).

An Infra-Red Study of Several Liquid Crystals

RICHARD TASCHEK AND DUDLEY WILLIAMS
University of Florida, Gainesville, Florida

(Received June 23, 1938)

The near infra-red spectra of three liquid crystals have been studied in the isotropic and anisotropic phases, and several band shifts have been observed. A detailed study of the transmission as a function of temperature was made at various wave-lengths. Pronounced changes in transmission were observed at melting and clearing points, the magnitude of the changes being greater at short wave-lengths. Rapid variations in transmission occurred in the mesophase. A qualitative explanation of the observed changes is given in terms of Ornstein's theory of scattering. The application of infra-red methods to the study of changes of state is discussed.

INVESTIGATIONS of the infra-red spectra of associated liquids have yielded information concerning the nature of the associational groups and the "structure" of the liquids themselves. The vibrational spectra of the liquids differ from those of the corresponding vapors in two principal respects: (1) the frequencies of certain atomic groups may be modified, and (2) new intermolecular bands may appear. The variation in the 3μ alcohol bands is illustrative of the first effect, while the 4.7μ, 20μ, and 60μ bands in the spectrum of liquid water are examples of the second. It has been suggested[1] that valuable information might be obtained from a study of the infra-red spectra of liquid crystals, in which the degree of association is known to be exceedingly high. There are numerous difficulties involved in making such a study both on account of the complexity of the molecules themselves and because of the relatively large magnitude of the local lattices or swarms. Rawlins and Taylor[2] have reported their inability to detect differences between the spectra of the isotropic and anisotropic phases of compounds having liquid crystalline properties.

TABLE I. *Melting and clearing points of compounds.*

	MELTING POINT	CLEARING POINT
Compound I. Iso-amyl *p*-(*p*-ethoxy benzalamino) cinnamate	81°C	137°C
Compound II. Anisal-amino α-methyl-*n*-propyl cinnamic ester	50°C	85°C
Compound III. Iso-amyl *p*-(*p*-ethoxy benzalamino) α-methyl cinnamate	83°C	90°C

(Hereafter the compounds will be referred to by number.)

The compounds chosen for study because of their low melting points are listed in Table I and were prepared by Mr. J. P. Bain of the local chemistry department. The melting and clearing points listed are taken from the *International Critical Tables*. For compounds II and III the melting points could be checked visually, but measurements of the melting point of compound I were difficult on account of marked supercooling. Cooling-curve data on compound I gave the melting point 77°C, indicating the presence of an impurity. The orienting action of container walls introduces difficulties in the determination of melting and transition temperatures.

The spectrometer previously described[3] has been modified by the addition of an optical amplifier.* The temperature of the sample being studied was controlled by means of a small oil bath consisting of concentric brass cylinders. The rocksalt cell containing the sample was placed in a massive brass support in the center of the inner cylinder, cell temperatures being determined by a thermocouple brazed into the support close to the cell. It was impracticable to place a thermocouple in the thin absorbing layer itself. The control bath, mounted on horizontal ways, could be moved into and out of a vertical light beam.

The spectra of the compounds in the isotropic and anisotropic liquid states are shown in Fig. 1.

[1] F. I. G. Rawlins, Trans. Faraday Soc. **29**, 993 (1933).
[2] F. I. G. Rawlins and A. M. Taylor, *Infrared Analysis of Molecular Spectra* (Cambridge University Press, 1929), p. 63.
[3] D. Williams and R. Taschek, J. App. Phys. 8, 497 (1937).

* The writers wish to express their appreciation to the A. A. A. S. for a grant which made possible the construction of the amplifier.

the temperatures being indicated. In every case the temperature of the sample was first raised above the clearing point and then lowered by the desired amount. Cell thicknesses were of the order of several hundredths of a millimeter. Since no marked differences of band positions in the spectra of isotropic and anisotropic phases of compound I were observed, only a part of the spectrum of each phase is shown, 108°C data from 2μ to 7.5μ and 156°C data from 7.5μ to 12μ.

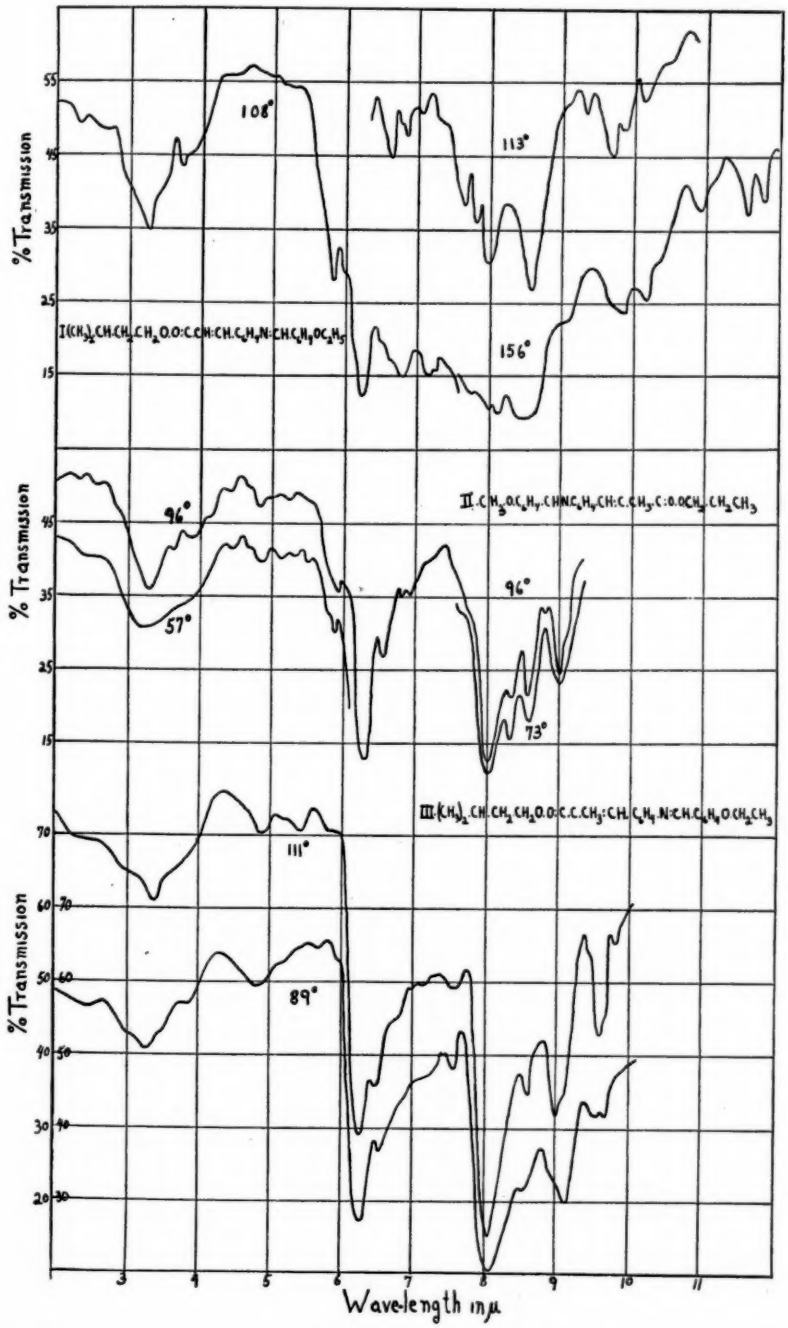

FIG. 1. The percentage transmission of compounds I, II, and III in isotropic and anisotropic liquid phases. The temperatures are indicated.

In order to observe bands which could not be resolved in thick samples, the 113°C data for an extremely thin cell were taken between 6.5μ and 11μ. For compound II no transmission curve for the anisotropic phase between 6.5μ and 7.7μ is shown, since the spectra of the two phases appear to be similar in this region. Although the spectra of the compounds are quite complex, the absorption arising from the inner vibrational frequencies of certain groups can be recognized. The bands near 3.3μ can be attributed to C−H vibrations, the broadness of the bands possibly arising from absorption by both aromatic and aliphatic groups. The bands near 6.9μ and 7.3μ in the spectra of most hydrocarbons were not observed, their presence possibly being masked by intense bands in adjacent spectral regions. The intense absorption with maximum at 6.25μ probably has its origin in the vibrations of the benzene ring, although the C=O, C=C, and C=N vibrations would be expected to give rise to bands in neighboring regions. It is difficult to assign the bands at 8.0μ, 8.6μ, 9.0μ, and 9.7μ to particular inner vibrations.

Although many slight shifts in band positions were observed, the shift of the 9.05μ band in the spectrum of compound III is especially noticeable. This band was studied at various temperatures and the transmission curves are given in Fig. 2. In the same figure are shown similar data for the 3.3μ band of compound I; in order to determine whether the orienting property of the surfaces had any effect on the observed spectrum, the curves on the left were obtained with a thin film between two rocksalt plates, while for those on the right the compound was spread upon a single plate. A study of the transmission at numerous temperatures shows the position of maximum absorption to be 3.27μ in the solid, 3.37μ in anisotropic, and 3.30μ in the liquid phase. The 6.25μ band showed a similar shift of 0.1μ to longer wave-lengths in the mesophase. Fig. 2 clearly indicates an increase in transmission and a change in band shape at higher tem-

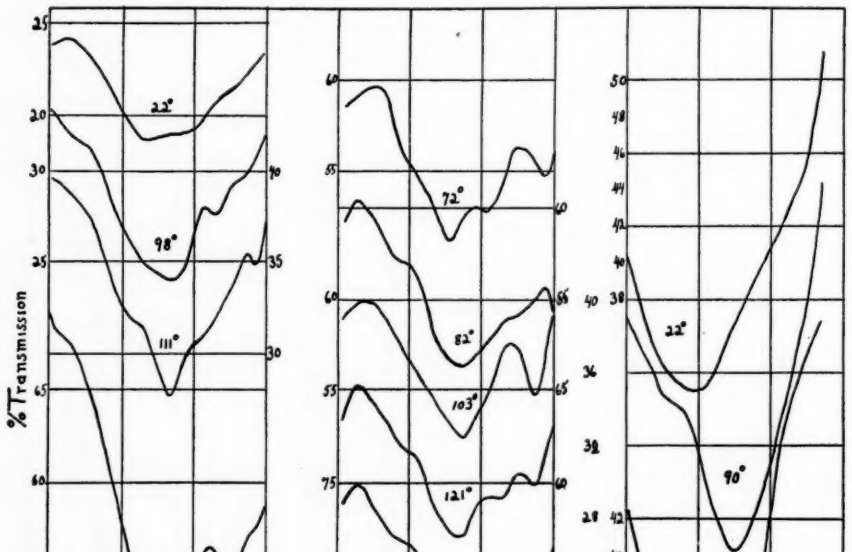

FIG. 2. The change in the position of certain bands with temperature variation: (*a*) 3.3μ band observed with compound I between rocksalt plates; (*b*) the same for a thin layer spread upon a single plate; (*c*) the 9.05μ band for compound III.

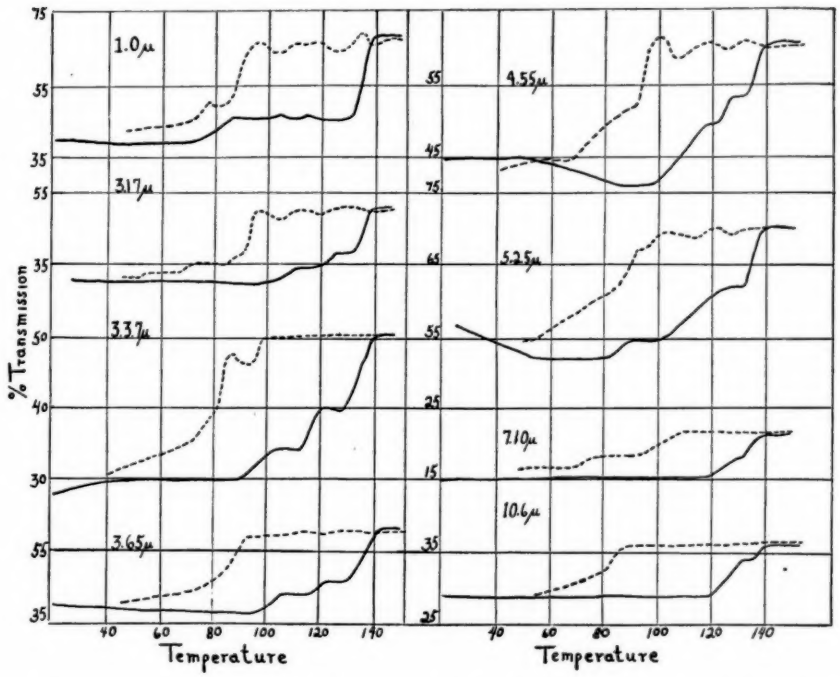

FIG. 3. Isochromatic curves for compound I showing percentage transmission as a function of temperature. The solid curve shows the data obtained while the temperature was being raised; the dotted line represents the data taken during cooling. *Note:* Isochromatics for a normal compound such as stearic acid show marked transmission increases only at the melting point.

peratures. The shift of the maximum apparently does not depend upon the method of supporting the sample. Although minor changes in the shape of the transmission curves are observed, no conclusions can be drawn as to the effects of the orienting action of the plates. The observed wave-length variation of the absorption maxima cannot be attributed to changes in the temperature of the prism, as the calibration was checked at each temperature by means of atmospheric bands.

The most pronounced difference in the spectra of the isotropic and anisotropic phases was a decrease in background transmission in the latter phase between 1μ and 6μ. Beyond 6μ there is little difference in intensity. The curves for compound III in Fig. 1 are illustrative of this decrease in transmission, as they were taken with the same sample. In order to study the variation in background transmission in more detail the data represented in Figs. 3, 4, and 5 were obtained. These curves indicate the transmission for given wave-lengths as the temperature was varied continuously. Readings were taken at two degree intervals from room temperature to temperatures well above the clearing point during heating and cooling; the rate of heating was approximately one degree per minute. All curves show an increase in transmission varying from 5 percent to 60 percent, the most rapid increase taking place over an interval including the clearing point. The transmission in the solid and isotropic liquid phases remains practically constant, as one might expect. Over the temperature intervals in which the compounds are in the anisotropic phase one or more "arrests" occur in the heating curves for compounds I and II, while sharp maxima and minima appear in those for compound III. In the cooling curves a marked "hysteresis" in transmission is apparent, the percentage transmission remaining constant until the temperatures of solidification are approached; at these points transmission decreases rapidly and subsequently approaches the values for the solid or anisotropic liquid. For example, the isochromatics for compound I show that on

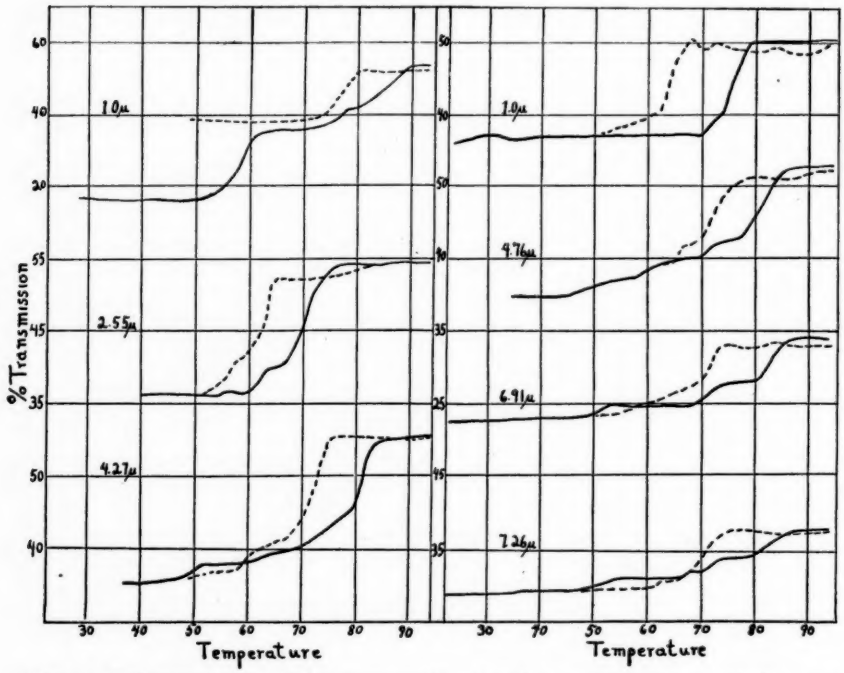

FIG. 4. Isochromatic curves for compound II showing percentage transmission as a function of temperature. Solid line represents heating measurements; the dotted line, cooling data.

cooling the sample invariably solidifies. For compound II two sets of 1μ data are shown, the first curve representing data obtained on initial heating; the other curves for this compound indicate that the low temperature data correspond to the transmission value for the anisotropic state. Other measurements show that thin films of compound II remain in a supercooled anisotropic state for several days. A similar effect was observed in the case of compound III, although supercooling was not so prolonged. The second set of 1μ data for compound III was taken immediately after the first set; a rather interesting change may be observed in that a *rise* in temperature apparently caused the supercooled anisotropic liquid to solidify. In all compounds the *total* change in transmission is greatest at 1μ and decreases rapidly beyond 6μ. Most of the data presented in the figures are for regions in which strong characteristic absorption is not present, but isochromatic curves taken in the center of absorption bands are not noticeably different. (See the 3.37μ curve of Fig. 3.)

Table II lists the temperature intervals in which marked transmission changes and arrests occur. Although the previous history of the sample and rates of heating and cooling undoubtedly have an influence on the temperatures at which critical changes occur, the variations caused by these factors are surprisingly small in view of the drastic temperature changes to which the samples were subjected. Data obtained with different samples checked excellently. The cooling rate had little effect on the "hysteresis" mentioned above. In determining the exact temperatures at which "arrests" and minima occur a slow heating rate and a continuous recorder would be desirable. An interesting effect observed with compound III is the growth of the high temperature minimum with increasing wave-length. It is especially noticeable in the isochromatics for compounds I and II that the transmissions of the solid and anisotropic liquid phases approach the same value at long wave-lengths.

The increase of transmission with temperature can be explained qualitatively in terms of scattering by the swarms present in the mesophase, the low transmission of the solid probably arising from scattering and reflection by small

crystals. Einstein[4] and Smoluchowski[5] have derived an expression for the scattering of light by dense media. The intensity of the scattered raditation is given in terms of the index of refraction of the medium, and hence the applicability of this expression to the case of doubly refracting liquids is questionable. Assuming that the Einstein expression can be applied and that an average of n_0 and n_e is a suitable index, one finds that a decreasing scattering volume is the chief factor which could account for the observed increases in transmission; there are other factors in the Einstein-Smoluchowski equation which indicate a decrease in transmission with increasing temperature. Approximate calculations of the change in transmission with wave-length reveal that the observed changes are not in agreement with the values given by the Einstein relation.

A theory more readily applicable to the present problem has been developed by Ornstein.[6] Because of birefringence and random distribution of swarms, gradients of refractive index occur, which, according to Ornstein, give rise to a scattering coefficient proportional to the square of the difference between ordinary and extraordinary indices. Stumpf[7] and Van Wyk[8] have measured these indices in the visible region for a number of anisotropic liquids and find that the difference between the indices is a decreasing function of temperature. A discontinuity of index occurs at the clearing point. If one assumes a random distribution of swarms in the samples used in this study, Ornstein's scattering theory can be applied. If Stumpf's data can be extrapolated to the infra-red, the coefficient decreases with increasing temperature and becomes zero at the clearing point.

Although probably due to a combination of swarm volume change and birefringence variation, the greater part of the increase in transmission with temperature must be attributed to the decrease in birefringence $(n_0-n_e)^2$. Otherwise at wave-lengths as long as 10μ most of the increase should take place as soon as the compound melts.[9] Actually, however, at long wave-lengths

[4] A. Einstein, Ann. d. Physik **33**, 1275 (1910).
[5] M. V. Smoluchowski, Ann. d. Physik **25**, 205 (1908).
[6] L. S. Ornstein, Ann. d. Physik **74**, 445 (1924).
[7] F. Stumpf, Ann. d. Physik **37**, 351 (1912).
[8] A. Van Wyk, Ann. d. Physik **3**, 879 (1929).
[9] Measurements of the dielectric and diamagnetic anisotropy of liquid crystals show that the volume of the

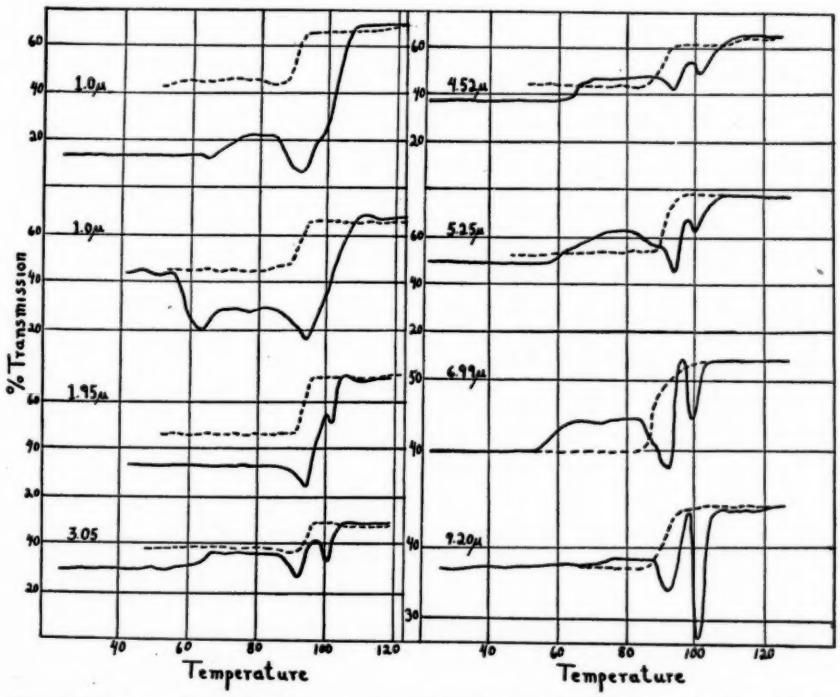

FIG. 5. Isochromatic curves for compound III showing percentage transmission as a function of temperature. Solid line indicates heating data; dotted line, cooling data.

TABLE II. *Temperatures of characteristic transmission changes.*

WAVE-LENGTH	INITIAL RISE	ARRESTS	SECOND RISE	COOLING DECREASE
		Compound I		
1μ	78–88°C	88–131°C	131–141°C	96–92°C
3.17	100–110	110–120 126–133	133–140	96–91
3.37	94–103	103–115 121–130	130–139	87–78
3.65	100–106	106–117 120–133	133–142	93–75
4.76	102–127	127–134	134–140	100–94
5.25	85–90	94–108 127–133	133–141	102–88
7.10	120–134 (slow rise)		134–142	111–95 (slow decrease)
10.60	124–135 (slow rise)		135–143	89–75 (slow decrease)
		Compound II		
1μ (from solid)	47–56°C	56–68°C	68–80°C	73–65°C
1μ (from liquid crystal)	69–74		74–79	68–62
2.55	61–63	63–68	68–76	64–59
4.27	48–52	52–76 (slow rise)	79–84	75–67
4.76	48–62 (slow rise)	62–69 69–77	77–85	75–65
6.91	50–54	54–68 75–80	80–85	73–67
7.26	50–54	54–69 74–79	79–85	74–67

WAVE-LENGTH	INITIAL RISE	FIRST DECREASE	FIRST MINIMUM	FIRST MAXIMUM	SECOND MINIMUM	FINAL MAXIMUM	COOLING DECREASE
			Compound III				
1μ (from solid)	63–71°C	82°C	91°C			105°C	94–88°C
1μ (from liquid crystal)	63–70	82	91			107	94–89
1.95		83	94	98°C	101°C	104	94–90
3.05	62–68	83	91	96	100	104	96–89
4.52	62–70	88	94	98	101	106	94–88
5.25	57–70	89	94	97	100	106	96–89
6.99	80–90	85	92	96	99	104	96–86
9.20	71–75	82	92	98	100	104	94–89

the transmissions of solid and mesophases are approximately the same and the increase occurs at the clearing point.[10] The comparatively small total change in transmission can possibly be explained in terms of a decreasing (and in the case of compound I an almost constant) birefringence factor $(n_0-n_e)^2$ with increasing wave-length. This type of decrease was found in the visible region by Stumpf and Van Wyk[8] and can probably be extrapolated to the infra-red.[11]

Since there is no evidence to indicate that the indices n_0 and n_e vary discontinuously with temperature in any one phase, the arrests and minima in the isochromatics may arise from polymorphism in the liquid crystalline phase, as observed by Dorn and Lohman[12] in their measurements of refractive index, the variation of arrests and minima with wave-length depending upon the variation of $(n_0-n_e)^2$ with wave-length. The observed "hysteresis" in transmission is probably due to a tendency of the molecules to maintain the random distribution characteristic of the isotropic liquid phase. As mentioned above, the temperature interval over which supercooling persists is apparently independent of the cooling rate.

Attention is called to the fact that the presence of the increased transmission of compound III in the temperature interval 63°C to 84°C may indicate the existence of an intermediate phase not previously detected. On cooling to the normal solid phase the compound apparently does not pass through this state. The presence of the intermediate phase may be due to polymorphism in the solid.

Although the observed variations in band shape and position with change of state may be attributed to associational effects, it would be necessary to study a large number of substituted compounds before any definite conclusions as to the associational mechanisms could be drawn. The isochromatic data indicate pronounced variations in transmission with change of state, the liquid crystalline phase being more closely related to the solid than to the true liquid. The present method provides a sensitive means of studying change of state and for anisotropic liquids is superior to ordinary cooling-curve measurements and visual observations. In common with methods involving polarized light, the present scheme necessitates the use of thin layers. If the interpretation in terms of Ornstein's theory is correct, isochromatic data should enable one to estimate the magnitude of birefringence at infra-red wave-lengths.

The writers wish to express their appreciation to Mr. J. P. Bain for preparing the compounds, to Mr. H. B. Messec for aid in construction of apparatus, and to Mr. R. G. Larrick, who assisted in taking some of the data.

swarms is of the order of 10^{-15} cm³. G. Foex and L. Royer, Comptes Rendus **180**, 1912 (1925). W. Kast, Ann. d. Physik **73**, 145 (1924).

[10] This is especially noticeable in the isochromatics of compound I.

[11] L. R. Ingersoll (Phys. Rev. **44**, 399 (1933)) reports a decrease of this type in the case of the Kerr constant.

[12] E. Dorn and W. Lohman, Ann. d. Physik **29**, 533 (1909).

The Infra-Red Absorption Spectrum of Methyl Alcohol

AVIS BORDEN AND E. F. BARKER
University of Michigan, Ann Arbor, Michigan
(Received June 20, 1938)

Using a grating spectrometer having a KBr foreprism the spectrum of methyl alcohol vapor was studied in the region from 2.5 to 26μ. This molecule has bands at 3683, 2978, 2845, 2054, 1477, 1455, 1340, 1034.18 cm^{-1} and a very broad band extending from 860 to beyond 380 cm^{-1}. These bands are typical perpendicular and parallel bands and indicate that the molecule is only slightly asymmetric.

From the fine structure of the 1034.18 cm^{-1} parallel band and from certain assumptions about the structure of the molecule the two largest moments of inertia, A and B, were found to be 35.18 and 33.83×10^{-40} g cm^2, respectively. It was not possible to measure C directly but it was estimated to be approximately 6.8×10^{-40} g cm^2.

The low frequency band is probably due to the vibration of the hydroxyl hydrogen atom perpendicular to the O—H bond and perpendicular to the figure axis of the molecule. The presence of this band indicates that the hydroxyl group is not free to rotate, at least in the ground state. There is evidence of rotation in the structure of the band near the high frequency edge. The spacing increases toward high frequencies and finally there is a group of lines having a spacing of about 40 cm^{-1} between 600 and 860 cm^{-1}. Since these lines are very weak and occur at such high frequencies it appears that free rotation exists only in states of high excitation. A quantitative study of free rotation in a symmetric molecule has been made. This investigation indicates that in a first approximation free rotation should give rise to groups of lines having a spacing of about 40 cm^{-1} between each group.

INTRODUCTION

A STUDY of the infra-red absorption spectrum of methyl alcohol has been made by Bartholomé and Sachsse[1] using a prism spectrometer. Earlier studies have also been made by Titeica[2] and Lecomte.[3] In addition, the Raman spectrum of methyl alcohol has been well established by the work of a number of investigators.[4] These studies were of value in establishing the positions of the bands but they were unable to give information about their character. Moreover, due to the absorption of the rocksalt prisms used in the infra-red investigations it was not possible to work with wave-lengths longer than 16μ.

In the present work the absorption spectrum was studied under high dispersion using the grating spectrometer designed by Hardy.[5] With this instrument it was possible to resolve lines having a separation of less than 1 cm^{-1} over most of the range. By using a KBr foreprism it was possible to extend the spectral region to 26μ. This extension of the spectral region and the ability to resolve the fine structure of the bands made it possible to assign the frequencies more accurately and to gain further information about the structure of the molecule.

The form of the methyl alcohol molecule is known from sterochemical evidence and from infra-red data on other similar molecules. The carbon atom lies within a tetrahedron formed by hydrogen atoms at three of its corners and by the hydroxyl group at the fourth. The hydroxyl hydrogen atom stands out at an angle, somewhat greater than a right angle, from the C—O line.

Such a molecule should possess twelve fundamental frequencies. Since the molecule is very nearly symmetrical, however, it turns out that only nine of the frequencies are distinct, three being double perpendicular frequencies. Of these nine, six correspond to the frequencies found for the methyl halides. Following Dennison's notation,[6] the first six frequencies are assigned to those modes of vibration which also occur in the methyl halides. ν_7, ν_8 and ν_9 are assigned to the frequencies associated with vibrations within the hydroxyl group.

[1] E. Bartholomé and H. Sachsse, Zeits. f. physik. Chemie **B30**, 40 (1935).
[2] R. Titeica, Comptes rendus Acad. Sci., Paris **196**, 391 (1933).
[3] J. Lecomte, Comptes rendus Acad. Sci., Paris **180**, 825 (1925).
[4] J. O. Halford, L. C. Anderson, G. H. Kissin, J. Chem. Phys. **5**, 927 (1937). V. S. Mizushima, Y. Morina, G. Okamoto, Bull. Chem. Soc. Japan **11**, 698 (1936). K. W. F. Kolhrausch, *Der Smekal-Raman Effekt*, p. 309.
[5] J. D. Hardy, Phys. Rev. **38**, 2162 (1931).
[6] D. M. Dennison, Rev. Mod. Phys. **3**, 280 (1931).

Experimental Results

The positions of the bands, the approximate amounts of gas required, the gratings used and the slit widths are given in Table I. A 25 cm

Table I. *Position of the bands.*

Frequency in cm^{-1}	Pressure cm Hg	Grating Lines Per Inch	Slit Width in cm^{-1}
ν_7 3683	5	4800	2.0
ν_2 2978	1	4800	1.3
ν_1 2845	1	4800	1.3
$2\nu_5$ 2054	9	4800	0.65
ν_4 1477	9	1200	1.8
ν_3 1455	9	1200	1.8
ν_6 1340	9	1200	1.5
ν_5 1034.18	0.5	2400	0.5
ν_8 860–650	9	1200	0.8
ν_8 630–380	9	1200	0.5
ν_8 630–380	9	360 (2nd order)	0.5

absorption cell with KBr windows was used for all the bands except for the region between 860 and 650 cm^{-1}. Here it was necessary to use a meter cell to obtain sufficient absorption. It was impossible, however, to measure the pressure of the gas in the long cell since it could not be evacuated.

ν_1 and ν_2 are very intense bands which have their centers at 2845 and 2978 cm^{-1}, respectively, Fig. 1. These two frequencies are associated with the vibrations of the three hydrogen atoms in the methyl group, ν_1 being a parallel vibration and ν_2 a double perpendicular vibration. Although the amplifier was used at its limit of sensitivity and the slits were made as narrow as possible it was impossible to resolve the fine structure of either of these bands.

ν_3 and ν_4 are also associated with vibrations within the methyl group. ν_3 is a parallel band having its zero branch at 1455 cm^{-1}. ν_4 is another double perpendicular band which has its center at 1477 cm^{-1}, Fig. 2. These two bands fall in a region where the atmospheric absorption due to water vapor is very intense. For this reason it was very difficult to resolve the fine structure of the bands except for a few lines near the center of the perpendicular band. These lines have the frequencies: 1463.2, 1471.7, 1479.9 cm^{-1}. It was impossible to obtain the fine structure of the parallel band even with a finer grating and narrower slits.

These four methyl frequencies found in methyl alcohol are in good agreement with those found in the methyl halides and are almost identical with the frequencies of methyl fluoride.[7] In the spectra of the methyl halides, however, another parallel band is usually observed between ν_1 and ν_2, which has been interpreted as the overtone of ν_4.[8] This frequency was not observed in the spectrum of methyl alcohol although the region was examined carefully with different amounts of gas. The perpendicular band is not symmetrical, however, and it may be that there is a faint band on the low frequency side of it.

The double perpendicular band ν_6 consists of the vibration between the methyl and hydroxyl

[7] W. H. Bennett and C. F. Meyer, Phys. Rev. **32**, 888 (1928).
[8] A. Adel and E. F. Barker, J. Chem. Phys. **2**, 627 (1934).

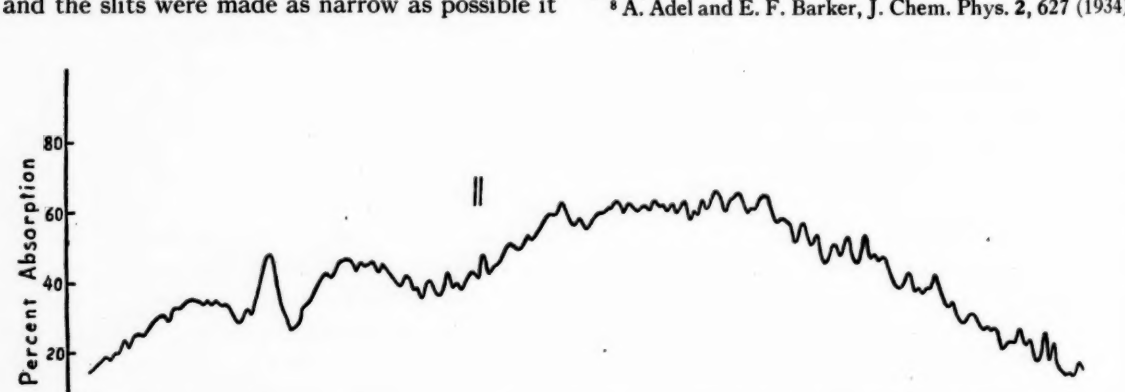

Fig. 1. The bands ν_1 at 2845 cm^{-1} and ν_2 at 2978 cm^{-1}.

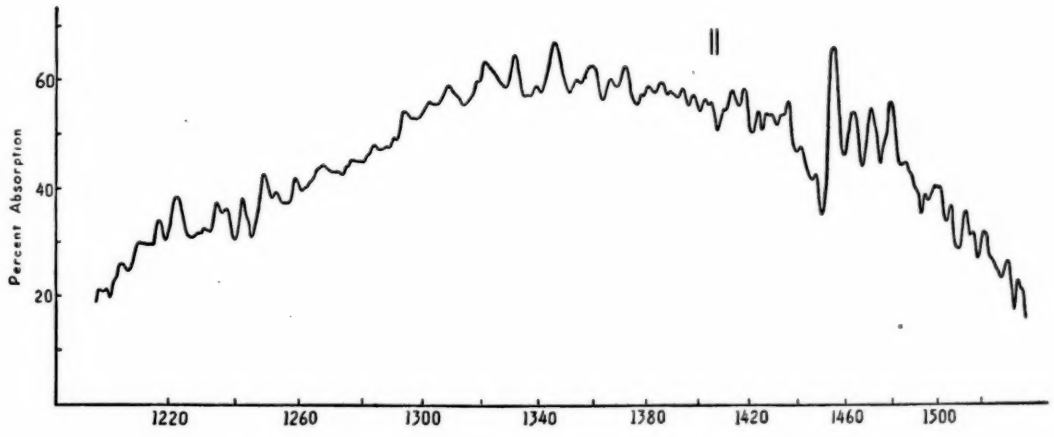

FIG. 2. The bands ν_3 at 1455 cm^{-1}, ν_4 at 1477 cm^{-1} and ν_6 at 1340 cm^{-1}.

groups and lies at 1340 cm^{-1}, Fig. 2. One might expect the two frequencies in this band to be separated, as was the case in the corresponding perpendicular band of formaldehyde, studied by Nielsen.[9] Such a splitting is not immediately apparent from the structure of the band. There is, however, considerable atmospheric absorption out to 1350 cm^{-1} which introduces uncertainties in the positions and intensities of the fine structure lines. The band does appear to be considerably broader than most of the other perpendicular bands of this molecule, thus indicating the possibility of a double frequency. Although the background is fairly clear beyond 1350 cm^{-1} the band does not show much structure except near the center and far out on the low frequency edge. The central lines have the frequencies: 1321.3, 1331.8, 1348.4, 1359.5 cm^{-1}.

The parallel vibration ν_5 between the methyl and hydroxyl groups gives rise to a very intense band at 1034.18 cm^{-1}, Fig. 3. The fine structure in this band is well resolved in both branches and fits the quadratic equation:

$$\nu = 1034.18 + 1.5975m - 0.0088m^2$$

where m is the number of the line counting from the center. The calculated and observed frequencies are given in Table II. Most of the calculated values fit the observed frequencies within 0.05 cm^{-1}.

The overtone of ν_5 occurs as a weak parallel band at 2054 cm^{-1}, Fig. 4. The fine structure could be resolved only in the negative branch. Here the spacing agrees well with the spacing found in ν_5.

ν_7 consists of the motion of the hydroxyl hydrogen atom along the O—H bond and lies at 3683 cm^{-1}, Fig. 5. The atmospheric absorption due to water vapor is particularly strong here and it was impossible to obtain more than just the envelope of the band. The central line, however, occurs between two water vapor lines and was observed several times. This band has the

TABLE II. *Frequencies of the fine structure lines in the 1034.18 cm^{-1} parallel band.*

m	Observed	Calculated	m	Observed	Calculated
−27	983.78	983.82	−2		1031.94
−26	986.68	986.69	−1		1032.57
−25	988.72	988.74	0		1034.18
−24	990.78	990.78	1		1035.77
−23	992.76	992.78	2		1037.34
−22	994.69	994.78	3	1038.79	1038.89
−21	996.77	996.76	4	1040.34	1040.43
−20	998.71	998.71	5	1041.92	1041.94
−19	1000.68	1000.65	6	1043.41	1043.45
−18	1002.57	1002.57	7	1044.94	1044.93
−17	1004.52	1004.48	8	1046.40	1046.40
−16	1006.36	1006.37	9	1047.75	1047.85
−15	1008.26	1008.24	10	1049.23	1049.28
−14	1010.01	1010.09	11	1050.64	1050.69
−13	1011.94	1011.92	12	1052.12	1052.08
−12	1013.78	1013.74	13	1053.55	1053.46
−11	1015.62	1015.55	14	1054.86	1054.93
−10	1017.40	1017.32	15	1056.18	1056.16
−9	1019.16	1019.09	16	1057.55	1057.49
−8	1020.86	1020.84	17	1058.82	1058.80
−7	1022.57	1022.57	18	1060.02	1060.09
−6	1024.26	1024.27	19	1061.23	1061.35
−5	1025.94	1025.98	20	1062.50	1062.61
−4	1027.58	1027.65	21	1063.80	1063.84
−3	1029.36	1029.31			

[9] H. H. Nielsen, J. Chem. Phys. **5**, 818 (1937).

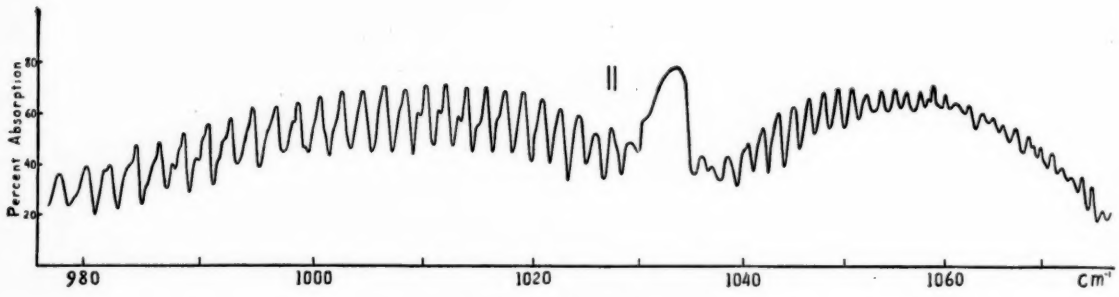

FIG. 3. The parallel bands ν_5 at 1034.18 cm^{-1}.

appearance of a perpendicular band with possibly a weak parallel component.

In the Raman spectrum of liquid methyl alcohol ν_7 was found at 3400 cm^{-1} instead of at 3683 cm^{-1}. This discrepancy is not an error in the results but is characteristic of the molecule when it passes from the liquid to the gaseous state. Errera and Mollet[10] have plotted this band in the infra-red using liquid alcohol and found it at 3μ. When they diluted the alcohol with CCl_4 this band disappeared and a faint one was detected at 2.7μ. They conclude that the 3μ band is due to association and that the fundamental is at 2.7μ. The dilution of the alcohol breaks up the association of the molecules. This agrees well with the results of the present investigation since no band was found at 3μ using alcohol vapor.

Another hydroxyl frequency ν_9 consists of the motion of the hydrogen atom perpendicular to the O−H bond and nearly parallel to the figure axis of the molecule. This band was never found in the infra-red. The Raman spectrum gives this frequency at 1107 cm^{-1}. In the molecule CH_3OD this band also is affected by association.[11] Its frequency is about 80 cm^{-1} lower than the Raman spectrum predicts. If a similar shift takes place in ordinary methyl alcohol this band should lie near 1030 cm^{-1} which is in the midst of the very intense 1034.18 cm^{-1} band, ν_5. The 1034.18 cm^{-1} band does have irregularities in its fine structure which may be due to the presence of this other band. But the hydroxyl frequency is essentially parallel and one should expect to find a zero branch somewhere. Although the region was studied a number of times with different amounts of gas no zero branch could be found unless it coincides with the zero branch of ν_5. These two frequencies are of the same symmetry class, however, and one would expect a resonance interaction to separate them. It is not possible to use much gas in this region before the absorption becomes complete. The hydroxyl frequency may be too weak to be detected here.

Finally, there is a frequency ν_8 in which the hydrogen atom moves perpendicular to the O−H bond and perpendicular to the axis of the molecule. If there were no restoring force this motion would result in the free rotation of the hydroxyl group about the axis of the molecule. The absorption band between 16 and 26μ indicates, however, that the hydroxyl group is not entirely free, Fig. 6. At 26μ the absorption of the KBr foreprism made it impossible to work at longer wave-lengths although the band probably con-

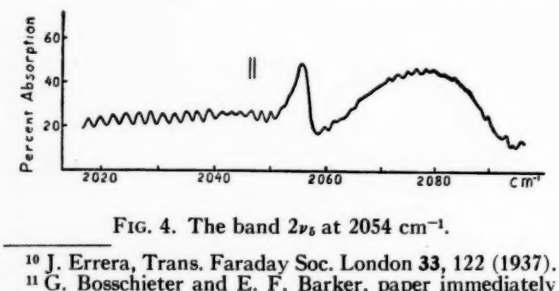

FIG. 4. The band $2\nu_8$ at 2054 cm^{-1}.

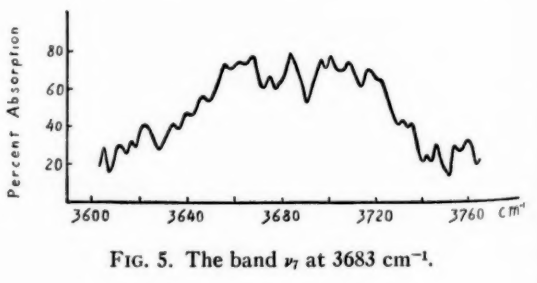

FIG. 5. The band ν_7 at 3683 cm^{-1}.

[10] J. Errera, Trans. Faraday Soc. London **33**, 122 (1937).
[11] G. Bosschieter and E. F. Barker, paper immediately following in J. Chem. Phys.

tinues for some distance. There are a number of water lines in this region. These become more numerous and more intense as one proceeds toward longer wave-lengths. The curve is drawn with broken lines where the atmospheric absorption makes the readings uncertain.

Toward the high frequency edge of the band the spacing between the lines becomes greater and the lines fall off in intensity. Between 650 and 860 cm^{-1} is a group of very faint lines with a regular spacing of about 40 cm^{-1} which are probably a continuation of ν_8, Fig. 7. Although these lines could be observed with the 25 cm absorption cell, their structure was better defined when the meter cell was used. In the region between 700 and 630 cm^{-1} there is intense atmospheric absorption due to CO_2. The line at 694.7 cm^{-1} was strong enough to stand out between the CO_2 lines. It appeared to be fairly broad but it was impossible to give its exact structure. In addition to the lines shown in Fig. 7, there is a region of absorption near 650 cm^{-1}. This absorption, also, was broad but no part of it was strong enough to stand out between the CO_2 lines. The frequencies of the most important lines of ν_8 are listed in Table III.

Discussion of Results

The energy of an asymmetric molecule has the form:[12]

$$E=(n+\tfrac{1}{2})h\nu+\frac{h^2}{8\pi^2}$$

$$\times\left\{(J^2+J)\left(\frac{1}{2A}+\frac{1}{2B}\right)+\left(\frac{1}{C}-\frac{1}{2A}-\frac{1}{2B}\right)W\right\},$$

where W is a parameter which makes the energy matrix diagonal and is not in general an integer. When the values of W are computed for the methyl alcohol molecule it turns out that only in the lowest states do they differ appreciably from squares of integers. This results in a displacement and splitting of the lowest levels but the effect is negligible for values of W greater than 4. This splitting affects the structure of the perpendicular bands slightly but, except for a slight broadening of the lines, it is unimportant in the parallel bands.

[12] H. H. Nielsen, Phys. Rev. **38**, 1432 (1931).

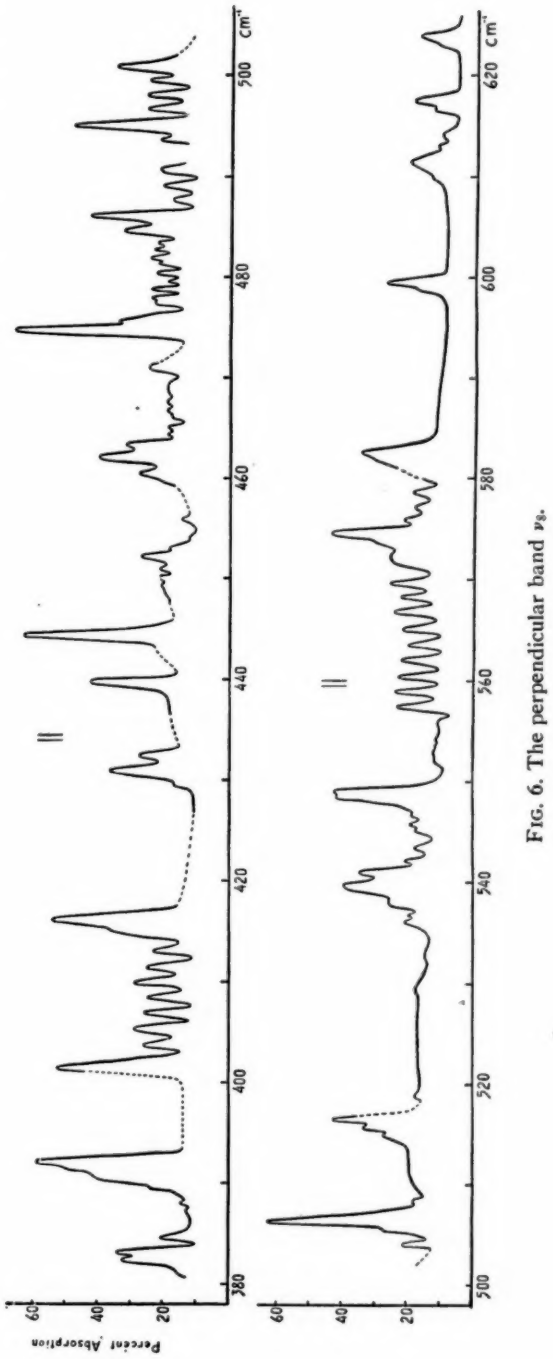

FIG. 6. The perpendicular band ν_8.

From the fine structure of the 1034.18 cm^{-1} parallel band an average value of the two largest moments of inertia of the molecule could be obtained. From further assumptions about the internuclear distances, using infra-red data on

TABLE III. *Lines of the perpendicular band ν_8.*

382.45 cm^{-1}	474.65 cm^{-1}	582.60 cm^{-1}
383.20	484.60	599.50
384.65	486.05	611.45
392.15	494.95	617.55
401.45	500.80	623.90
416.10	506.40	(650)
439.70	515.73	694.7
444.30	516.42	736.7
452.20	539.60	778.3
460.55	540.90	780.0
462.20	548.65	820.6
463.38	574.50	860.1

the methyl halides[13] and the water molecule,[14] it was possible to compute A and B with a fair degree of accuracy. $A=35.18\times10^{-40}$ g cm^2 and $B=33.83\times10^{-40}$ g cm^2. The C−H and H−H distances in the methyl group were assumed to be 1.11A and 1.81A, respectively. The O−H distance was taken to be 0.9558A as in water. In their experiments on electron diffraction Pauling and his co-workers[15] give 1.44±0.02A for the C−O distance in CH_3ONH_2. Results from the moments of inertia of methyl alcohol indicate that the C−O distance in methyl alcohol is between 1.42 and 1.43A and the angle between the O−H and the C−O bonds lies between 105° and 115°. These values cannot be known exactly until a more exact measurement of the least moment of inertia C is made. Although the present observations do not yield C directly its value can be estimated from the dimensions of the molecule. In making computations on the free rotation of the two parts of the molecule it is also necessary to know the approximate values of the moments of inertia of the hydroxyl and methyl groups separately about the figure axis of the molecule. For the hydroxyl group C_1 is between 1.3 and 1.4×10^{-40} g cm^2; for the methyl group $C_2=5.4\times10^{-40}$ g cm^2. The moment of inertia C is equal to the sum of C_1 and C_2 and lies between 6.7 and 6.8 g cm^2.

The perpendicular band ν_8 is a single frequency and should be unaffected by the internal angular momentum which changes the spacing in the double perpendicular bands of symmetric molecules. A simple calculation shows that if the hydroxyl group were completely bound one should expect an ordinary perpendicular band having a spacing of approximately 6.5 cm^{-1}. If, however, the hydroxyl group were a free rotator one should expect a series of rotation bands with a spacing of about 40 cm^{-1} between each band. The low frequency band shows an irregular spacing which increases from about 10 cm^{-1} to 30 cm^{-1} in the region from 380 to 600 cm^{-1} and finally has a spacing of about 40 cm^{-1} between 600 and 860 cm^{-1}. The increased spacing toward higher frequencies probably indicates that for higher energies the hydroxyl group is approaching rotation levels.

FREE ROTATION BANDS OF METHYL ALCOHOL

The problem of the torsion oscillator-rotator has already been treated by Nielsen.[16] For simplicity it will be assumed that the hydroxyl group can be approximated by a symmetrical top. Then the whole molecule can be represented by two symmetrical rotators having a common C axis. It will be convenient to refer to the two systems with the subscripts 1 and 2. The positions of the two parts of the molecule with respect to a set of fixed axes is best described by

[13] M. Johnston and D. M. Dennison, Phys. Rev. **48**, 868 (1935).
[14] H. M. Randall, D. M. Dennison, N. Ginsburg, L. R. Weber, Phys. Rev. **52**, 160 (1937).
[15] L. O. Brockway, J. Y. Beach, L. Pauling, Am. Chem. J. **57**, 2693 (1935).
[16] H. H. Nielsen, Phys. Rev. **40**, 445 (1932).

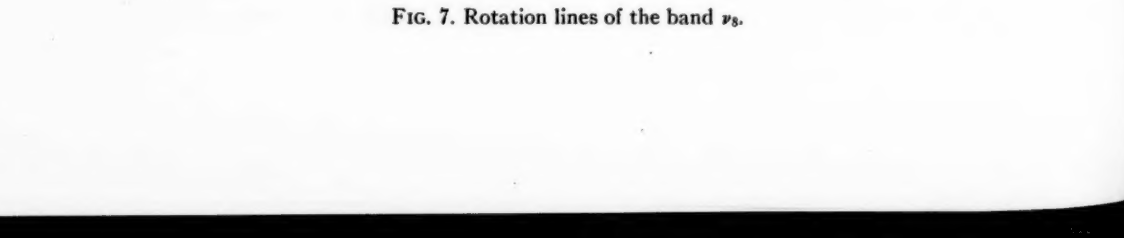

FIG. 7. Rotation lines of the band ν_8.

the Eulerean angles, θ, ψ, φ_1 and θ, ψ, φ_2; where θ is the angle between the fixed Z axis and the C axis of the molecule, ψ is the angle which describes the precession of the molecule, φ_1 and φ_2 are the angles of rotation about the C axis. Following Nielsen's procedure it will be advantageous to introduce the quantities φ and α defined as follows: $\varphi=[(C_1\varphi_1+C_2\varphi_2)/C]$, $\alpha=\varphi_2-\varphi_1$, where C_1 and C_2 are the moments of inertia of the two parts of the molecule and $C_1+C_2=C$, the total moment of inertia about the figure axis of the molecule. Since the potential energy depends only upon the angular displacement between the two parts of the molecule it is a function of α only.

Proceeding as Nielsen did the Schrodinger equation is separable, one part giving the energy of rotation of the molecule as a whole:

$$E_1=\frac{h^2}{8\pi^2}\left\{\frac{J^2+J}{A}+\left(\frac{1}{C}-\frac{1}{A}\right)K^2\right\}.$$

The other part leads to the differential equation:

$$\frac{d^2M}{d\alpha^2}+\frac{8\pi^2C_1C_2}{h^2C}\{E_2-V(\alpha)\}M=0.$$

Since the hydroxyl hydrogen atom has three positions of equilibrium between the hydrogen atoms of the methyl group the simplest potential function is: $V=V_0(1-\cos 3\alpha)$. This leads to the Mathieu equation. As was pointed out by Nielsen exact solutions for this equation are known only for every third state. The intermediate solutions can only be estimated.

It is of interest to investigate the solutions for extreme values of the potential. If the barrier is indefinitely high there will be simple harmonic motion. This will give rise to an ordinary perpendicular band with a spacing $(h/4\pi^2)(1/C-1/A)$. If there is no barrier, however, there will be free rotation of the two parts of the molecule. Then the energy of the molecule may be written:

$$E=\frac{h^2}{8\pi^2}\left\{\frac{J^2+J-K^2}{A}+\frac{\lambda_1^2}{C_1}+\frac{\lambda_2^2}{C_2}\right\}.$$

The eigenfunction has the form:

$$\psi=F(\theta)e^{iN\psi}e^{i\lambda_1\varphi_1}e^{i\lambda_2\varphi_2},$$

where $F(\theta)$ is the hypergeometric function. The notation used here is somewhat different from that employed by Nielsen. λ_1 and λ_2 are the azimuthal quantum numbers for the two parts of the top and may take on all integral values. K is the total azimuthal quantum number and $|K|=|\lambda_1+\lambda_2|$.

The selection rules are similar to those obtained for ordinary perpendicular bands. If the electric moment changes in the system denoted by the subscript 1: $\Delta J=0, \pm1$, $\Delta K=\pm1$, $\Delta\lambda_1=\pm1$, $\Delta\lambda_2=0$. If the electric moment changes in the other part of the molecule, then $\Delta\lambda_1=0$ and $\Delta\lambda_2=\pm1$. In the following discussion it will be assumed that the electric moment changes in the hydroxyl group, which will be assigned the subscript 1.

Using these selection rules the zero branches on the low frequency side of the center of the band have the frequencies:

$$\nu_{\lambda_1\ \lambda_2\ K\ J}^{\lambda_1-1\ \lambda_2\ K-1\ J}=\frac{h}{4\pi^2}\left\{\frac{\lambda_1-\frac{1}{2}}{C_1}-\frac{K-\frac{1}{2}}{A}\right\}$$

where $|\lambda_1+\lambda_2|=|K|$.

The fine structure lines associated with the Kth zero branch have the frequencies:

High frequency side of the center

$$\nu_{\lambda_1\ \lambda_2\ K\ J}^{\lambda_1-1\ \lambda_2\ K-1\ J-1}=\frac{h}{4\pi^2}\left\{\frac{\lambda_1-\frac{1}{2}}{C_1}-\frac{K-\frac{1}{2}-J}{A}\right\}$$

where $|J|\geq|K|$.

Low frequency side of the center

$$\nu_{\lambda_1\ \lambda_2\ K\ J-1}^{\lambda_1-1\ \lambda_2\ K-1\ J}=\frac{h}{4\pi^2}\left\{\frac{\lambda_1-\frac{1}{2}}{C_1}-\frac{K-\frac{1}{2}+J}{A}\right\}$$

where $|J-1|\geq|K|$.

Since J is never less than K certain of the fine structure lines will be missing. It is the same situation that arises in perpendicular bands of symmetric molecules and the band is constructed in the same way. On the low frequency side the first zero branch has the first rotation line on the low frequency side missing. The second zero branch has two lines missing on the low frequency side and one on the high frequency side. On the high frequency side the situation is just the reverse. A typical rotation band showing

how the zero branches and fine structure lines go together is drawn in Fig. 8. The asymmetry of the band will be explained later.

It is apparent from these equations and the diagram that the fine structure lines and the zero branches have the same spacing and in most cases a number of lines coincide. In computing the intensities it is necessary to find the sum of the intensities of all the lines falling at a particular place. It will be convenient to find the intensities of the zero branches and fine structure lines separately. The intensity formulae for perpendicular bands given by Dennison[6] may be adapted for use here. For the zero branches on the low frequency side of the center the intensity formula is:

$$I^{\lambda_1-1\,\lambda_2\,K-1\,J}_{\lambda_1\quad\lambda_2\,K\quad J}=A[x]\sum_{J=K}^{\infty}\frac{(2J+1)(J+K)(J-K+1)}{2J(J+1)}\times\exp\left(-\sigma[J^2+J-(K-1)^2+\gamma_1(\lambda_1-1)^2+\gamma_2\lambda_2{}^2]\right),$$

where $\sigma=\dfrac{h^2}{8\pi^2AkT}$, $\gamma_1=\dfrac{A}{C_1}$, $\gamma_2=\dfrac{A}{C_2}$.

A is a constant which depends upon the population in the initial state and the Boltzmann factor. The quantity $[x]$ is equal to one except when the quantum number λ_2 is zero or any multiple of three, in which case $[x]$ takes on the value two. This enhancement of every third line is due to the presence of the three protons (like particles with spin $\frac{1}{2}(h/2\pi)$) in the methyl group which doubles the population in every third state.

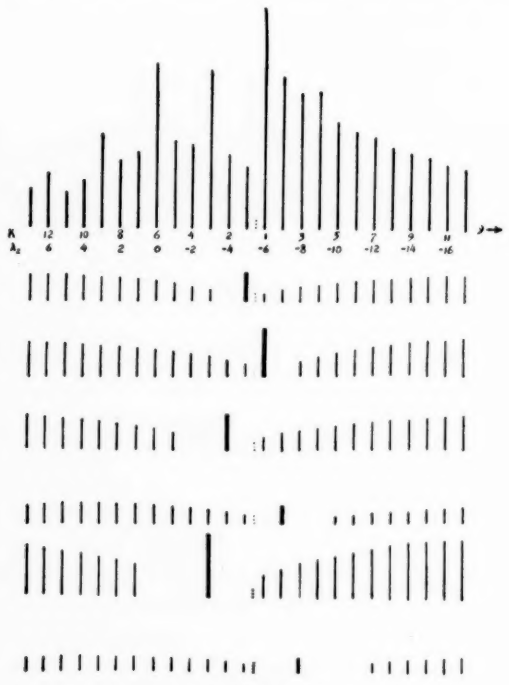

FIG. 8. The free rotation band $\lambda_1=6$.

In the approximation needed here it is convenient to change the sum into an integral:

$$I^{\lambda_1-1\,\lambda_2\,K-1\,J}_{\lambda_1\quad\lambda_2\,K\quad J}=\frac{A}{2}[x]\times\exp\left(-\sigma[\gamma_1(\lambda_1-1)^2+\gamma_2\lambda_2{}^2-(K-1)^2]\right)\times\left\{\frac{e^{-\sigma(K^2+K)}}{\sigma}-(K^2-K)\int_{\sigma(K^2+K)}^{\infty}\frac{e^{-u}}{u}du\right\}.$$

The integral which occurs here is the logarithmic integral for which tables have been computed. A similar expression is obtained for the zero branches on the high frequency side:

$$I^{\lambda_1-1\,\lambda_2\,K\quad J}_{\lambda_1\quad\lambda_2\,K-1\,J}=\frac{A}{2}[x]\times\exp\left(-\sigma[\gamma_1(\lambda_1-1)^2+\gamma_2\lambda_2{}^2-K^2]\right)\times\left\{\frac{e^{-\sigma(K^2-K)}}{\sigma}-(K^2-K)\int_{\sigma(K^2-K)}^{\infty}\frac{e^{-u}}{u}du\right\}.$$

The intensities of the fine structure lines can best be treated in two parts. First consider the fine structure associated with zero branches on the opposite side of the center of the band, and then consider the fine structure associated with zero branches on the same side of the center. In either case it is necessary to sum over all rotation lines of that class falling on the Kth zero branch.

Consider all rotation lines on the high frequency side of the band having zero branches on the low frequency side, which fall on the Kth zero branch on the high frequency side. The Kth zero branch has the frequency:

$$\nu^{\lambda_1-1\,\lambda_2\,K\quad J}_{\lambda_1\quad\lambda_2\,K-1\,J}=\frac{h}{4\pi^2}\left\{\frac{\lambda_1-\frac{1}{2}}{C_1}+\frac{K-\frac{1}{2}}{A}\right\},$$

where $K-1=-(\lambda_1+\lambda_2)$. The fine structure line

associated with the K'th zero branch on the low frequency side has the frequency:

$$\nu_{\lambda_1\ \lambda_2'\ K'\ J}^{\lambda_1-1\ \lambda_2'\ K'-1\ J-1}=\frac{h}{4\pi^2}\left\{\frac{\lambda_1-\frac{1}{2}}{C_1}-\frac{K'-\frac{1}{2}-J}{A}\right\},$$

where $K'=\lambda_1+\lambda_2'$ and $|J|\geq|K'|$. It is clear that this fine structure line coincides with the Kth zero branch if $K'=J-K+1$ and $\lambda_2'=J-K+1-\lambda_1$. Each fine structure line has the intensity:

$$I_{\lambda_1\ \lambda_2'\ K'\ J}^{\lambda_1-1\ \lambda_2'\ K'-1\ J-1}=A[x]\frac{(J+K'-1)(J+K')}{2J}\times\exp\left(-\sigma[J^2-J-(K'-1)^2+\gamma_1(\lambda_1-1)^2+\gamma_2\lambda_2'^2]\right)$$
$$=A[x]e^{-\sigma b}\frac{(2J-K)(2J-K+1)}{2J}\times\exp\left(-\sigma\gamma_2(J+a)^2\right),$$

where

$$a=\frac{2K-1-2\gamma_2(K+\lambda_1-1)}{2\gamma_2},$$
$$b=\gamma_1(\lambda_1-1)^2+\gamma_2[(K+\lambda_1-1)^2-a^2]-K^2.$$

The intensity of all the fine structure lines falling on the Kth zero branch may be found by summing this expression over J, from $J=K$ to infinity. It will be more convenient, however, to use the integral form, where 4/3 has been written for the average value of $[x]$.

$$I=\frac{4}{3}Ae^{-\sigma b}\int_K^\infty\left[2(J+a)-(2K-1+2a)+\frac{K^2-K}{2J}\right]\times\exp\left(-\sigma\gamma_2(J+a)^2\right)dJ.$$

The first term may be integrated at once and the other two may be written in a simpler form:

$$I=\frac{4}{3}Ae^{-\sigma b}\left\{\frac{e^{-\sigma\gamma_2(K+a)^2}}{\sigma\gamma_2}-\frac{2K-1+2a}{(\sigma\gamma_2)^{\frac{1}{2}}}\int_{(\sigma\gamma_2)^{\frac{1}{2}}(K+a)}^\infty e^{-x^2}dx+\frac{K^2-K}{2}\int_{(\sigma\gamma_2)^{\frac{1}{2}}(K+a)}^\infty\frac{e^{-x^2}}{x+(\sigma\gamma_2)^{\frac{1}{2}}a}dx\right\}.$$

The second integral is the probability integral for which tables have been computed. The third may be evaluated numerically.

Exactly the same expression may be obtained for the intensities of the fine structure lines on the low frequency side which are associated with zero branches on the high frequency side. Here, however,

$$a=\frac{2K-1-2\gamma_2(K-\lambda_1)}{2\gamma_2}$$

and

$$b=\gamma_1(\lambda_1-1)^2+\gamma_2[(K-\lambda_1)^2-a^2]-(K-1)^2.$$

In some cases a is negative and greater than K. Here the integral does not well approximate the sum. It is then more convenient to sum the first few terms until $J\geq a$. The integral form may be used for the remaining terms.

Now consider all the fine structure lines on the low frequency side associated with zero branches also on the low frequency side. The intensity of one of these lines which is associated with the K'th zero branch is:

$$I_{\lambda_1\ \lambda_2'\ K'\ J}^{\lambda_1-1\ \lambda_2'\ K'-1\ J}=A[x]\frac{(J-K'+1)(J-K')}{2J}\times\exp\left(-\sigma[J^2+J-(K'-1)^2+\gamma_1(\lambda_1-1)^2+\gamma_2\lambda_2'^2]\right).$$

A fine structure line associated with the K'th

TABLE IV. *Intensities of lines in the rotation band* $\lambda_1=6$.

Low Frequency Side				High Frequency Side			
K	Zero Branch	Fine St. Z B High	Fine St. Z B Low	K	Zero Branch	Fine St. Z B Low	Fine St. Z B High
1	7.78	0.58	—	1	12.60	17.21	—
2	9.85		—	2	4.50	16.18	—
3	21.30		0.03	3	3.03	15.23	0.05
4	11.50	0.21		4	3.89	14.41	
5	11.70			5	1.20	13.45	
6	22.50		0.15	6		12.82	0.19
7	10.40			7			
8	8.98		0.34	8		11.37	
9	14.98			9			
10	5.90		0.42	10		9.82	
11	4.52			11			
12	6.52		0.94	12		8.44	0.51
13	2.16			13			
14	1.49		1.01	14		6.66	0.52
15	1.85						
16	0.54		1.04				
17							
18			0.86				

zero branch will coincide with the Kth zero branch if $K'=K-J$ and $\lambda_2'=K-J-\lambda_1$. It is only high K values, Fig. 8, which receive contributions from this class of fine structure since $J\geq K'+1$, or $J\geq(K+1)/2$ if K is odd and $J\geq(K+2)/2$ if K is even. Also, since $J=K-K'$, only those values of $J\leq K-1$ can give contributions to the Kth zero branch. The intensity of all these fine structure lines falling on the Kth zero branch is:

$$I=Ae^{-\sigma b}\sum_{\substack{J=(K+1)/2\ K\text{ odd.}\\ J=(K+2)/2\ K\text{ even.}}}^{K-1}\frac{(2J-K)(2J-K+1)}{2J}\times\exp\left(-\sigma\gamma_2(J+a)^2\right)$$

where $$a=\frac{2K-1-2\gamma_2(K-\lambda_1)}{2\gamma_2}$$

and

$$b=\gamma_1(\lambda_1-1)^2+\gamma_2[(K-\lambda_1)^2-a^2]-(K-1)^2.$$

The same sum is obtained for the intensities of the fine structure lines on the high frequency side of the band which are associated with zero branches also on the high frequency side. In this case, however,

$$a=\frac{2K-1-2\gamma_2(K+\lambda_1-1)}{2\gamma_2}$$

and $$b=\gamma_1(\lambda_1-1)^2+\gamma_2[(K+\lambda_1-1)^2-a^2]-K^2.$$

Since it is only in states of high excitation that the hydroxyl group approaches free rotation the intensities of some of the lines in the band where $\lambda_1=6$ are computed in Table IV. This band is drawn in Fig. 8. The quantum number K changes from $K-1$ to K for the lines on the low frequency side of the center of the band and from K to $K-1$ for the lines on the high frequency side. In each rotation band there are two particularly strong zero branch lines having the quantum number $\lambda_2=0$ and -3. In the first rotation band where $\lambda_1=1$ these strong lines would occur at the center of the band and the fine structure lines would be distributed evenly on both sides. In each successive band, however, these strong lines are displaced farther from the center toward lower frequencies by an amount $h/(4\pi^2A)$. In high rotation states this displacement brings most of the important zero branches on the low frequency side of the center. Thus the important contributions from the fine structure in the high rotation bands is that associated with zero branches on the low frequency side. These fine structure lines always begin at a distance $h/(8\pi^2A)$ from the center of the band on the high frequency side but they build up more slowly on the low frequency side. For this reason the bands have an unsymmetrical appearance and are very intense on the high frequency side since so many fine structure lines coincide here. This effect is enhanced in each successive band as λ_1 increases.

These bands do not compare very well with the structure of the lines in Fig. 7. These are not single lines, however. It may be that, when interactions between the two parts of the molecule are considered, the rotation bands will have quite a different form.

The results of the present investigation are highly suggestive from a qualitative point of view. It has been shown that, if the motion of the hydroxyl group were entirely free, one should expect a series of rotation bands with a separation of about 40 cm^{-1} between each band. This is clearly not the case here. The very fact of the existence of a low frequency band shows that the levels must in some measure possess a vibration-like character. This indicates that the hydroxyl atom is confined within a threefold potential barrier produced by the three hydrogen atoms of the methyl group. If this barrier were very high the particle would vibrate in one of its positions of equilibrium and give rise to a typical perpendicular band. This band would not be affected by vibration-rotation interaction and should have a spacing of about 6.5 cm^{-1}. The spacing in the low frequency band is between these two extremes. At the low frequency edge of the band the spacing approaches the bound case but near the high frequency edge the distance between the lines indicates that the hydroxyl atom is nearly free.

While the evidence is not at all conclusive, it suggests that the height of the barrier might be estimated by correlating it with that part of the band where the distance between the lines begins to approach the spacing expected on the basis

of free rotation. This would appear to correspond to a quantum number of the order of magnitude of 5 in the energy of the free hydroxyl rotator. This estimate of the barrier is accordingly between 400 and 600 cm^{-1}. A study of the far infra-red would be helpful in fixing this value.

It is beyond the scope of the present paper to discuss the transition between vibrational and rotational states. Since the potential function of the alcohol molecule is intermediate between the two extremes discussed here, it is clear that both the rotational and vibrational states are complicated by the presence of the three minimum potential barrier.

In conclusion the authors wish to express their gratitude to Professor D. M. Dennison for his interest in the work and for many helpful discussions during the development of the theory.

SEPTEMBER, 1938 JOURNAL OF CHEMICAL PHYSICS VOLUME 6

The Infra-Red Absorption Spectra of CH_3OD and CH_2DOD

E. F. Barker and G. Bosschieter
Department of Physics, University of Michigan, Ann Arbor, Michigan

(Received June 23, 1938)

The infra-red absorption spectra of CH_3OD and CH_2DOD between 2.5μ and 24μ have been examined with a KBr prism spectrometer, and with appropriate gratings. The observed bands represent all of the fundamental vibrations except the one of lowest frequency which is associated with torsional vibrations about the C−O bond. Since these molecules depart only slightly from axial symmetry, the bands, with the exception of three due to the hydroxyl radical, correspond in position and appearance to those of the methyl halides. The rotational structure for the 10μ band (ν_5) of CH_3OD has been resolved, and partial resolution is obtained in some other bands. The band ν_8 in CH_2DOD has two components arising probably from two forms of the molecule in which the hydroxyl D atom occupies different valleys of the threefold potential. The deformation vibration (ν_7) is single for CH_3OD but has four components in CH_2DOD, indicating a separation of levels which for the former molecule are degenerate. A comparison of the frequencies obtained with gaseous and liquid samples indicates large displacements of the bands arising from the hydroxyl valence and deformation vibrations, the former toward greater wave-lengths in the liquid, and the latter toward smaller wave-lengths.

THE Raman spectra of ordinary methyl alcohol in the liquid phase, and of two methyl alcohols containing deuterium, have recently been described by Halford, Anderson and Kissin.[1] While the particular modes of vibration to be associated with each observed frequency may be decided almost by inspection, it is only through measurements in the infra-red that the character of the motions is revealed. Moreover the true molecular frequencies must be observed for the gaseous state. A comparison of infra-red data for the gases with Raman data for the liquids yields information of interest particularly in connection with the problem of association.

The molecule of methyl alcohol departs slightly from axial symmetry, since the line connecting the atoms O and H is nearly perpendicular to that connecting C and O. The minimum moment of inertia corresponds to an axis which is very nearly parallel to the C−O line, and which, for convenience, may be referred to as the symmetry axis. The relatively large electric moment may be attributed principally to the hydroxyl group. Twelve fundamental vibrations are to be expected, some of which occur in pairs, corresponding to two dimensional oscillators with nearly equal frequencies in the plane determined by the atoms C, O and H, and normal to it. Six of these are associated primarily with the methyl radical, three with the C−O bond, and three with the hydroxyl group, the first nine being conveniently designated as in the methyl halides.[2]

[1] Halford, Anderson and Kissin, J. Chem. Phys. **5**, 927 (1937). See also Mizushima, Morino and Okamoto, Bull. Chem. Soc. Japan **11**, 698 (1936).

[2] Dennison, Rev. Mod. Phys. **3**, 280 (1931).

The infra-red spectrum of CH_3OH has been reported in the preceding paper.[3] The observations here presented include certain bands of particular interest in the spectra of CH_3OD and of CH_2DOD. We are indebted to Professors Halford and Anderson for the preparation of these materials; the specimens are in fact the same ones upon which the Raman observations were made. Professor Randall kindly placed at our disposal a recording prism spectrograph for exploratory measurements, the absorption cell being a metal tube with windows of KBr and an optical path length of 80 cm. For measurements at high resolution a prism-grating spectrometer was used, with a 60° NaCl foreprism, and gratings ruled 4800 and 2400 lines per inch. With this instrument the absorption cells were 25 cm glass tubes without stopcocks, the windows being attached with Apiezon wax. A side arm held the liquid sample in sufficient quantity to saturate the chamber at room temperature; when intense absorption bands were under observation the vapor pressure was reduced by cooling this reservoir.

The Methyl Vibrations

In the region of 3.5μ the two methyl frequencies ν_1 and ν_2 occur. These consist primarily of motions in which the hydrogen atoms approach and recede from one another. In ν_1 the change in electric moment is along the methyl axis, and the band is of the parallel type. It appears at 2850 cm^{-1} in CH_3OD, and at 2874 cm^{-1} in CH_2DOD. The displacement toward higher frequencies in the latter case in spite of increased mass is caused by a slight change in the direction of vibration. The second fundamental vibration ν_2, is perpendicular in character. In CH_3OD it involves two oscillations normal to one another and of almost identical frequencies. The band center, at approximately 2965 cm^{-1}, can be determined only to within three or four wave numbers, since almost no structure is apparent. Whether or not there is also absorption in this region due to the parallel component of $2\nu_4$, as indicated by Raman scattering, cannot be determined because of the breadth and intensity of the perpendicular band. The observations are represented by curve *a* of Fig. 1. The two corresponding motions in CH_2DOD are of very different frequencies. One is only slightly displaced, giving rise to a band at about 2944 cm^{-1}, but the second appears at about 2180 cm^{-1}. These are shown on curves *b* and *c* of Fig. 1. In the latter curve there appears also a fairly intense zero branch at 2158.4 cm^{-1} which may be the harmonic $2\nu_5$, although in CH_3OD the latter appears at 2065.4 cm^{-1}, as indicated in curve *d*.

The second pair of methyl frequencies, ν_3 and ν_4, lie in the region between 6.8 and 8.0μ, and are difficult to locate because of the strong atmospheric absorption due to water vapor. The frequencies ν_3 are 1459 cm^{-1} for CH_3OD and 1357 cm^{-1} for CH_2DOD, corresponding to vibrations in which the three hydrogen atoms move in phase approximately at right angles to the carbon bonds. In ν_4 the motions are similar except that the three hydrogens oscillate with phases differing by equal intervals, producing bands of the perpendicular type. In the spectrum these appear as groups of lines in the neighborhood of 1480 cm^{-1} with a second group appearing in CH_2DOD near 1330 cm^{-1}.

[3] Borden and Barker, J. Chem. Phys. **6**, 553 (1938).

FIG. 1. Transmission at 3.4μ and 4.8μ. *a*, ν_1 and ν_2 for CH_3OD, 25 cm cell at −30°C. *b*, ν_1 and ν_2 for CH_2DOD, at −30°C. *c*, ν_2' for CH_2DOD, at 20°C. *d*, $2\nu_5$ for CH_3OD, at 20°C.

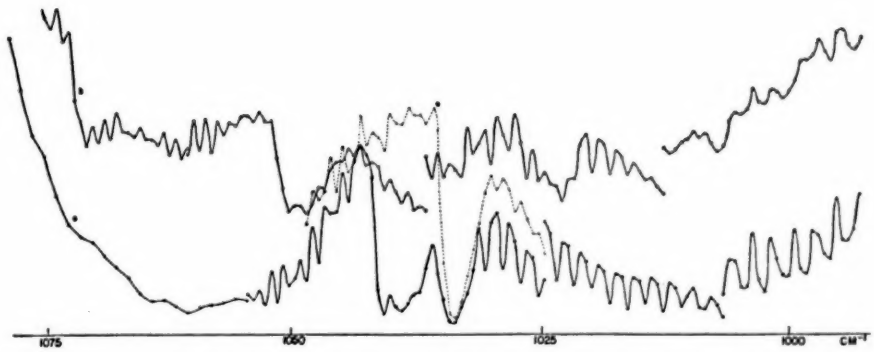

FIG. 2. Transmission at 10μ, showing ν_5. *a*, CH_3OD (with some CH_3OH). *b*, CH_2DOD. *c*, CH_3OH. Discontinuities indicate changes in prism setting.

THE C–O VIBRATIONS

In the methyl halides two frequencies are associated with the single carbon bond, one (ν_5) giving rise to a parallel band and the other (ν_6) to one of the pependicular type. The absorption due to ν_5 is very intense in the methyl alcohols, and is indicated in Fig. 2. With CH_3OD two zero branches were observed, one at 1034 cm^{-1} and the other at 1040 cm^{-1}. The fact that the former coincides exactly with the band of CH_3OH as indicated by the broken line, suggests that this sample had been contaminated with ordinary hydroxyl hydrogen, the tendency to exchange in this position being well known. Observations at 2.7μ showed that the OH band was present also. The second maximum at 1040 cm^{-1} is ν_5 for CH_3OD. It is somewhat broader than the one at 1034, indicating that the replacement of the hydroxyl hydrogen by deuterium produces a molecule somewhat farther removed from axial symmetry. The increase in frequency again indicates a larger restoring force due to the change in direction of vibration.

In the absorption curve for CH_2DOD there are also two maxima which appear to be rather broad zero branches at 1023 and 1049 cm^{-1}. These are probably to be explained by the fact that this compound exists in two forms depending upon the azimuthal position of the hydroxyl D with respect to the methyl D. In approximately two-thirds of the molecules the hydroxyl D will lie between an H and a D of the methyl group, the obliquity of the vibration with respect to the C–O line with being even greater than in CH_3OD, and the frequency correspondingly higher. The fact that no maxima appear in this spectrum at 1034 and 1040 cm^{-1} indicates that no exchange of hydrogens occurs in the methyl group, and also demonstrates the effectiveness of the procedure employed for the preparation of the material.

The band obtained with CH_3OD shows a distinct rotational structure, somewhat falsified, no doubt, by lines due to CH_3OH. As shown in Table I, the frequencies agree reasonably well with those computed from the equation

$$\nu = 1040.6 \pm 1.58m - 0.008\ m^2,$$

where m is the ordinal number of any line counting from the center. This indicates a mean moment of inertia for axes normal to the symmetry line, of approximately 35.0×10^{-40} g cm^2, a little more than 1 percent greater than for CH_3OH.

The perpendicular band ν_6 has not been observed for CH_3OD. In CH_2DOD two broad maxima consisting of groups of lines were located at about 1330 cm^{-1} and 1270 cm^{-1}. Whether the higher frequency group is a component of ν_6, which should be double, or belongs to ν_4 is not clear.

THE O–H AND O–D VIBRATIONS

The characteristic valence oscillation of the hydroxyl radical (ν_7) occurs at approximately 2.7μ for OH, and at 4.0μ for OD. The former is indicated in Fig. 3 as an absorption maximum around 3680 cm^{-1} in the lower curve (*C*) taken with low dispersion, using CH_3OH vapor. The determination of this band under high dispersion

TABLE I. *Observed and computed frequencies for the band* ν_5.

m	ν OBS.	ν COMP.	m	ν OBS.	ν COMP.
+9	1053.7	1054.2	−13	1018.4	1018.6
+8	1052.5	1052.8	−14	1016.7	1016.8
+7	1051.3	1051.3	−15	1015.0	1015.1
+6	1050.0	1049.8	−16	1013.4	1013.3
+5	1048.2	1048.4	−17	1011.7	1011.4
+4	1047.0	1046.8	−18	1009.8	1009.5
+3	1045.8	1045.3	−19	1007.8	1007.3
+2	1044.0	1043.8	−20	1005.9	1005.8
			−21	1004.0	1003.9
−6	1030.5	1030.8	−22	1002.0	1002.0
−7	1028.7	1029.1	−23	1000.1	1000.1
−8	1027.7	1027.4	−24	998.0	997.8
−9	1025.3	1025.8	−25	996.4	995.8
−10	1023.5	1024.2	−26	994.2	994.1
−11	1021.8	1022.2	−27	992.1	992.1
−12	1020.1	1020.4	−28	990.5	990.0

is a matter of some difficulty because of the intense absorption due to atmospheric water vapor, which is indicated in curve *A*. Measurements taken under the same conditions with CH_3OD in the cell are recorded in curve *B*. The very considerable absorption is evidence of the presence of hydroxyl H.

The region in which the O−D valence vibration occurs is a much more favorable one, since no atmospheric absorption interferes. Fig. 4 shows the band observed with CH_2DOD, its center having the frequency 2718.8. An almost identical curve was obtained for CH_3OD, with the center at 2720.4 cm^{-1}. The change in electric moment associated with this motion has components parallel to and perpendicular to the symmetry axis, both of course having the same frequency. The perpendicular one is probably greater in magnitude, and the band associated with it should exhibit a strong central maximum consisting of a family of zero branches spaced at intervals of approximately 5 cm^{-1}. These zero branches correspond to $\Delta K = \pm 1$, where K measures the angular momentum about the symmetry axis. There is some indication of such structure, but superposed upon it are a set of lines with spacing appropriate to the parallel band, as in ν_5. The small number of rotation lines observed on each side is evidence that this parallel band is superposed upon a strong and rather narrow background, probably attributable to the perpendicular transitions.

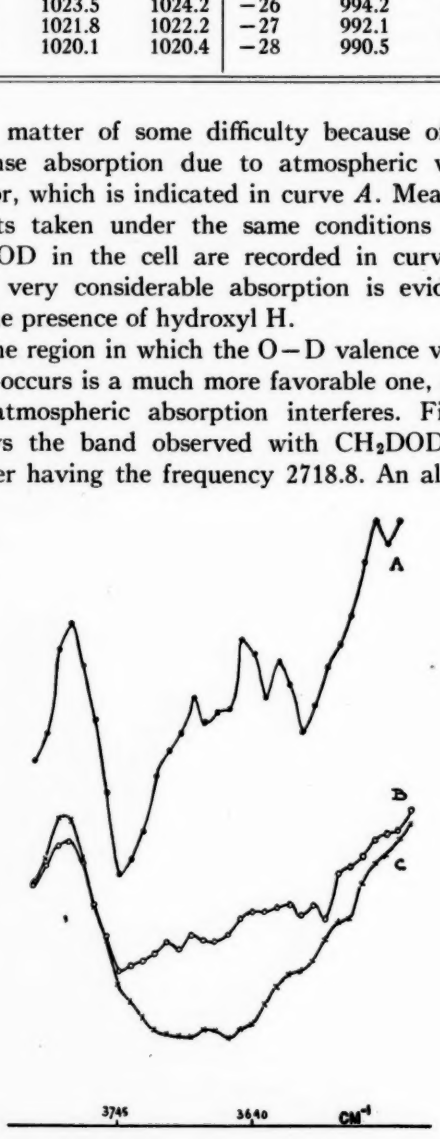

FIG. 3. Transmission at 2.7μ. *a*, Atmospheric water. *b*, CH_3OD (with some CH_3OH). *c*, CH_3OH.

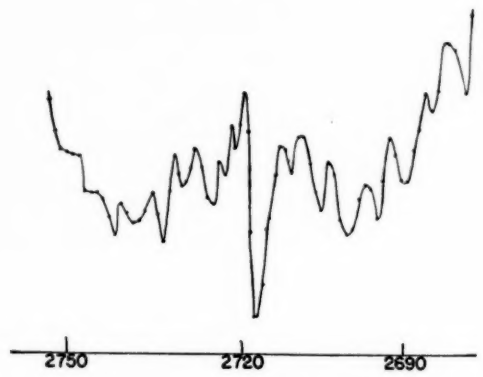

FIG. 4. Transmission at 3.7μ for CH_2DOD. Hydroxyl valence vibration $\nu_7 = 2718.8$ cm^{-1}.

A second degree of freedom (ν_8) for the hydroxyl D atom involves motions of low frequency normal to the D−O−C plane. In the absence of restraints this would become free rotation on the single carbon band. While the evidence here presented is not conclusive, it appears probable that free rotation occurs in only a relatively small number of molecules which have been excited to upper states of this motion, and that the normal state is an oscillation in one of the potential minima provided by the methyl radical. There is at least the negative argument that free rotation should introduce low states of considerable population, and in consequence,

combination bands which could hardly escape detection. For CH_3OD the three potential valleys are identical, and the lowest vibration state should be single while the second is double but degenerate. In CH_2DOD, however, one of the valleys differs from the other two, and this degeneracy would be removed, so that two low frequency bands should appear. Prism curves including the region from 13 to 22μ, taken with the 80 cm cell, indicated no absorption by CH_3OD. In CH_2DOD two very weak bands appeared near 16μ; these, however, could not be observed with the grating instrument in which it was necessary to use the shorter cell.

The so-called hydroxyl deformation vibration is normal to the O−D line, but in the D−O−C plane. This introduces a change in electric moment with its major component parallel to the symmetry axis. The resulting bands have strong zero branches, somewhat broadened, and degraded toward higher frequencies. They are shown in Fig. 5. The CH_3OD gives a single band at 863 cm^{-1}. In CH_2DOD four frequencies are observed, the two different types of molecules previously mentioned each being responsible for a pair of bands. The frequencies are 952.9, 892.3, 829.5, and 810.1 cm^{-1}. It might be expected that the splitting of the excited state would be greater in the more prevalent than in the less prevalent molecular type, the latter having a plane of symmetry, but it is not yet clear how these four bands are to be assigned.

The Effect of Association

Condensation from the vapor to the liquid state modifies some of these frequencies very considerably. This effect is apparent from a comparison of Raman and infra-red data, and has also been verified by observations upon the absorption of liquids. The methyl bands, and ν_5 due to the C−O bond, are not appreciably shifted, but the hydroxyl frequencies show a large displacement. The O−H valence vibration ν_7, found at 3650 cm^{-1} in CH_3OH vapor is reduced in frequency to about 3300 cm^{-1} in the liquid, as has been shown by Errera and others. The corresponding bands for CH_3OD and CH_2DOD are shifted from 2720 cm^{-1} to about 2500 cm^{-1}. The deformation bands ν_9 in the deuterium alcohols move to higher frequencies in the liquid phase, from 863 cm^{-1} to about 940 cm^{-1} for CH_3OD.[4] This effect could not be verified for CH_3OH, since ν_9 has not been observed in the vapor. Its position is indicated by Raman measurements as 1104 cm^{-1} in the liquid, and in the vapor it is probably obscured by the

[4] G. Bosschieter, J. Chem. Phys. 5, 992 (1937).

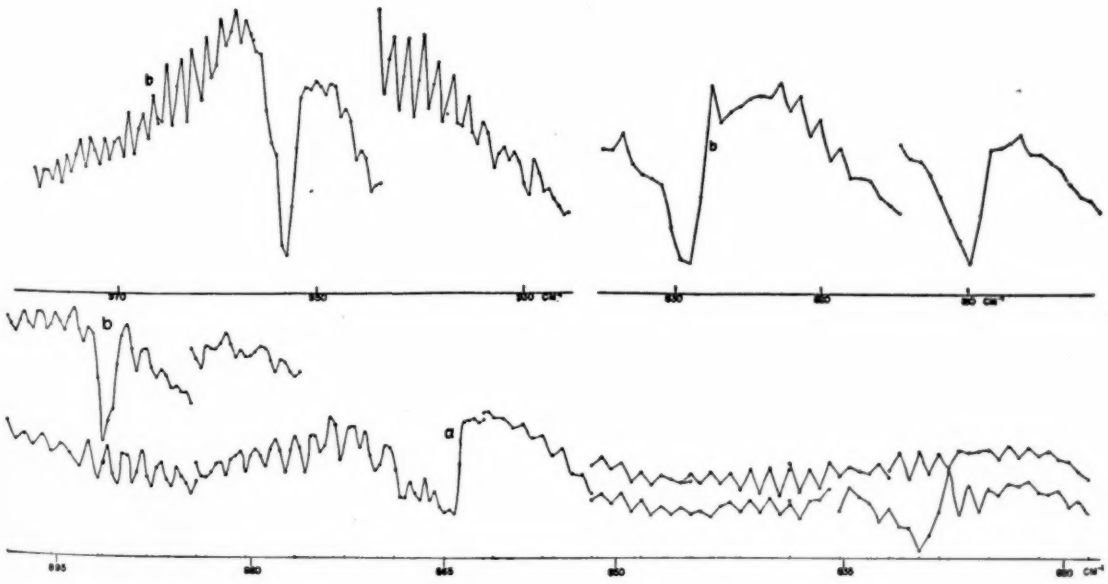

FIG. 5. Transmission at 12μ showing ν_9. *a*, CH_3OD. *b*, CH_2DOD.

intense 10μ band. A considerable intermolecular influence upon ν_6 might also be expected in the liquid. A bond between hydroxyl groups in adjacent molecules[5] would result in a further separation of the two components of this motion, though one of the components might be excluded from Raman transitions by considerations of symmetry. The only line in the Raman spectrum which can be assigned to ν_6 has a frequency of approximately 1160 cm^{-1} for both CH_3OH and CH_3OD, as compared with about 1340 cm^{-1} for the gases.

This investigation owes partial support to the Faculty Research Fund of the University of Michigan, which assistance is gratefully acknowledged.

[5] W. H. Zachariasen, J. Chem. Phys. **3**, 158 (1935).

LETTERS TO THE EDITOR

This section will accept reports of new work, provided these are terse and contain few figures, and especially few halftone cuts. The Editorial Board will not hold itself responsible for opinions expressed by the correspondents. Contributions to this section must reach the office of the Managing Editor not later than the 15th of the month preceding that of the issue in which the letter is to appear. No proof will be sent to the authors. The usual publication charge ($3.00 per page) will not be made and no reprints will be furnished free.

The Free Energy of the Producer-Gas Reaction, and the "Zero-Point" Entropy of Graphite[1]

In 1933, calculations made by Gordon[2] on the change in free energy for the producer-gas reaction indicated the possibility of the existence in graphite of a "zero-point" entropy of about 0.5 calorie per degree per mole. In an extensive study reported in 1934, Terebesi[3] compared, for five different reactions involving graphite, the experimentally determined equilibrium constants with those evaluated from calorimetric data and statistical calculations. According to Terebesi, the data on three of these reactions pointed strongly toward the nonexistence of a "zero-point" entropy for graphite, while the data on the other two reactions, one of them the producer-gas reaction, were inconclusive.

New calorimetric data on the heats of combustion of graphite[4, 5] yield new values, significantly different from the older ones, for the heats and free energies of formation of carbon dioxide[6] and carbon monoxide.[7] It seems desirable, therefore, to calculate a new value for the heat and free energy of the producer-gas reaction, and to ascertain the effect of the new values on the question of the "zero-point" entropy of graphite.

The new values for the heat and free energy of formation of carbon dioxide are, per mole:[6]

$$\text{C } (c, \text{ graphite}) + \text{O}_2\ (g) = \text{CO}_2\ (g), \tag{1}$$

$$\Delta H^0_{298.16} = -393{,}355 \pm 46 \text{ NBS international joules, or } -94{,}030 \pm 11 \text{ calories,}^{8} \tag{2}$$

$$\Delta F^0_{298.16} = -394{,}228 \pm 58 \text{ NBS international joules, or } -94{,}239 \pm 14 \text{ calories.} \tag{3}$$

For carbon monoxide, the writer[7] gives the following recalculated value for the heat of combustion, per mole:

$$\text{CO } (g) + \tfrac{1}{2}\,\text{O}_2\ (g) = \text{CO}_2\ (g), \tag{4}$$

$$\Delta H^0_{298.16} = -282{,}937 \pm 120 \text{ NBS international joules, or } -67{,}635 \pm 29 \text{ calories,} \tag{5}$$

and for the heat and free energy of formation, per mole:

$$\text{C } (c, \text{ graphite}) + \tfrac{1}{2}\,\text{O}_2\ (g) = \text{CO}\ (g), \tag{6}$$

$$\Delta H^0_{298.16} = -110{,}418 \pm 129 \text{ NBS international joules, or } -26{,}395 \pm 21 \text{ calories,} \tag{7}$$

$$\Delta F^0_{298.16} = -137{,}160 \pm 133 \text{ NBS international joules, or } -32{,}788 \pm 32 \text{ calories.} \tag{8}$$

Combination of the foregoing values, together with appropriate values[6, 7] of $H^0_{298.16} - H^0_0$, yields for the producer-gas reaction, per mole:

$$\text{C } (c, \text{ graphite}) + \text{CO}_2\ (g) = 2\text{CO}\ (g), \tag{9}$$

$$\Delta H^0_{298.16} = 172{,}519 \pm 244 \text{ NBS international joules, or } 41{,}240 \pm 58 \text{ calories.} \tag{10}$$

$$\Delta F^0_{298.16} = 119{,}908 \pm 248 \text{ NBS international joules, or } 28{,}663 \pm 59 \text{ calories,} \tag{11}$$

$$\Delta H^0_0 = 165{,}603 \pm 244 \text{ NBS international joules, or } 39{,}587 \pm 58 \text{ calories.} \tag{12}$$

Combination of the above value for ΔH^0_0 with the appropriate values of $(F^0 - H^0_0)/T$, reported by Clayton and Giauque,[9] Johnston and Davis,[10] and Kassel,[11] permits calculation of the equilibrium constant for reaction 9 for any given temperature:

$$\log_{10} K = -(1/2.3026R)[\Delta H^0_0/T + \Delta(F^0 - H^0_0)/T]. \tag{13}$$

In this manner, there may be calculated the following values of $\log_{10} K$: 1000°K, 0.2689; 1100°K, 1.0772; 1200°K, 1.7467; 1300°K, 2.3093; 1400°K, 2.7891; 1500°K, 3.2022. These values of the equilibrium constant are found to be in excellent accord with the experimentally determined equilibrium constants within the relatively large limits of uncertainty of the latter (see the summaries by Eastman,[12] Chipman,[13] and Terebesi[3]). It may be concluded, therefore, that the data on the producer-gas reaction are in accord with the nonexistence of a "zero-point" entropy for graphite.

FREDERICK D. ROSSINI

National Bureau of Standards,
Washington, D. C.,
August 10, 1938.

[1] Publication approved by the Director of the National Bureau of Standards, United States Department of Commerce.
[2] A. R. Gordon, J. Chem. Phys. **1**, 308 (1933).
[3] L. Terebesi, Helv. chim. Acta **17**, 819 (1934).
[4] P. H. Dewey and D. R. Harper, III. Forthcoming paper in Nat. Bur. Standards J. Research.
[5] R. S. Jessup. Forthcoming paper in Nat. Bur. Standards J. Research.
[6] F. D. Rossini and R. S. Jessup. Forthcoming paper in Nat. Bur. Standards J. Research.
[7] F. D. Rossini. Forthcoming paper in Nat. Bureau Standards J. Research.
[8] The superscript zero indicates, for gases, the hypothetical thermodynamic standard state of unit fugacity (1 atmosphere); a subscript indicates the absolute temperature; the calorie is conventionally defined as 4.1833 NBS international joules.
[9] J. O. Clayton and W. F. Giauque, J. Am. Chem. Soc. **54**, 2610 (1932); **55**, 5701 (1933).
[10] H. L. Johnston and C. O. Davis, J. Am. Chem. Soc. **56**, 271 (1934).
[11] L. S. Kassel, J. Am. Chem. Soc. **56**, 1838 (1934).
[12] E. D. Eastman, Circular 6125, U. S. Bur. Mines (1929).
[13] J. Chipman, Ind. Eng. Chem. **24**, 1013 (1932).